Corrosion Detection and Classification using Acoustic Emission and Machine Learning Based Approach

MUHAMMAD FAHAD SHEIKH

00000117373

Supervisor

DR. KHURRAM KAMAL

DEPARTMENT OF MECHATRONICS ENGINEERING

COLLEGE OF ELECTRICAL & MECHANICAL ENGINEERING

NATIONAL UNIVERSITY OF SCIENCES AND TECHNOLOGY

ISLAMABAD

FEBRAURY, 2018

Corrosion Detection and Classification using Acoustic Emission and Machine Learning Based Approach

Author

MUHAMMAD FAHAD SHEIKH

00000117373

A thesis submitted in partial fulfillment of the requirements for the degree of

MS Mechatronics Engineering

Thesis Supervisor:

DR. KHURRAM KAMAL

Thesis Supervisor's Signature: _____

DEPARTMENT OF MECHATRONICS ENGINEERING

COLLEGE OF ELECTRICAL & MECHANICAL ENGINEERING

NATIONAL UNIVERSITY OF SCIENCES AND TECHNOLOGY,

ISLAMABAD

FEBRAURY, 2018

Declaration

I certify that this research work titled "*Corrosion Detection and Classification using Acoustic Emission and Machine Learning Based Approach"* is my own work. The work has not been presented elsewhere for assessment. The material that has been used from other sources it has been properly acknowledged / referred.

Signature of Student

MUHAMMD FAHAD SHEIKH

00000117373

Language Correctness Certificate

This thesis has been read by an English expert and is free of typing, syntax, semantic, grammatical and spelling mistakes. Thesis is also according to the format given by the university.

Signature of Student

MUHAMMAD FAHAD SHEIKH

00000117373

Signature of Supervisor

Dr. Khurram Kamal

Copyright Statement

Acknowledgements

I am thankful to my Creator Allah Subhana-Watala to have guided me throughout my life and in this work at every step and for every new thought which You setup in my mind to improve it. Indeed, I could have done nothing without Your priceless help and guidance. Whosoever helped me throughout the course of my thesis, whether my parents or any other individual was Your will, so indeed none be worthy of praise but You.

I am profusely thankful to my beloved parents and family who raised me when I was not capable of walking and continued to support me morally and financially throughout in every department of my life. Whatever I am today, is due to their prayers.

I would also like to express special thanks to my supervisor Dr. Khurram Kamal for his help throughout my thesis and for Machine Learning course which he has taught me. I can safely say that I haven't learned any other engineering subject in such depth than the one which he has taught. Dr. Khurram Kamal showed personal interest, tremendous support and cooperation in this thesis. He personally monitored me during experimentation phase. Each time I got stuck in something, he came up with the solution. Without his help I wouldn't have been able to complete my thesis. I appreciate his patience and guidance throughout the whole thesis. I can easily say that he is more than teacher and mentor for me. I would also love to thank Dr. Kashif Khan from Coventry University England for his cooperation and guidance on this research work.

I would also like to thank Dr. Umar Shahbaz, Dr. Mahmood Anwar Khan for being on my thesis guidance and evaluation committee. I would like to thank and acknowledge the efforts of Tayyab Zafar, Faheem Khattak, Salman Sabir, Hassan Zaheer and Yousaf Mahmood for their help during thesis. I would like to express my special Thanks to my dearest class mates Muhammad Arslan, Ubaid-Ur-Rehman, Nabeel-Ur-Rehman, Altaph Chaudhary, Muhammad Zaeem, Hassan bin Younis and Muhammad Usman for their continuous support. I am also thankful to my beloved friends, Abdul Basit and Muhammad Sadam Sajid for being there for me every time I needed.

Finally, I would like to express my gratitude to all the individuals who have rendered valuable assistance to my study.

ABSTRACT

Degradation caused by corrosion in complex engineered systems strongly affects the economic and industrial growth of a country. Failure caused by corrosion in industries are the major cause of breakdown maintenance. Corrosion detection and monitoring techniques can diagnose health of industrial structures and reduce their life-cycle cost. Corrosion detection and monitoring techniques can be classified into two categories namely destructive testing and Nondestructive testing techniques (NDT). Various NDT techniques like Ultrasonic, Acoustic emission, Guided waves, Eddy currents, Radiographic testing and Magnetic flux leakage have been applied by researchers for corrosion monitoring. Acoustic emission being a passive NDT technique has greater potential to be used as corrosion detection and monitoring technique. Acoustic emission during the accelerated corrosion testing is a reliable method for corrosion detection, however, classification of these acoustic emission signals by machine learning techniques is still in its infancy. To overcome this problem, machine learning based classifier approach is proposed that extracts the statistical features of the acquired acoustic emission signals from accelerated corrosion testing of mild steel samples and then use these distinct statistical features as inputs to the classifier to classify corrosion and no-corrosion state and further corrosion severity level prediction. Proposed method automatically extracts distinct statistical features like AE Mean, AE Energy, AE RMS, Skewness and Kurtosis of each acquired acoustic signal and then present these distinct features as inputs to classifier for classification. Acoustic emission signals for accelerated corrosion process were acquired using acoustic sensor, NI Elvis kit and LabView interface. Three different algorithms, back propagation neural network, radial basis function neural network and naive bayes classifier have been used as supervised learning algorithms for classification of ‘corrosion’ and ‘no corrosion’ state and corrosion severity level prediction. For multi-class problem, five corrosion severity levels have been made based on the mass loss occurred during accelerated corrosion testing. For bi-classification problem, Naive Bayes, BP-NN and RBF-NN showed accuracy of 98.68%, 98.57%, and 100% respectively. For five-class corrosion severity level problem, Naive Bayes, BP-NN and RBF-NN showed accuracy of 90.4%, 94.57%, and 100% respectively. Radial basis function neural network outperformed the other two classifiers and showed the best classification accuracy for corrosion severity level prediction due to presence of gaussian activation function in network hidden layer neurons.

Table of Contents

List of Figures

List of Tables

1. INTRODUCTION

This chapter presents an introduction to corrosion detection and monitoring techniques using various methods while focusing on importance of corrosion monitoring in industry, research aims, scope of the research and the motivation lying behind the thesis.

1.1. Introduction to Thesis

Corrosion is a natural phenomenon which degrades the metals into its components by reacting chemically or electrochemically with its environment. Corrosion is the metal's chemical disintegration into its components. Corrosion has always been an immense problem for engineering community because complex engineering structures such as bridges, aircrafts, ships, nuclear power plants, and industrial pipelines are always subjected to such conditions that leads to corrosion. However, environmental conditions such as humidity, temperature and presence of any reactive substance strongly affects rate of corrosion. Corrosion affects the strength of the materials and reduces the life cycle of an equipment. Corrosion has many types namely general attack corrosion, pitting corrosion, stress corrosion cracking, galvanic corrosion and flow assisted corrosion.

Degradation caused by corrosion in these complex engineered systems strongly affects the economic and industrial growth of a country. According to world Corrosion Organization annual direct cost of corrosion is 2.2 trillion US dollars worldwide which accounts for over 3% of worldwide GDP [1]. Direct costs include the costs of materials, repair, maintenance and the replacement cost of equipment damaged due to corrosion. Production loss, environmental impacts, transportation disruptions, injuries, and fatalities are the indirect costs associated to corrosion. Failure caused by corrosion in industries are the major cause of breakdown maintenance. Corrosion detection and monitoring techniques can diagnose health of industrial structures and reduce their life-cycle cost. Major portion of the life-cycle cost goes towards finding and then fixing the fault. Early diagnosis of faults can save up to 30% of the total ownership cost [2]. Corrosion detection and monitoring techniques can save a lot of cost in terms of predictive maintenance. According to researchers $20 - 25$ % of the annual direct cost

of corrosion can be saved by applying the available technologies [1][3]. Intelligent health monitoring systems for detection and monitoring of corrosion are under great focus these days. Corrosion detection and monitoring techniques can be classified into two categories namely destructive testing and Nondestructive testing techniques (NDT). NDT techniques inspect and evaluate materials and assemblies without affecting their future usefulness. Various NDT techniques like Ultrasonic, Acoustic emission, Guided waves, Eddy currents, Radiographic testing and Magnetic flux leakage have been applied by researchers in this regard [4]. Each technique has its own benefits and limitations; however, the main benefit of NDT techniques is that the part can still be used when the part is under inspection.

In active type NDT techniques, external energy is used as an excitation source, therefore, transmitting transducer and receiver both are required. Acoustic emission testing relies on the energy initiated within the material or component under test so only receiving transducers are required. Acoustic emission is defined as emission of transient elastic waves generated by rapid release of energy due to deformation in the materials. Acoustic emission being a passive NDT technique has greater potential to be used as corrosion detection and monitoring technique. There are two types of acoustic emission namely air-borne acoustic emission and structure-borne acoustic emission. In corrosion detection and monitoring systems, Air-borne acoustic emission is commonly used but it has issues such as environmental noise. Structure-born acoustic emission during the accelerated corrosion testing is a reliable method for corrosion detection, however, classification of these acoustic emission signals by machine learning techniques is still in its infancy. To overcome this problem, machine learning based classifier approach is proposed that extracts the statistical features of the acquired acoustic emission signals from accelerated corrosion testing and then use these distinct statistical features as inputs to the classifier to classify corrosion and no-corrosion state and further corrosion severity level prediction. Proposed method automatically extracts distinct statistical features like AE Mean, AE Energy, AE RMS, Skewness and Kurtosis of each acquired acoustic signal and then present these distinct features as inputs to neural network based classifier for corrosion classification.

The thesis is organized in following sections. Chapter 2 presents the previous work related to corrosion monitoring techniques, classifiers and statistical signal processing. Chapter 3 explains the theory behind the chosen methods and chapter 4 explains the experimental setup and data acquisition while chapter 5 explains the results and detailed discussion respectively. Chapter 6 discusses the challenges related to implementation of the proposed technique and chapter 7 explains the conclusion and future work.

1.2. Summary

- Corrosion is a naturally occurring phenomenon in which metal's chemical disintegration into its components occurs. Corrosion affects the strength of the materials and reduces the life cycle of an equipment. Production loss, environmental impacts, transportation disruptions, injuries, and fatalities are the indirect costs associated to corrosion.

- Degradation caused by corrosion strongly affects the economic and industrial growth of a country. Annual direct cost of corrosion is 2.2 trillion US dollars worldwide. Failure caused by corrosion in industries are the major cause of breakdown maintenance.

- For better accuracy and efficiency of automated corrosion inspection systems, acoustic emission based corrosion detection needs to be combined with machine learning based classification techniques.

2. LITERARTURE REVIEW

This chapter provides a discussion on various methods that have been used to detect and monitor corrosion. A comparison of discussed technique is also provided in the chapter. Various techniques for detection and monitoring of corrosion using acoustic emission are also explained. Lastly, a discussion on machine learning based classifiers for classification purpose in contrast with the corrosion detection and monitoring systems is also included in the chapter.

2.1. Corrosion and Types of Corrosion

Corrosion can be defined as the deterioration of the metal. Metals disintegrate into their components due to corrosion. Corrosion costs billions of dollars a year in maintenance and repair. Corrosion occurs due to the chemical or electrochemical reaction of a metal with its environment. Main cause of corrosion is the chemical instability, so they react with environment to form a chemically stable form. Metals such as gold and platinum are found in their stable form. All other metals found in nature in form of ores are unstable in environmental conditions and have natural tendency to react with environment and form a chemically stable form. Natural corrosion is a slow process, however, environmental conditions such as pH, temperature, stress and humidity can accelerate the process [5]. Chemical mechanism of corrosion can be explained by the reaction of a metal with a strong acid. When pure iron metal reacts with hydrochloric acid, Iron oxidizes. Oxidation reaction produces ferric chloride and hydrogen gas is produced in the form of bubbles which will rise to the surface of solution. Chemical reaction of the above corrosion process is given in the following equations below.

$$Fe + 2HCl \rightarrow FeCl_2 + H_2 \quad (2.1)$$

$$Fe + 2H^+ + Cl^{2-} \rightarrow Fe^{2+} + Cl^{2-} + H_2 \quad (2.2)$$

Due to above reactions iron will start losing gradually and the rapid release of hydrogen bubbles at the top. Iron metal has been oxidized by leaving two electrons and hydrogen atom has been reduced by gaining two electrons. This transfer of electrons is taking place at the surface of the metal hence metal loss occurs. Corrosion has many types, mainly depending upon the type of loss that occurs on metal and the reaction that happened with the environment. Understanding the type of corrosion can help researchers to find the remedy to

prevent and monitor corrosion. Different types of corrosion have been reported in the literature [5-6] which are given below.

A. Uniform Corrosion

Uniform corrosion also known as general attack corrosion is the most common form of corrosion. When metal loss occurs evenly over the whole exposed surface area it is known as uniform corrosion. Metal loss rate is an important parameter while considering the uniform corrosion. Metal loss rate is generally expressed as millimeters per year. Material with metal loss more than 50 millimeter per year are not acceptable for critical engineering applications.

B. Localized Corrosion

When the corrosion attacks at the specific portions of the material it is known as localized corrosion. Localized corrosion is considered as more dangerous as compared to uniform corrosion due to its ability to localize at a point.

Localized corrosion can be divided into following types.

- **Pitting Corrosion**

  Pitting corrosion is the highly localized loss of material to form a pit or hole on the surface of the material. Pitting starts with the breakage of protective passive film from the surface of metal and it initiates the pit. Leakage and breakdown of Industrial pipelines are mostly caused by this type of corrosion.

- **Crevice Corrosion**

  Type of localized corrosion which occurs at the gap or crevice joining the two surfaces. This type of corrosion generally attacks at the stagnant locations where physically access is limited. Small localized attack at such locations can be magnified with intense environmental conditions [7].

C. Galvanic Corrosion

Galvanic corrosion occurs when two different metals are placed in a common electrolyte and a driving force such as voltage is applied between them. Applied potential difference causes the flow of electrons between anode and cathode and consequently the metal loss occurs.

D. Stress Corrosion Cracking

Stress corrosion cracking occurs when the metal and alloys are exposed to corroding environment and stresses simultaneously. Amount of stress applied, and temperature have significant effect on rate of corrosion. Extensive cracking of Stainless steel SS-304 can be generated in hours when placed in boiling magnesium chloride solution.

E. Intergranular Corrosion

Intergranular corrosion is a chemical or electrochemical attack on the grain boundaries of a metal. This often occurs due to impurities in the metal, which tend to be present in higher contents near grain boundaries. As attack penetrates individual grains are separated from the layer and the grain structure of the layer changes, making the surface layer porous. Porous surface leads to rapid powdery metal loss.

F. Erosion Corrosion

This type of corrosion occurs due to the combination of erosion due to mechanical wear and then corrosion due to the presence of some liquid. Erosion corrosion can lead to an accelerated metal loss. Erosion corrosion can cause cavitation in tubes and pipelines.

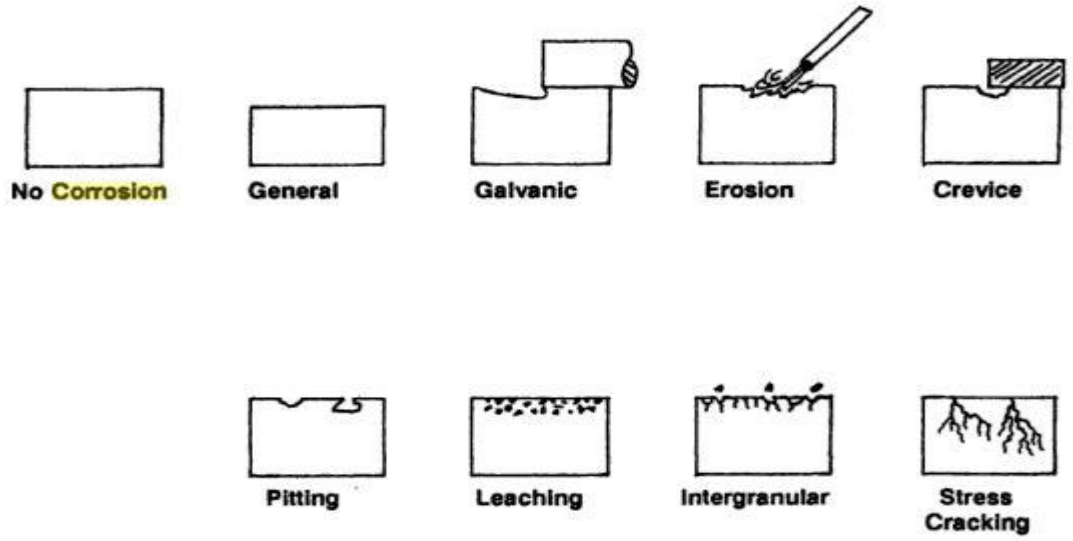

Figure 2. 1: Types of corrosion *[5]*

2.2. Corrosion Monitoring Techniques

Different researchers proposed different corrosion monitoring techniques. These techniques can be divided into two categories, destructive testing and non-destructive testing techniques.

While performing destructive testing, specimen under test is subjected to load until its breakdown. Common example of destructive testing is the crash test used in automotive industry, stress testing and the hardness test. Non-destructive testing is to inspect and evaluate materials without affecting their serviceability. Common NDT techniques include visual testing, ultrasonic testing, magnetic flux leakage, eddy current, radiographic testing and acoustic emission [8]. Benefits and the limitations of the destructive and non-destructive testing are summarized below.

- Destructive testing yields only the mechanical properties of the materials such as corrosion resistance, ultimate tensile strength, yield point, hardness, ductility and toughness.
- Destructive testing yields accurate and reliable data from test which is generally used for design purposes.
- Destructive testing can give precise information about the specimen characteristics; however, the specimen is destroyed so it cannot be used again.
- Destructive testing requires large and expensive laboratory equipment.
- Non-destructive testing can inspect parts while in service, and without affecting their future usefulness.
- Non-destructive methods are cost effective, long term and portable.
- Data gathered from Non-destructive testing needs interpretation.

Main goal of corrosion inspection and detection techniques are to inspect for corrosion without dismantling the structure. Visual methods for corrosion inspection and detection are the most commonly used non-destructive testing methods. Visual methods involve the periodic visual inspection of the structure for any defects and disorders. Common visual methods for corrosion detection and inspection involves boroscope and charge couple devices (CCD) [2]. Boroscope is an optical device that uses telescope with a light source. This optical device allows visual inspection of internal surfaces for corrosion defects. Diffracto D-sight, edge of sight, optical profilometry and video imaging are common CCD techniques. These techniques make use of

CCD cameras to acquire the images and then process them using computer programs to look for corrosion related defects. Pidaparti et al. [9] proposed an image processing-based technique for classification of corrosion defects. Proposed technique uses Scanning Electron Microscope (SEM) images of NiAl bronze, exposed in different corrosive and stress environment. These SEM images are cropped to the size of 256×256 pixels. Wavelet packet transform, and fractal analysis are used as image analysis techniques. The flow chart of the proposed technique is shown in the figure 2.2.

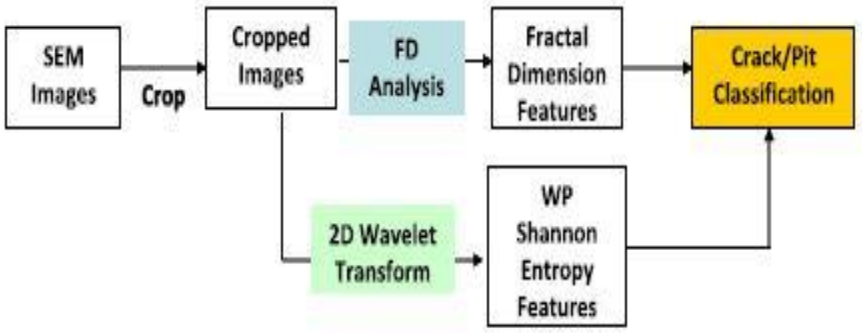

Figure 2. 2: Flow chart of the proposed defect detection technique using image processing *[9]*

SEM Image is decomposed into one approximation and three detail images through discrete wavelet packet transform (DWPT). A second level decomposition is applied on the resultant of the first decomposition. Combination of high-pass and low-pass filters are used to implement a 2-D DWPT. Feature extraction involves the calculation of energy and entropy of these images. Fractal analysis of SEM images involves the calculation of fractal dimension to measure the roughness in these images. Power spectral density (PSD) of the surface image f (x,y) is calculated. where F (u,v) is the Fourier transform of f (x, y), and u and v are the spatial frequencies (number of waves per unit wave length) in the x and y directions, respectively.

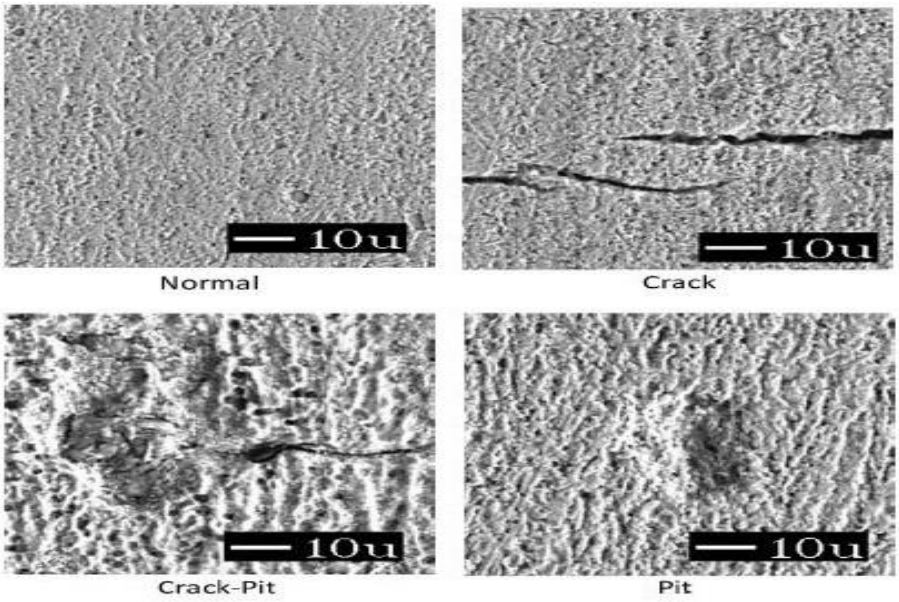

Figure 2. 3: Typical Corrosion defects (SEM images) *[9]*

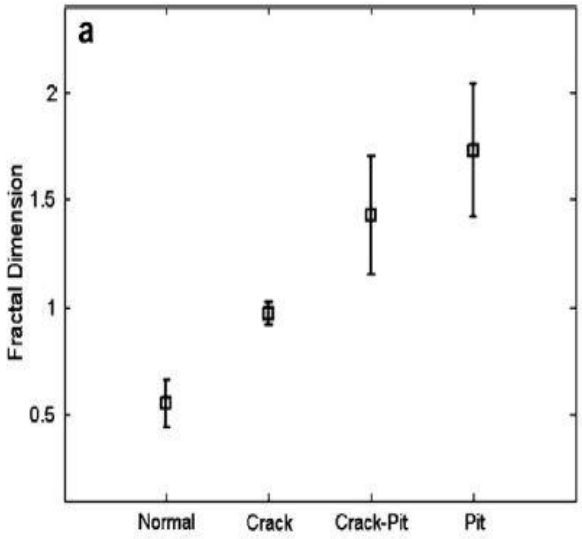

Figure 2. 4: Results of classification of corrosion defects from SEM images using Fractal Dimension *[9]*

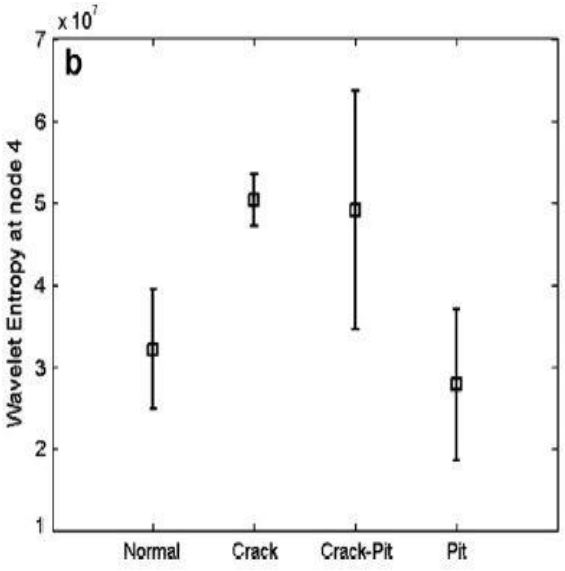

Figure 2. 5: Results of classification of corrosion defects from SEM images using Wavelet Transform *[9]*

Visual inspection for long range systems is a very tedious and labor-intensive task. Vision based monitoring of corrosion needs offline processing of images and has physical limitations like accessibility issues. These systems are generally not considered as reliable testing methods for critical applications.

Magnetic flux leakage based corrosion PIGs were conventionally used to detect corrosion defects. Magnetic flux leakage is the most widely used non-destructive evaluation technique for in-service inspection of pipelines [10]. Wall of the pipe is magnetized and when metal loss occurs due to corrosion, magnetic flux is leaked and is sensed by the sensor. Magnetic saturation of the pipe wall is the requirement of Magnetic flux leakage technique because it forces the magnetic field to leave the material during the metal loss, hence, small diameter and thick pipe walls cannot be inspected by this technique. Gloria et al. [11] proposed an internal corrosion sensor that uses magnetic flux leakage and magnetic perturbation [12] technique to detect internal corrosion in pipelines. Proposed technique measures the direct magnetic response from small pipe area and it is not affected by the thickness of the pipe wall. Magnetic flux lines tend to remain inside the material with better magnetic properties. Due to defects caused by metal loss, deformation is produced in the magnetic flux lines and this deformation is sensed by the proposed sensor. Best configuration of the sensor is proposed by the finite element calculations.

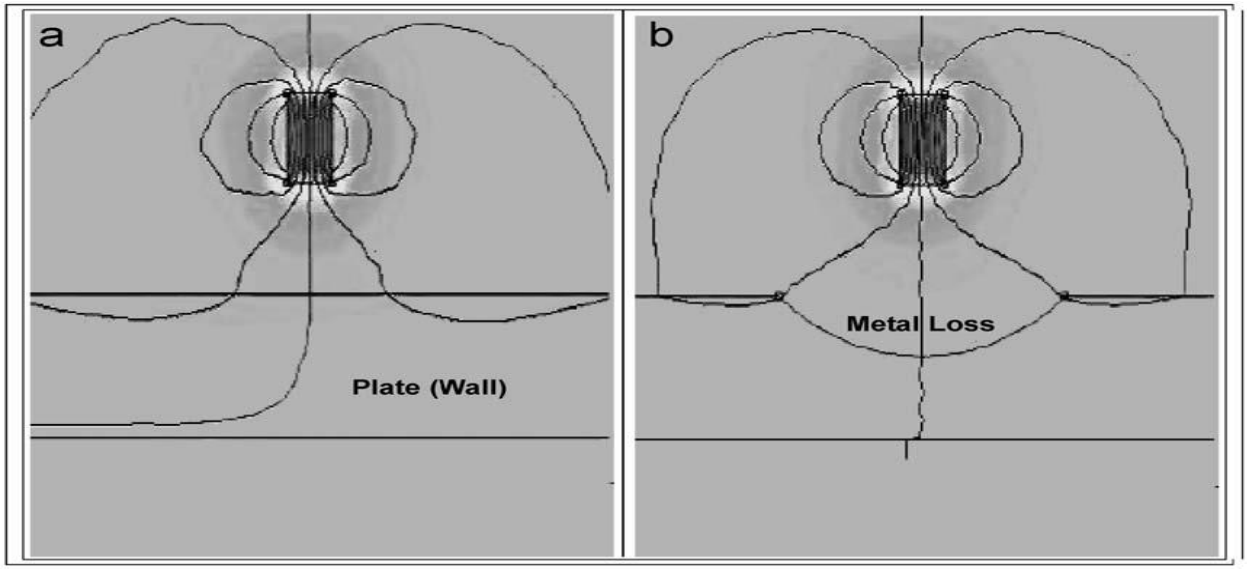

Figure 2. 6: Principles of operation of ICS sensor based on the difference between the magnetic. (a) in the absence of a defect (b) in the presence of a metal loss defect *[12]*

Kim et al. [13] proposed an eddy current based stress corrosion crack detection for gas transmission pipelines. The addressed problem in this technique is to detect the stress corrosion cracking colonies oriented axially along the length of the pipeline. The proposed technique uses ploy-phase rotating magnetic field to setup eddy currents and magnetic fields. Remote field region is used to make measurements of the decaying eddy currents away from the exciter.

A three-phase power supply, induction motor rotor, pick-up coil, lock-in-amplifier (LIA), PC-based motion controller and a personal computer are required to setup the experiment. Four different defects were induced at different depth level at the outer wall of the pipe. Electromagnetic field within the remote field region that penetrates through pipe is sensed by the pick-up coil. Remote field eddy current (RFEC) based scanning is performed by moving pick-up coil circumferentially and axially in both directions. Results of RFEC based scanning at the induced defects pipe is shown in the figure 2.7. For estimation of defects, a boundary detection algorithm has been employed. Detected phase signal has been de-trended and filtered through wavelet de-noising scheme. X-axis in the figure depicts the inches in circumferential direction and Y-axis shows the degrees in axial direction.

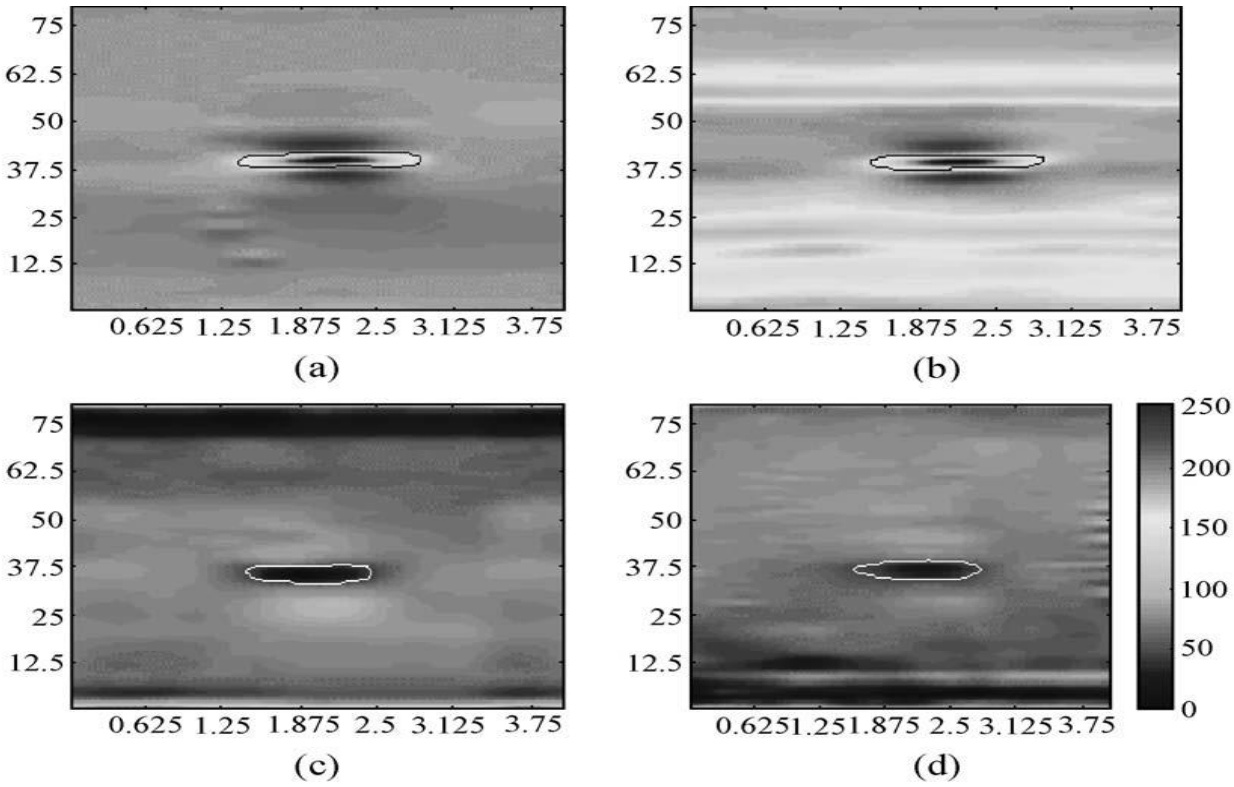

Figure 2. 7: RFEC scanning of defects: (a) 80%, (b) 60%, (c) 40%, (d) 20% depth *[13]*

Guided waves are the stress waves that are bounded to follow the boundaries of the structure [14]. Guided waves based structural health monitoring (SHM) systems are considered as an important tool for damage detection in civil, mechanical and aerospace structures. SHM provides accurate information to user about the health of structure and it can also help in predicting the remaining useful life of the structure. Early diagnosis of defects by SHM saves a lot of maintenance cost by changing the scheduled maintenance to condition based maintenance. Guided wave testing being an active non-destructive testing technique, excites the structure and then examine it for the damage. Pulse-echo and pitch-catch are two common guided wave SHM schemes. In pulse-echo scheme, structure is excited with a known narrow bandwidth pulse and a sensor is used to listen the echoes coming from discontinuities. Because of the known frequency of the boundary signals they can be filtered out and the remaining signal is of the defect if present. In pitch-catch scheme, a pulse is sent across the structure subjected to test and sensor at the other end of structure receives the signal. Characteristics of received signal reveals the information about the damage. Figure 2.8 explains the essential steps involved in Guided wave SHM. Guided waves are passed through the structure under

test, reflected signals are collected and processed for the feature extraction and then the final step involves the implementation of pattern recognition and machine learning techniques.

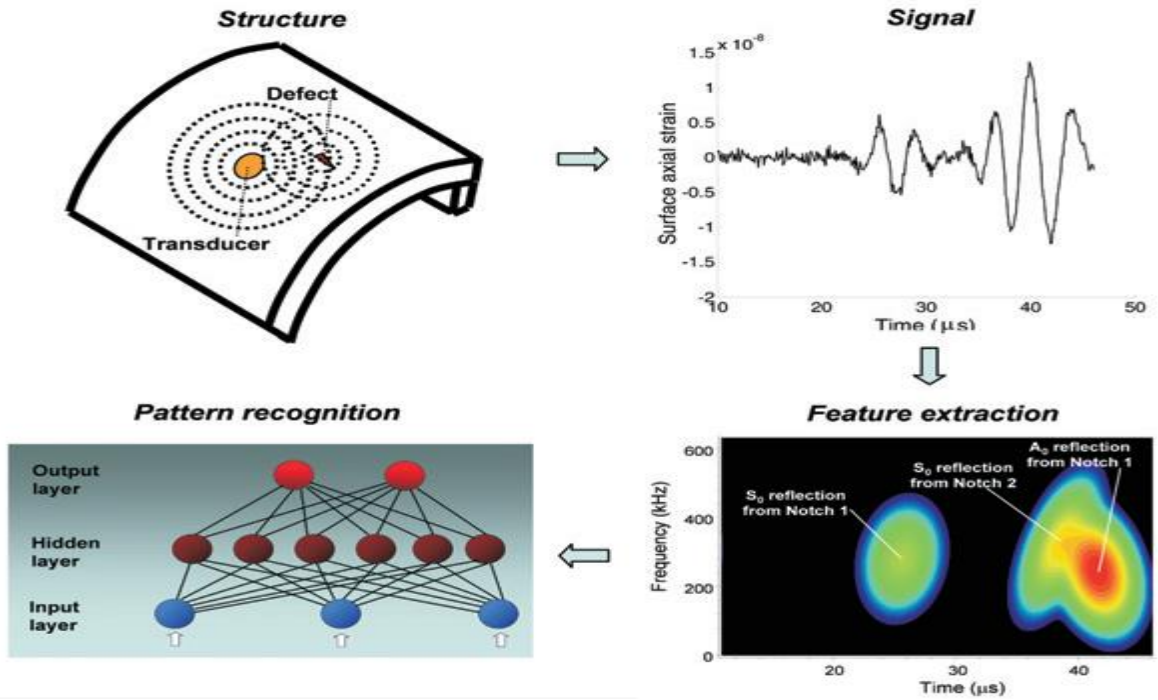

Figure 2. 8: Steps involved in guided wave structural health monitoring system *[14]*

Detection of corrosion in insulated pipelines is very important in chemical industries. Insulation needs to be removed to inspect the pipelines, hence, making it an expensive and time-consuming task. Solution to the problem of Corrosion under Insulation (CUI) was proposed by Lowe et al. [15]. Proposed technique makes use of guided waves that propagates along the wall of the pipe. Main benefit of this technique is that insulation needs to be removed from just one location on pipe. Proposed technique uses the pulse-echo arrangement of guided waves that uses ring of piezoelectric transducers for wave excitation and receiving. Reflections of guided waves and their arrival time reveals the presence of defects and their axial location. The proposed technique has the ability to inspect pipelines for corrosion defects up to fifty meters. Figure 2.9 explains the general pulse echo guided wave inspection technique for pipes.

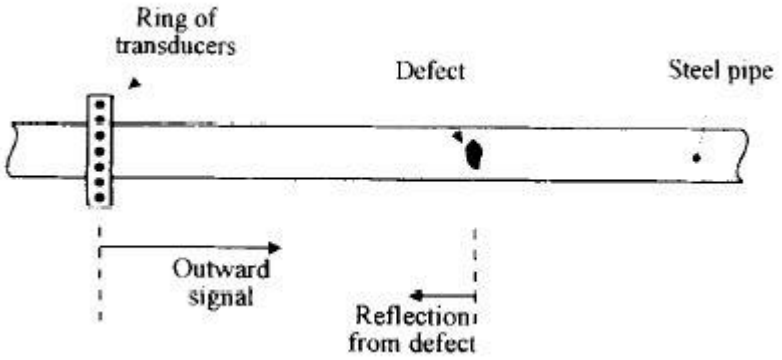

Figure 2. 9: Pulse echo inspection system for pipelines *[15]*

Proposed inspection system uses 70 kHz axially symmetric mode of guided waves for excitation of the structure. Selection of high frequency narrow band single mode is justified by the fact that it gives good signal strength and avoids dispersion over long ranges.

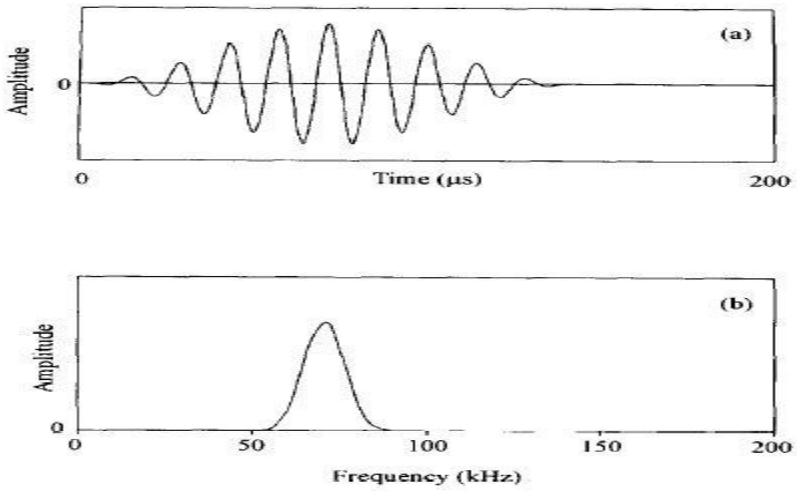

Figure 2. 10: Narrow band signal 70 KHz a) Time domain signal b) Frequency spectrum *[15]*

Figure 2.11 shows the reflected signal that was generated by reflection of the high frequency single mode excitation signal when it encounters the other end and the notches.

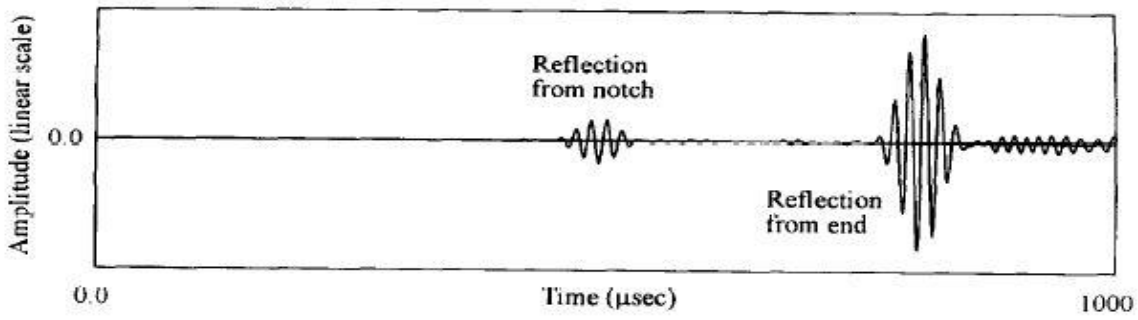

Figure 2. 11: Time vs Amplitude of reflected signal *[15]*

Mokhles et al. [16] proposed Long Range Ultrasonic Testing (LRUT) for long distance pipeline inspection. Proposed technique uses guided ultrasound wavelet for detection and inspection of external and internal metal loss due to corrosion in pipelines. Ultrasonic signal used in the proposed technique is above human hearing range normally of 10-100 KHz. Relationship between signal amplitude and pipe line distance is obtained in each LRUT scan. High amplitude peaks are produced by the pipe line features and defects produced by corrosion.

2.3. Acoustic Emission as Corrosion Monitoring Technique

The above reviewed non-destructive techniques for corrosion detection and monitoring are active in nature because they involve the excitation of the structure by means of some external energy and then receiving these signals. Acoustic emission being a passive NDT technique just listen to the micro seismic activity happening inside the structure. Acoustic emission (AE) testing detects the high frequency elastic waves produced under stress loading and then conversion of these waves to electrical signals. Corrosion detection and monitoring through AE is reviewed.

Droubi et al. [17] proposed the use of acoustic emission for defect detection and identification in carbon steel welded joints. Four samples of carbon steel, one non-defective reference sample and three induced defects samples of crack, porosity and slag are used for experimentation. Data acquisition system used in experimentation make use of piezoelectric AE sensor, a pre-amplifier unit, data acquisition card and Labview software data acquisition interface.

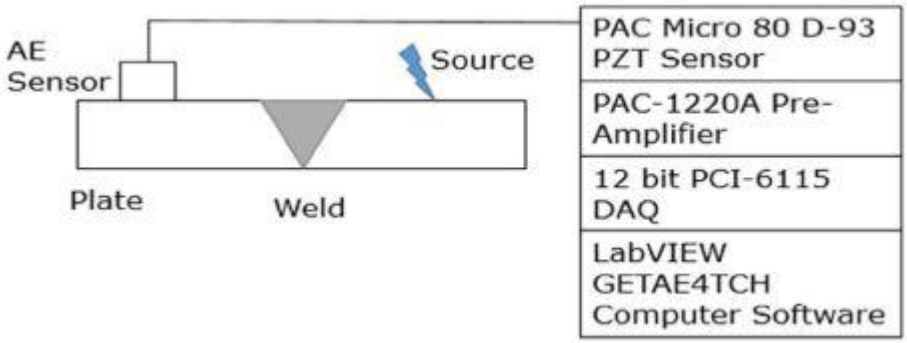

Figure 2. 12: Schematic layout of the AE data acquisition system *[17]*

Peak amplitude, AE energy, rise time, decay time and RMS are extracted from the acquired AE signal. Figure 2.13 shows that each defect has different amplitude level hence providing clear identification of defects.

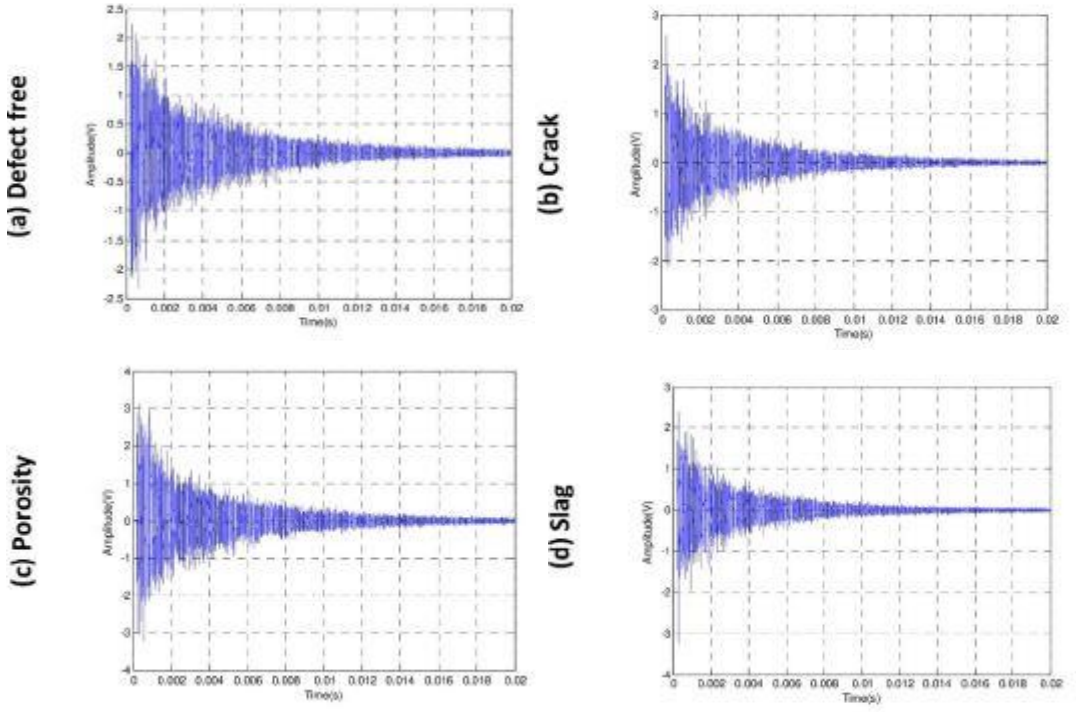

Figure 2. 13: Amplitude vs Time of acquired AE signal a) No defect b) Crack c) Porosity d) Slag *[17]*

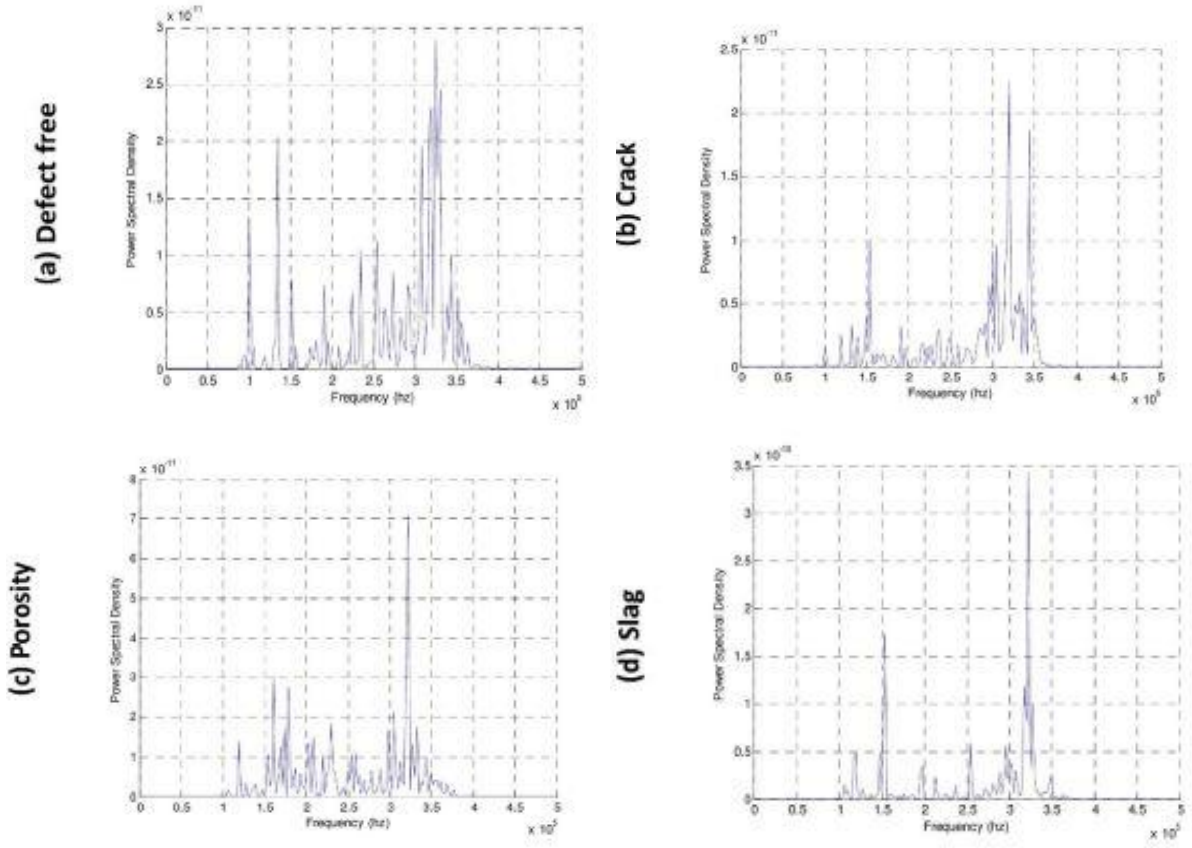

Figure 2. 14: Frequency Spectrum of acquired AE signal a) No defect b) Crack c) Porosity d) Slag *[17]*

Kaige Wu et al. [18] monitored pitting corrosion of stainless steel (SS) 304 with the help of Acoustic emission. Proposed technique makes use of hydrogen bubbles acoustic emission produced in the pitting process. 10 mm×10 mm sample of Commercial SS-304 was used in the experiment. Pitting corrosion was controlled by anodic polarization using potentiodynamic method. Experiment make use of three-electrode electrochemical cell with AgCl electrolyte having 3 % NaCl and pH of 2. R15 Physical acoustic sensor, Pre-amplifier and AE data acquisition software were used to make Acoustic emission measurements. AE behavior shows three stages of corrosion, Stage I when bubbles form but no AE signal detected, Stage II when series of single bubbles break and Stage III when bubbles breaking up. Fig shows the morphology of bubbles during stage II and then FFT and magnitude plot of the acquired acoustic signal during stage II.

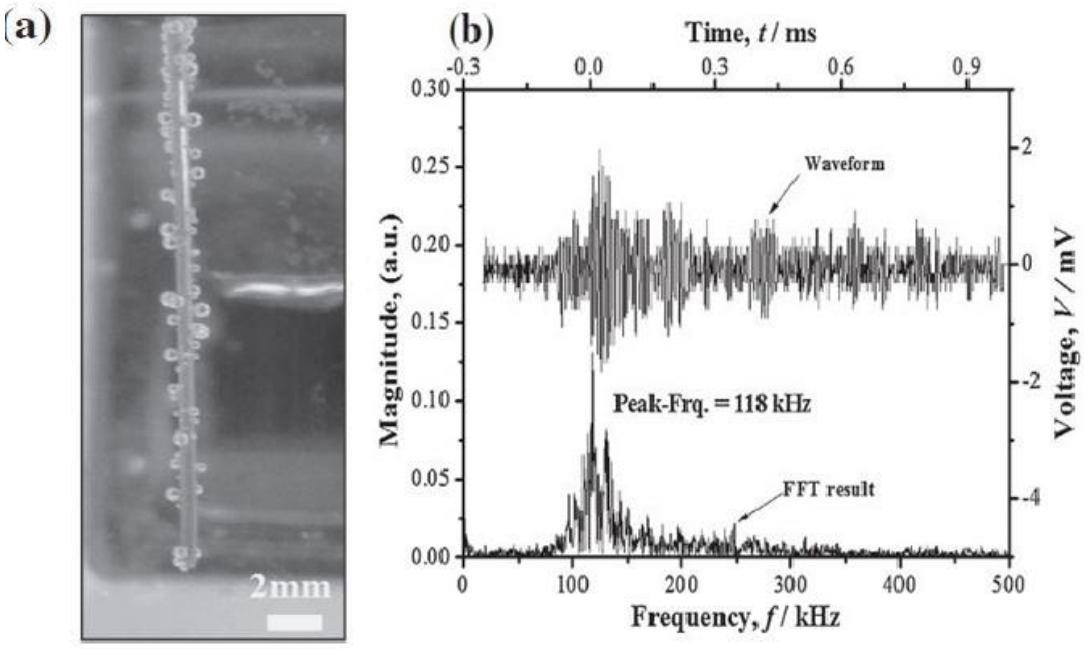

Figure 2. 15: (a)The morphology of bubbles generated during AE stage II breaking up as a series of "single bubble", (b) the typical AE waveform of AE stage II and its corresponding FFT result *[18]*

Patil et al. [19] proposed an acoustic emission based technique for evaluation of accelerated corrosion testing. Due to slow process of natural corrosion, proposed technique uses the accelerated corrosion testing in steel reinforced concrete (RC) structures. Experimentation involved the specimen to be submerged into 5% NaCl solution and then drying it in ambient conditions for 255 days. For AE activity monitoring, Acoustic sensor, pre-amplifier and AE data acquisition setup was used. Threshold level of 40 dB was determined and sampling rate of 1 million Samples per second (SPS) was set for AE data acquisition. Different AE parameters like signal strength were extracted and Cumulative signal strength have shown promising results for corrosion monitoring in accelerated corrosion testing.

Prateepasen et al. [20] also monitored the pitting corrosion using acoustic emission. Proposed technique used accelerated corrosion testing of 4×6×0.05 cm^3 SS-304 specimen, having ground surface with silicon carbide paper, rinsed with distilled water and dried in air. 3% NaCl was mixed in HCl electrolyte and a pH of 2 was maintained. AE data acquisition system involves PAC R15 acoustic sensor and 60 dB gain pre-amplifier and a LOCAN frequency spectrum analyzer and data acquisition system.

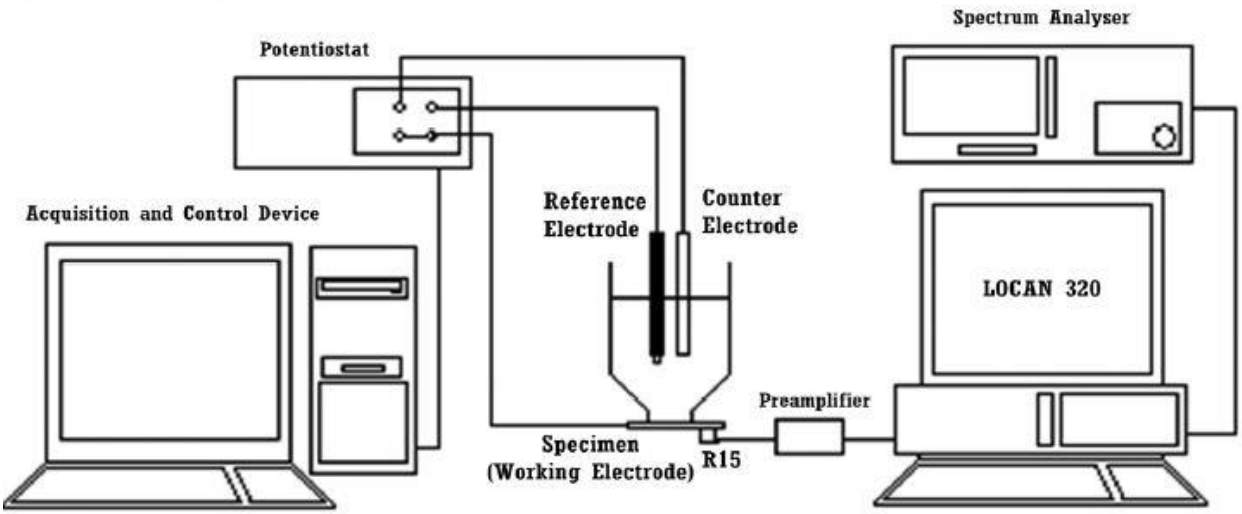

Figure 2. 16: Electrochemical corrosion setup with AE data acquisition system *[20]*

Constant potential was supplied for twenty hours and frequency and time domain data of acoustic emission was collected every ten minutes. Pit nucleation, metastable pit growth and stable pit growth are the three stages associated to pitting corrosion process. Different AE parameters were extracted. AE hit rate has shown important relationship with pit growth. Fig shows as hit rate goes on increasing, pit depth increases too.

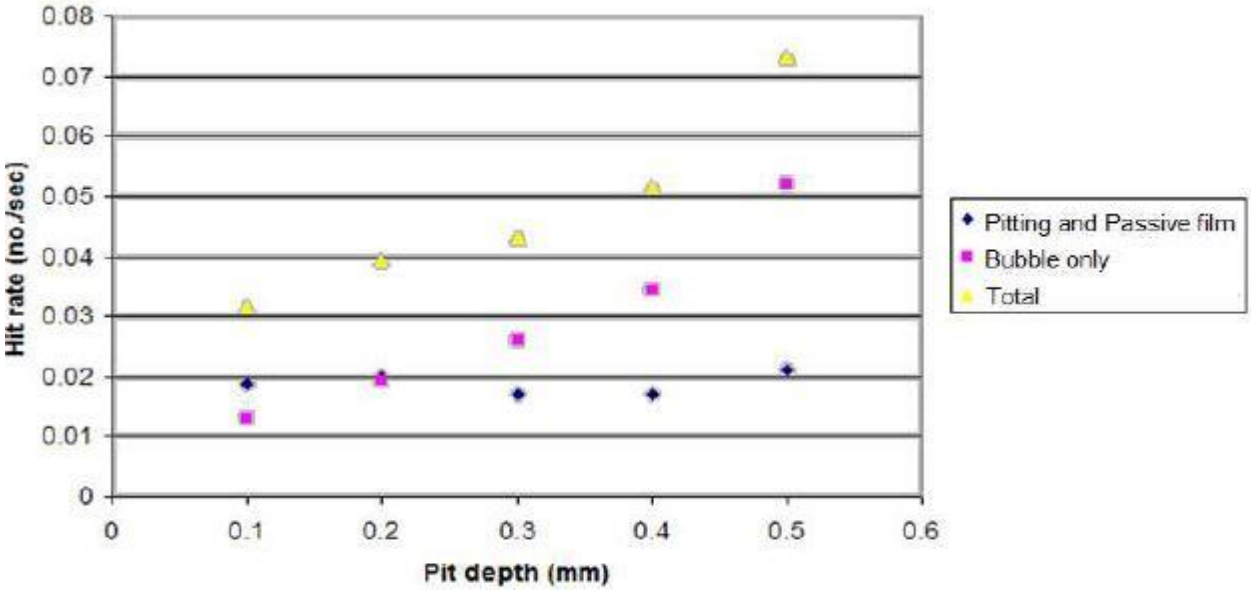

Figure 2. 17: Relationship of Pit depth and Hit rate (AE extracted parameter) *[20]*

Table 2. 1: Comparison of Non-Destructive Corrosion Monitoring Techniques

Corrosion Monitoring Technique	Advantages	Limitations
Visual Inspection	✓ Direct Method ✓ Inexpensive	▪ Labor Intensive ▪ Time Consuming ▪ Limited Access Issues ▪ Limited to surface inspection
Vision Based Inspection	✓ Reliable Monitoring ✓ Inexpensive	▪ Off-line Processing ▪ Computationally Expensive ▪ Limited Access Issues
Magnetic Flux Leakage	✓ Active type NDT ✓ Fast surface and sub-surface inspection ✓ Relatively Inexpensive	▪ Limited to ferromagnetic materials ▪ Alignment between magnetic flux and defects is necessary
Guided waves Based Inspection	✓ Active type NDT ✓ On-line Monitoring	▪ High frequency Ultrasonic waves are required ▪ Cross-talk issues ▪ Expensive
Radiographic Inspection	✓ Active type NDT ✓ Not limited by Material type ✓ Accurate and Reliable	▪ Safety Hazards ▪ Expensive ▪ Required Interpretation for Results
Acoustic Emission	✓ Passive type NDT ✓ On-line Monitoring ✓ Relatively Inexpensive	▪ Interpretation of AE is important

2.4. Machine Learning Techniques in Corrosion Monitoring

With advancements in the field of machine learning and artificial intelligence, focus is to produce hybrid technologies that have better accuracy and reliability. Neural networks serve as an important tool of machine learning which have the capability to handle complex systems that cannot be modeled. Machine learning techniques that have been blended with corrosion monitoring are in great focus now days. Artificial Neural Networks (ANN) applied to corrosion monitoring have been reviewed in the literature [21].

Saenkhum et al. [22] proposed the use of Artificial Neural Network (ANN) for classification of corrosion that was detected by acoustic emission. SS-304 specimen with size of 4×6×0.05 cm^3 was subjected to electrochemical corrosion in 3% NaCl and HCl solution having pH of 2. Proposed technique involves the extraction of statistical features like rise time, amplitude, count, and AE energy from recorded signals. The features that expressed a good correlation with corrosion were then used to train a feed forward neural network, aiming to classify the corrosion severity. Figure 2.19 shows the relationship of different AE levels with corrosion severity levels.

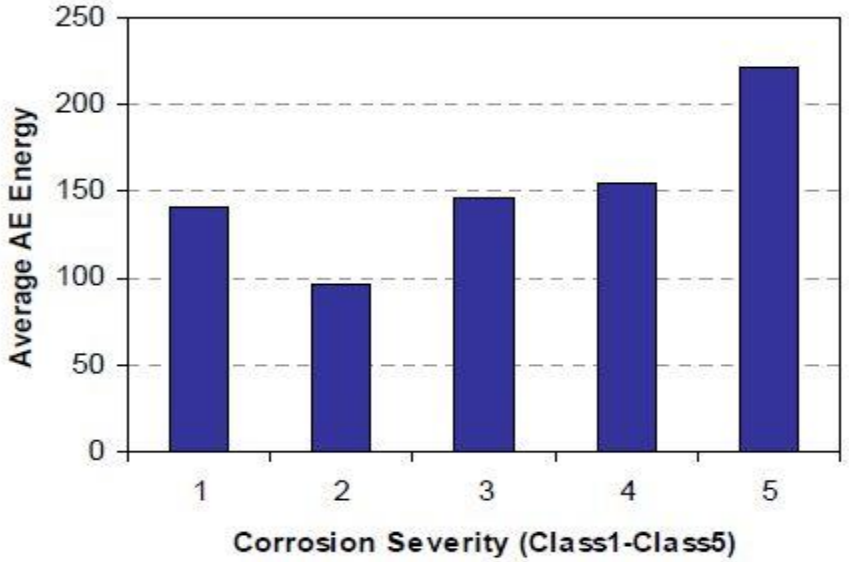

Figure 2. 18: Relationship of AE energy levels with corrosion severity levels *[22]*

Single layer feed forward neural network is used to classify corrosion severity levels. Four features AE energy, amplitude, rise time and count extracted from experiments are used as

inputs to neural network. Dataset is preprocessed using data scaling and adaptive moving average (AMA) techniques. One half of the original dataset is used as training, one fourth as testing and one fourth as validation dataset. Network architecture employs the use of 4 input neurons, 8 hidden layer neurons and 5 output neurons for corrosion severity levels. Tan-sigmoid activation function is used in hidden layer neurons and log-sigmoid activation function is used in output neurons. Levenberg-Marquardt algorithm was used for optimizing the training of the network. Figure 2.20 shows confusion matrix in for the training and testing phase of neural network, which indicates very less misclassification rate and a very good generalization capability. Confusion matrix reveals the training accuracy to be 96.41 % and testing accuracy to be 94.35 %.

Desire / Actual	Class1	Class2	Class3	Class4	Class5
Class 1	100	0	0	0	0
Class 2	1.34	97.66	0	0	0
Class 3	0	0.07	98.51	0.71	0
Class 4	0	0	0.13	98.03	0.26
Class 5	0	0	0	8.87	87.86
Classification rate (Train) = 96.41%					

Desire / Actual	Class1	Class2	Class3	Class4	Class5
Class 1	96.40	1.80	0	0	0
Class 2	3.33	95.33	0	0	0
Class 3	0	0	97.59	1.21	0
Class 4	0	0	0.07	96.59	0.20
Class 5	0	0	0	10.49	85.83
Classification rate (Test) = 94.35%					

Figure 2. 19: Confusion matrix for training and testing datasets of Neural Network *[22]*

Hendi et al. [23] proposed the use of artificial neural networks (ANN) for concrete corrosion monitoring in sewage systems against the attack of Sulphuric acid. Proposed technique uses ANN to learn from past and predict an output based on the value of input. Distinct experimentation features were used as inputs and back propagation neural network (BP-NN) is trained to predict the metal loss based on the learning that used sigmoidal activation function in its hidden layer neurons. 60% of the whole dataset is used for training and 40% is used for

testing and validation purposes. Network used 9 input neurons with two hidden layers having 8and 6 neurons respectively and one output neuron used for prediction. Mass loss and volume loss both were predicted with same inputs and same network architecture. Network Mean squared error (MSE) for mass loss and volume loss are found to be 0.44 and 1.18 respectively.

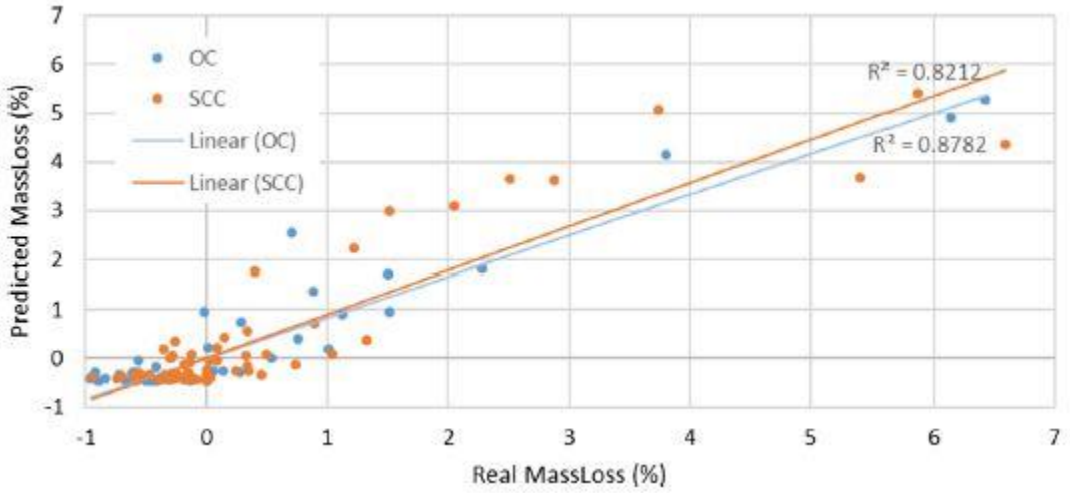

Figure 2. 20: Comparison of real mass loss vs predicted mass loss by ANN *[23]*

De Masi et al. [24] made the corrosion assessment in subsea pipelines using machine learning based approach. Proposed technique uses data driven machine learning model for internal corrosion assessment that poses great threats to integrity of pipelines. Geometrical pipeline characteristics and fluid dynamics multiphase variables were used as input features to the neural network. Fitting neural network (FNN) based regression approach was used to predict the corrosion rate, metal loss, area of defects and number of defects. Non-linear input-output relationship is fitted by feed forward fitting network with two or more hidden layers. Figure 2.21 shows that the architecture of proposed fitting neural network, that contains 14 input neurons, 20 hidden layer neurons and a single output neuron. Corrosion rate, Metal loss, Number of defects and Area of defects were predicted using single output neuron. Network is trained using Levenberg-Marquardt back propagation algorithm was used to minimize the error function by weight and bias updation.

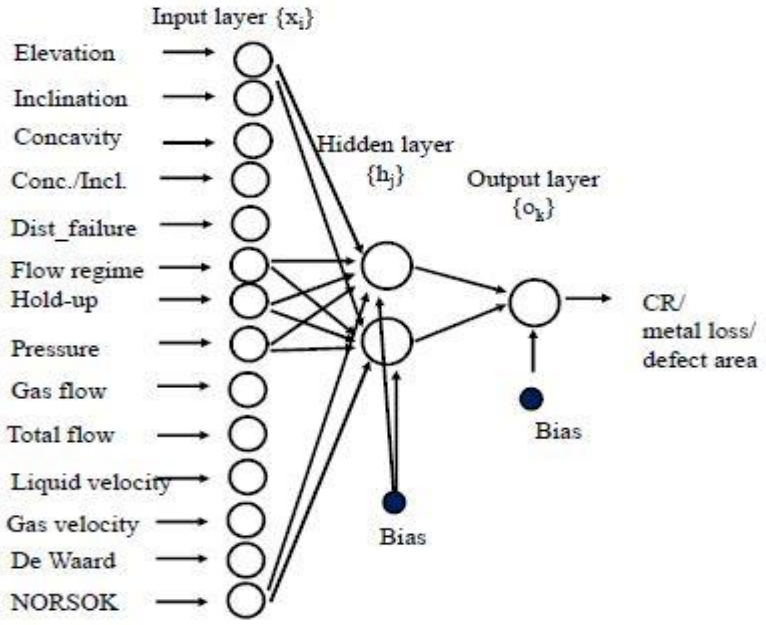

Figure 2. 21: Architecture of proposed Fitting Neural Network *[24]*

Figure 2.22 shows comparison of actual target values and predicted values produced by Fitting Neural Network for volume loss prediction.

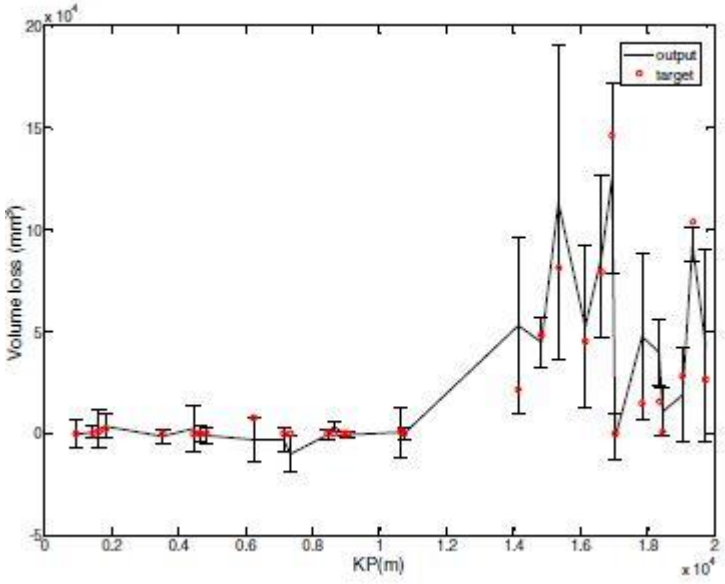

Figure 2. 22: Comparison of target vs output of FNN for Volume Loss prediction *[24]*

Liao et al. [25] used hybrid machine learning algorithms for numerical corrosion rate prediction in internal corrosion assessment of gas pipelines. Basic corrosion inspection data was gathered from seven pipelines in Sichuan China and was arranged into 116 groups. Metal

material and metal surface state, the fluid nature, and pipeline operating parameters were main groups from which of main corrosion influencing parameters were identified and used for numerical corrosion rate prediction. Back Propagation Neural Network (BPNN) and hybrid neural network approaches like Genetic Algorithm (GA) and BPNN, Particle Swarm Optimization (PSO) and BPNN are used as numerical prediction model. GA and PSO in these hybrid approaches are used as optimization methods for weights and biases. Internal corrosion influencing parameters were then processed using grey rational analysis which ranked the parameters based on correlation degree. Dataset is divided into training and testing dataset. 95 groups of data out of 116 are divided into training dataset and 21 are divided into testing dataset. Figure 2.23 shows the architecture of the proposed network.

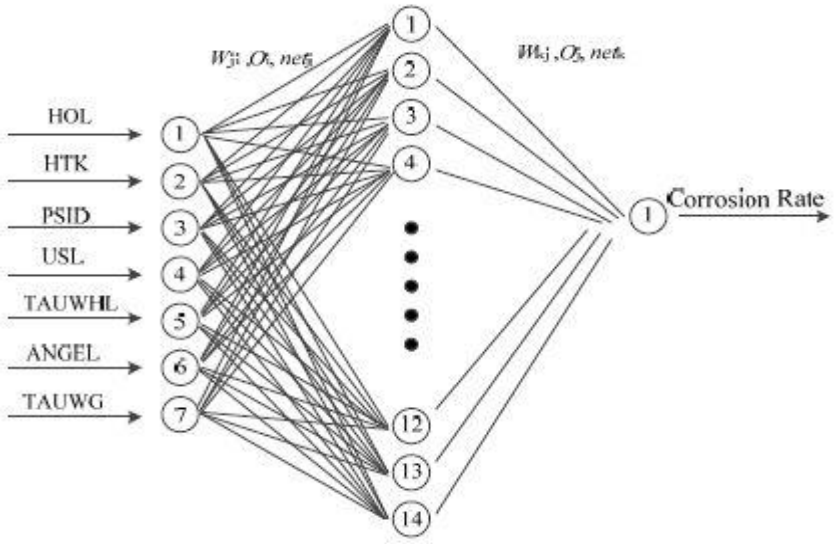

Figure 2. 23: Architecture of proposed ANN *[25]*

Liquid holdup, heat transfer coefficient of inner wall, deposition rate, superficial velocity total liquid film, liquid maximum wall shear stress, pipe angle and as maximum wall shear force are chosen as input parameters of network based on grey rational analysis. Network contain 7 input neurons, 14 hidden layer neurons and a single output neuron for corrosion rate prediction. ANNs are trained to minimize the Mean Squared Error (MSE). Inspected corrosion rates are compared with the predicted corrosion rates produced by BP, genetic algorithm optimized BPNN and particle swarm optimized BPNN in figure 2.24. GA optimized BPNN showed the best corrosion prediction rate than other two techniques based on its least absolute error.

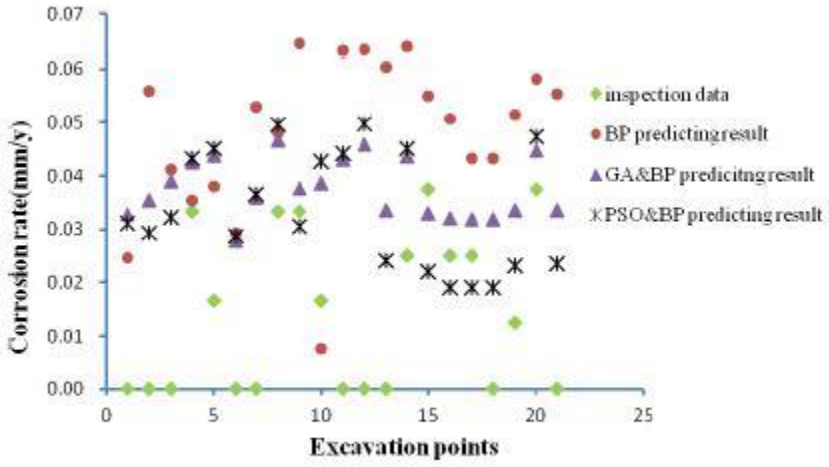

Figure 2. 24: Corrosion rate prediction comparison between inspection, BP, GA&BP and PSO&BP *[25]*

Jian et al. [26] proposed the use of machine learning methods for determining corrosion types. Proposed technique uses data gathered through Electrochemical Noise (EN) measurement and then machine learning techniques for accurate corrosion type determination. EN is the fluctuations of potential and current generated during spontaneous corrosion process. Experimentation involves the exposure of SS-304 sample for 72 hours in three electrodes set up to generate pitting, uniform and passivation corrosion. Raw EN data is then processed to extract feature vectors that includes 10 useful parameters including energy of 7-level wavelet crystal. Feature vectors are then processed through data normalization in the range of 0-1 to minimize gap between features. Figure 2.25 represents the flow chart of the proposed technique.

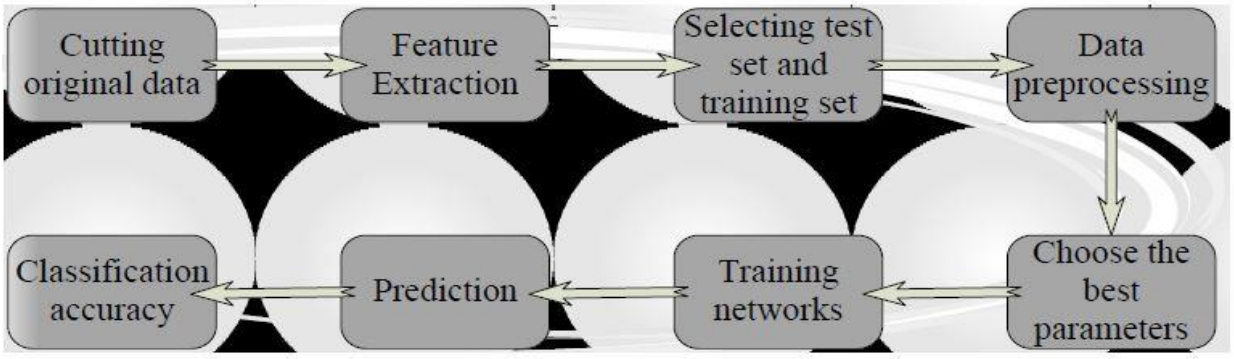

Figure 2. 25: Flow chart for the development of ANN corrosion classification *[26]*

Data set comprises of 100 feature vectors that are randomly selected representing the EN data for corrosion. 80% of Dataset is divided into training and 20% is divided into testing dataset. Back Propagation Neural Network (BPNN) and Support Vector Machines (SVM) are used as classifiers. BPNN is used as pattern recognition tool trained with 10 input neurons, 9 hidden layer neurons and two output neurons to minimize the Mean Squared Error (MSE). Network best training performance is achieved in 26 iterations of training with an MSE reduced to 2.1381×10^{-6}. Accuracy of the network is shown in terms of confusion matrix which shows the overall accuracy of the network as well as the individual accuracy of each class of corrosion predicted by BPNN. Figure 2.27 shows the confusion matrix of BPNN against training, testing and validation data. Confusion matrix reveals the classification accuracy of BPNN to be 99.7 %. SVM uses kernel based learning functions to solve classification and regression problems with better accuracy. Figure2.28 Shows the architecture of SVM with kernels in the middle layer. SVM combines kernels like linear, polynomial, radial basis and sigmoid with optimization algorithms like GA and PSO. Proposed SVM model uses cross validation technique to find best parameters for training. After completion of training, network is tested to predict corrosion type using testing dataset. Figure 2.26 shows the comparison of actual versus predicted corrosion type by SVM. Actual type is represented by 'o' and predicted type by '*'. Classification accuracy of SVM comes out to be 100 %. SVM has shown better classification performance than BPNN in the presented scenario.

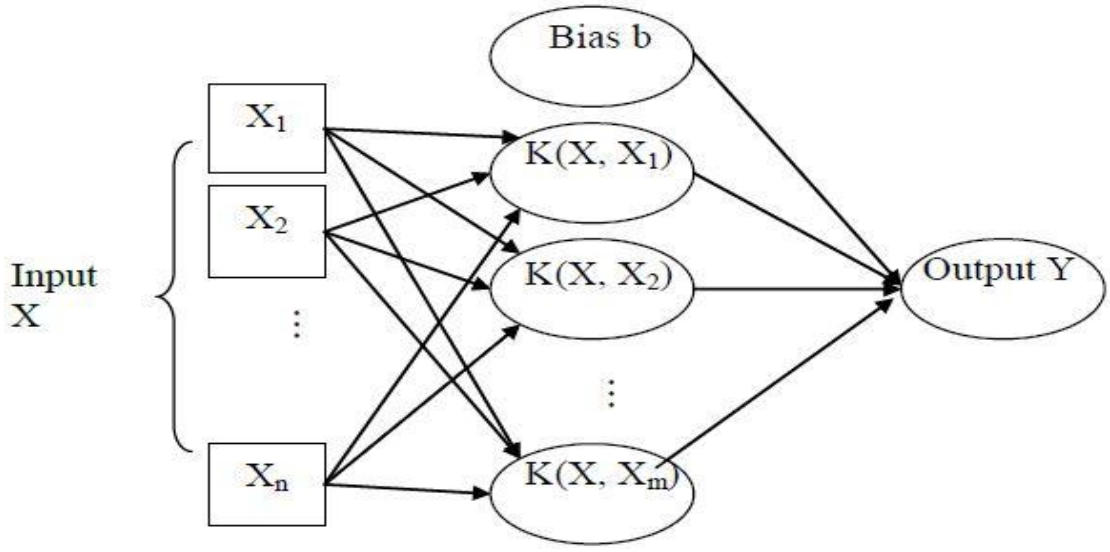

Figure 2. 26: Generalized architecture of SVM *[26]*

Figure 2. 27: Confusion matrix for the proposed BPNN Classifier model *[26]*

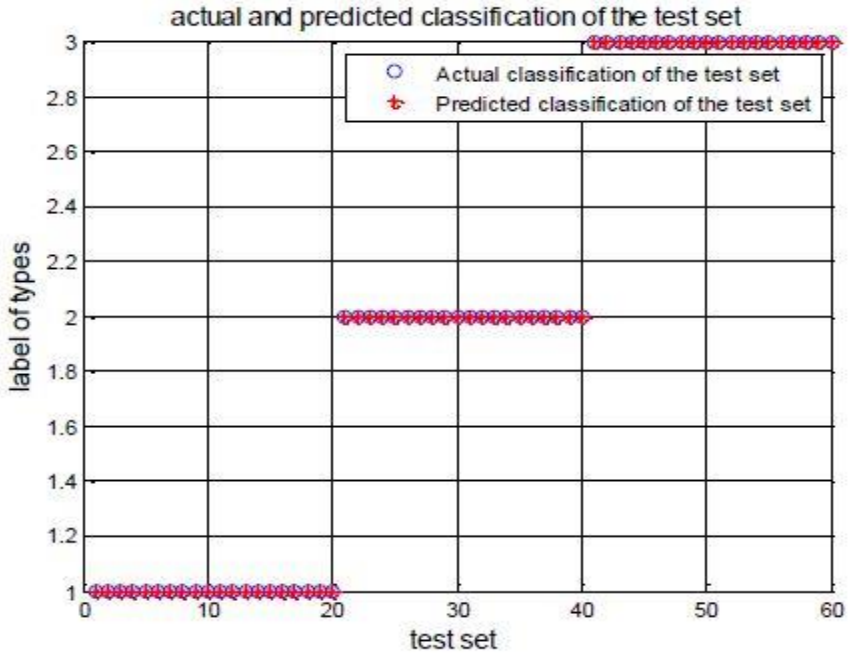

Figure 2. 28: Comparison of actual and predicted corrosion type on testing dataset (SVM Classifier) *[26]*

2.5. Thesis Aims and Objectives

The scope of the research is quite broad, however, according to level of research and based on the literature review, the thesis aims and objectives can be defined as follows

I. To develop a novel technique to detect and classify corrosion using acoustic emission and machine learning based approach.

II. To study state of the art techniques in corrosion monitoring.

III. To develop a user-friendly interface to classify acoustic corrosion data.

2.6. Summary

The chapter can be summarized as follows:

- Corrosion has many types, mainly depending upon the type of loss that occurs on metal and the reaction that happened with the environment. Understanding the type of corrosion can help researchers to find the remedy to prevent and monitor corrosion. Different types of corrosion found in literature are uniform corrosion, pitting corrosion, crevice corrosion, stress corrosion cracking, galvanic corrosion, intergranular corrosion and erosion corrosion etc.

- Main goal of corrosion inspection and detection techniques are to inspect for corrosion without dismantling the structure. Vision based methods, Eddy current, Magnetic flux leakage, Guided waves and Acoustic emission are NDT techniques that may be used for corrosion detection. However: each technique has its own advantages and limitations. Acoustic Emission being a passive NDT technique is a low-cost and effective corrosion Monitoring technique.

- Different AE schemes for defect detection have been reviewed from the literature. Acoustic emission data acquisition for the accelerated corrosion testing has been reviewed. Classification of AE data for better accuracy and reliability is taken as a major issue in implementation of acoustic emission as corrosion monitoring technique in industrial environments.

- Different Machine Learning based classifiers used in corrosion monitoring have been reviewed from literature. Different classification and regression based models have been employed for corrosion monitoring applications.

3. TOOLS AND TECHNIQUES

This chapter explains the techniques used to fulfill the scopes of thesis as well as the background theory related to them. The Chapter is divided into two main sections; explaining the acoustic emission and different paradigms of machine learning based classifiers for classification of corrosion signal.

3.1. Acoustic Emission

Acoustic Emission (AE) is the rapid release of transient elastic waves due to sudden redistribution of stress in the material. AE has become an important NDT technique for evaluation and monitoring of structures and materials. J. Kaiser introduced AE in 1950s [27]. AE relies on listening the energy initiated within the component. Frequencies of AE released during mechanically loaded structures are usually above the audible range. Common examples of the processes that involve acoustics are, crack growth due to hydrogen embrittlement, stress corrosion cracking, fatigue, creep etc. AE falls into the category of non-destructive testing techniques because it does not affect the serviceability of the part subjected to test and it can be used as an online structural integrity inspection technique. However, AE is different from the other NDT techniques because AE just listens to the release of energy within the component hence, making AE a passive NDT technique. Active NDT uses external source of energy for creating some effect in the component. Radiographic and Ultrasonic are common examples of Active NDT techniques.

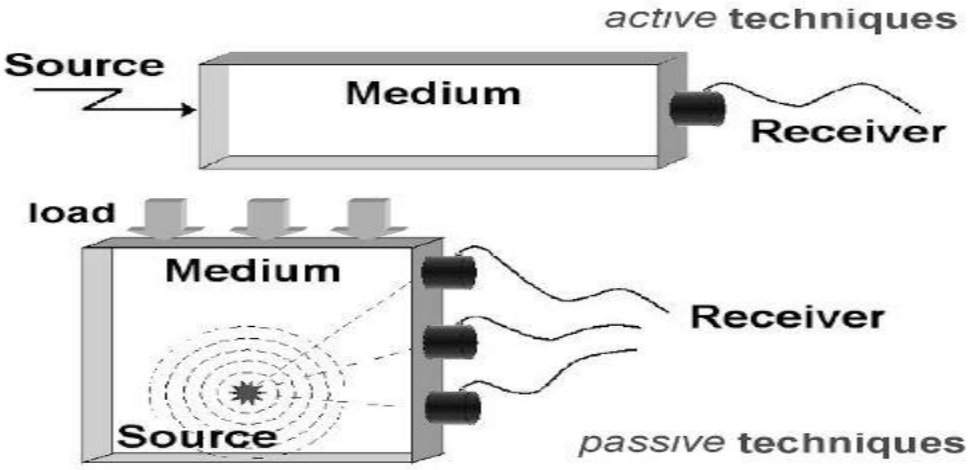

Figure 3. 1: Comparison of Active and Passive NDT techniques *[28]*

3.1.1. AE Principle

Component subjected to stress or mechanical loading release energy due to discontinuities. Stress acts on body and produce local plastic deformation in the material that lead to breakdown of material at specific regions. This breakdown is the source of energy that travels outside of a material. Released energy travel in the form of high frequency stress waves. These waves are received by acoustic sensors and transducers that convert stress waves to voltage. Signal conditioning circuits amplify that voltage for AE data acquisition. AE data is further processed for analysis and interpretation. Stress and structural loading are the main sources of AE activity.

3.1.2. AE Sensors

Acoustic sources emit acoustic energy at different frequency ranges instead of a single frequency band. Acoustic sensors are mainly of two types namely broadband sensor and narrow-band sensor depending upon the source emitted frequency. Broadband sensors are normally used when the requirement is the detection of a wide range of frequencies. Narrow-band sensors are normally preferred, dealing with a specific range of frequency. Narrow-band sensors are normally preferred in practical AE data acquisition systems due to their better performance against noise problems. Resonant sensors are more sensitive and less expensive than broadband type sensors. Resonant sensors operate in a defined operating frequency range which helps in optimizing their performance against attenuation and noise.

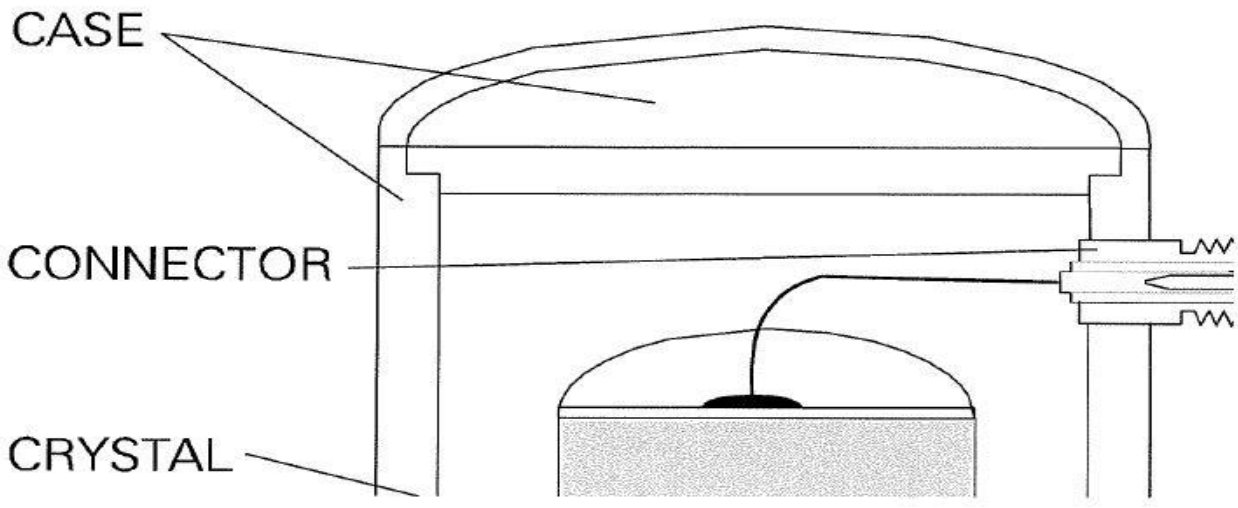

Figure 3. 2: Schematic diagram of AE sensor *[27]*

AE sensors uses piezoelectric crystals for AE wave sensing. Piezoelectric materials generate electric voltage when they were deformed subjected to stress waves. Incoming stress waves from AE sources produce elastic deformation in the piezoelectric crystal that converts it into electric voltage [28].

AE sensor sensitivity is defined as the ratio of the output voltage and input motion. If sensor produce output voltage proportional to the input motion its response is said to be linear. Sensitivity of AE sensor mainly depends upon the frequency of motion and highest sensitivity of the element is achieved at resonant frequency. Sensor calibration curves shows how sensor sensitivity varies with frequency. Sensitivity of sensor does not only depend upon the frequency but also on the direction of motion because AE sensors unlike accelerometers respond to motion in any direction. AE sensors come with calibration certificates that have sensitivity in terms of decibels.

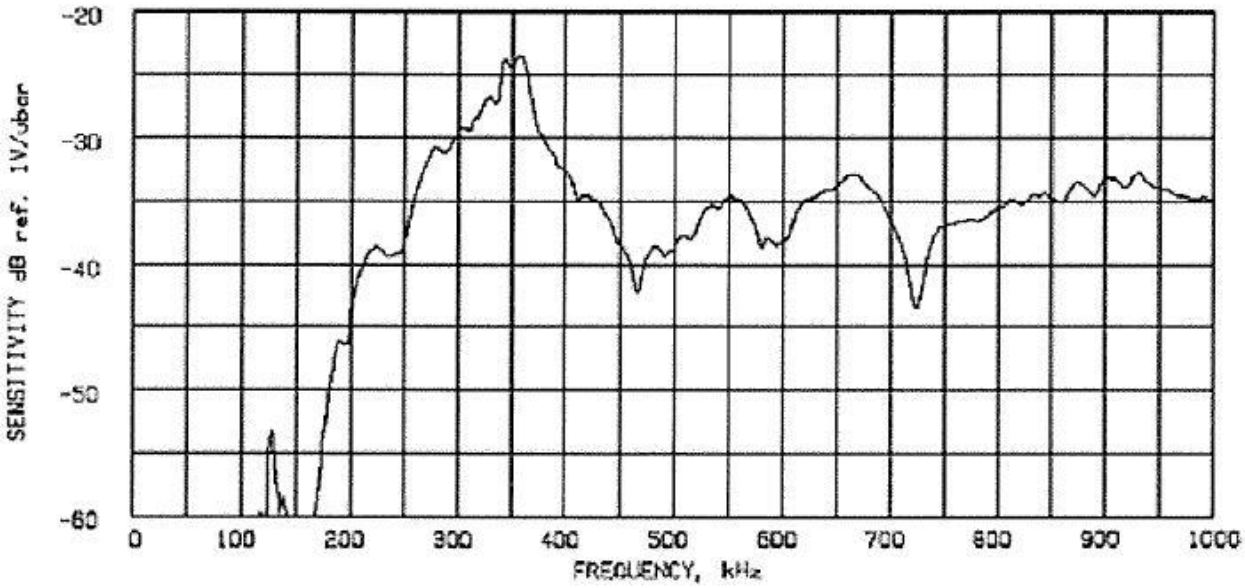

Figure 3. 3: Typical AE sensor calibration curve *[27]*

3.1.3 AE Signal and Wave Prorogation

AE signals can be characterized into two categories mainly depending upon the type of source namely continuous and burst signal. Burst signals are produced due to the spontaneous release of energy due to cracking and other material deformation process. Continuous AE signals are released by the sources that continuously emits energy.

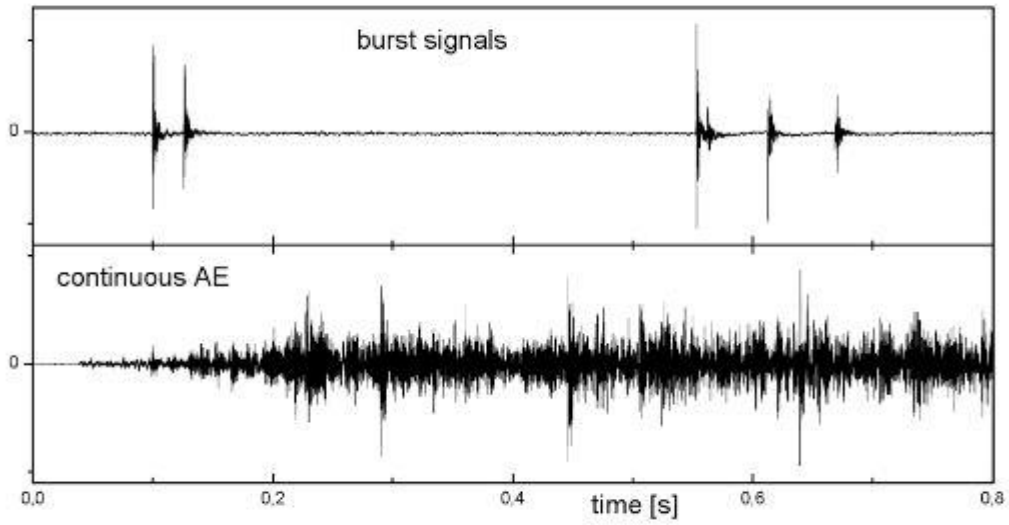

Figure 3. 4: Comparison of burst vs continuous AE signal *[28]*

AE signal has a chain of controlling links that influence the size and shape of the measured signal. The signal produced by the acoustic source is very much different from the signal that is acquired at the final stage. The AE signal chain has four links namely the source, the wave propagation, the sensor and the signal-conditioning circuit. Signal-conditioning circuits involve the use of amplifiers to amplify the low amplitude signals, and usage of filters for acquiring the right frequency band of signal to get rid of noise.

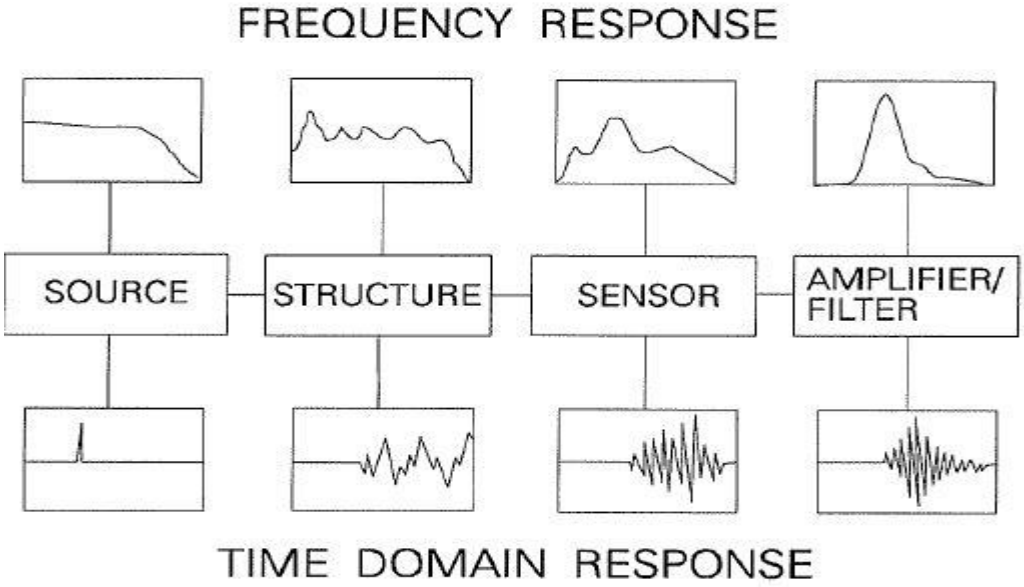

Figure 3. 5: Signal shaping chain *[27]*

AE wave propagation involves two major problems namely signal attenuation and wave velocity. Attenuation means the decay of signal amplitude as acoustic signal travels outside the source. Effect of attenuation is due to several factors namely geometric spreading, scattering at structural boundaries, and absorption. Geometric spreading means that the sound wave tries to spread to the whole volume of structure. Scattering depicts the reflection of acoustic waves at structural discontinues that tends to decrease signal amplitude. Absorption refers to the phenomenon in which kinetic and elastic energies in the acoustic wave are absorbed in the material from which they are passing through. Absorption is greater at higher frequencies due to their shorter wavelengths.

For better AE data acquisition, sensor must be in good contact with the structure, so it can detect AE wave and deliver a strong signal. Sensor mounting techniques play a vital role in accurate measurement. Sensor is mounted at clean and smooth surface with sensor face having liquid or adhesive that will act as acoustic couplant [27].

3.2. Machine Learning Based Classifiers

Classifier is a function f that maps input feature vectors $x \in X$ to output class labels y $\in${1, . . . ,C}, where X is the feature space [29]. Machine learning involves programming of computers to optimize a problem by learning from the past experiences and data. Learning can be classified into two categories, supervised and supervised learning. If the classes of the data are known then the obvious choice is supervised learning in which we provide a teaching signal to classifier to learn. Unsupervised learning is used where class labels are unknown and algorithm clusters the data by using the patterns within data.

3.2.1. Back Propagation Neural Network

Different neural network based classifiers have been proposed in the literature for classification of corrosion and for corrosion severity prediction using acoustic emission signal. Techniques involve mainly the use of back-propagation neural network (BP-NN) as a supervised learning technique for classification purpose.

Artificial Neural Networks (ANN) are biologically inspired computational models that mimics biological brain in their working. ANN consists of simple information processing units that are called as neurons. These interconnected neurons process information to solve a certain problem based on input it receives. Like biological neurons, artificially generated neurons have adjustable gains that influence on the output of the network. Information from system is fed into the network as input pattern. Then input is then amplified using adjustable weights of neurons which are further processed using activation functions to form an output. These adjustable weights attached with neurons slowly adjust to produce the output patterns based on input patterns presented to the network. Adjustment of weights is called the training phase of the network. After training, network is tested against the new input patterns which is called as the recall phase of the network.

Back-propagation neural network is a feed forward neural network that generally consists of three layers; an input layer, hidden layer and output layer respectively. Architecture of the feed forward neural network is shown in the figure 3.6.

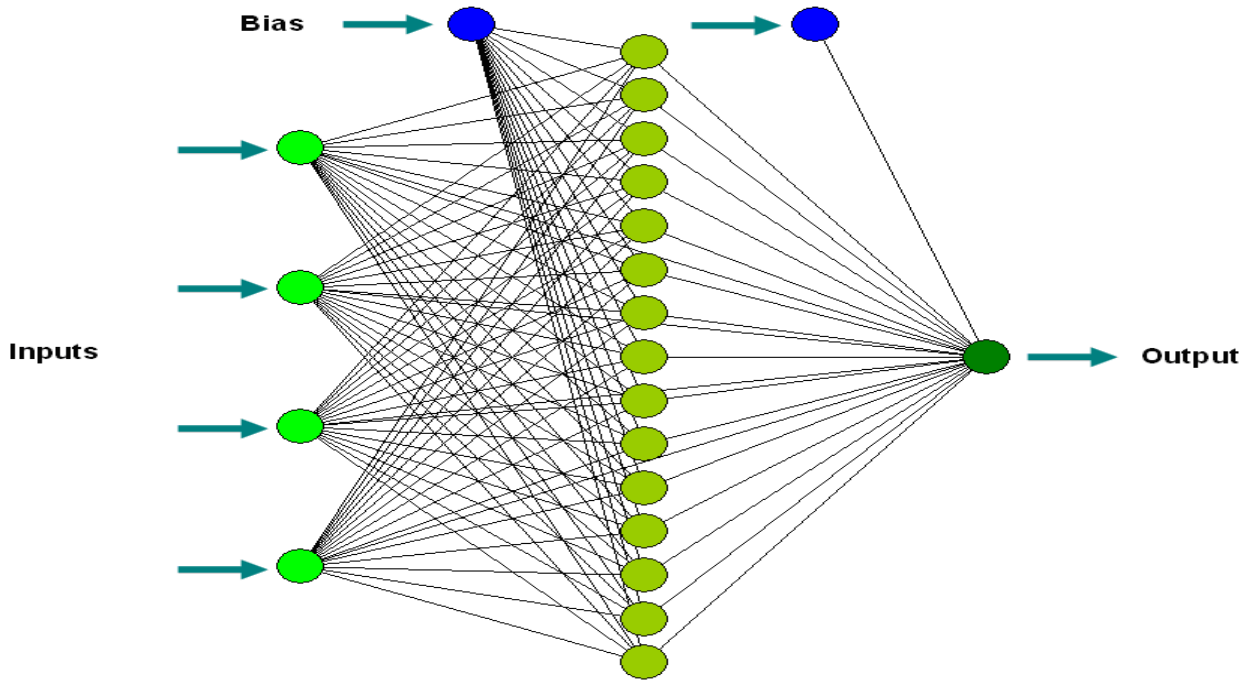

Figure 3. 6: Structure of a Feed Forward Neural Network *[30]*

Number of input neurons of the network is equal to the number of features of the data. Number of output neurons depends upon the output classes. Number of hidden layer neurons can be varied against the network optimum performance. Back propagation neural network is a multi-layer feed forward network is trained with gradient descent method commonly known as back propagation. The input layer is connected to hidden layer and hidden layer is fully interconnected to output layer. All these interconnections have weights that amplify the input and hidden layer neurons have activation function. Threshold, sigmoidal, tan-sigmoidal are commonly used activation functions. Back propagation training algorithm involves four basic steps [31].

- Weights initialization
- Feed forward operation
- Back propagation of errors
- Updation of weights and biases

During the feed forward stage network is initialized with small random values of weights and then these weights are used to form an output. Network output is compared with the desired output and an error signal is generated. That error signal is then fed back into the network layers and weights and biases are updated against that back propagation of error.

Input layer, hidden layer and output layer of the network are denoted as **i**, **j** and **k** respectively. X is the input training vector where X= [x_1, x_2…… x_n] and T is the desired target vector where T= [t_1, t_2……t_n]. Input layer **i** is connected to the hidden layer **j** through V_{ij}. Hidden layer j and output layer are connected through weights W_{jk}. After Initialization of small random value to the weights V_{ij} and W_{jk}, each input unit receives the input signal x_i and transmits it to all units in hidden layer. Sum y at each hidden unit is calculated using following equation.

$$y_{in} = \sum V_{ji} x_i + b \tag{3.1}$$

Where b is bias, and it is the weight whose activation function is always one. At each hidden unit, an activation function is applied from following equation and the resulting signal is sent to the output layer.

$$f(y) = \frac{1}{1+e^{-y}} \tag{3.2}$$

$$z_j = f(y_{in}) \tag{3.3}$$

Signal then gets multiplied with the weights of hidden and output layer W_{jk} using following equation.

$$y_{ink} = \sum W_{ji} z_{j_i} + b \tag{3.4}$$

$$Y_k = f(y_{ink}) \tag{3.5}$$

Once each output unit receives output pattern based on the input pattern, error term is generated using the following equation.

$$\delta_k = (t_k - y_k) f(y_{ink}) \tag{3.6}$$

$\boldsymbol{\delta}_k$ is the error term at output unit that is fed to the hidden layer where further error is calculated using the same way and then weights and biases are updated.

$$W_{jk}(new) = W_{jk}(old) + \nabla W_{jk} \tag{3.7}$$

∇W_{jk} is the change that is produced in the weight when error is fed back into the network layers.

$$\nabla W_{jk} = \alpha \delta_k z_j \tag{3.8}$$

Where α is learning rate, whose value lies with in [0-1] range. Equation 3.8 also represents the generalized delta rule which is the base of back propagation algorithm.

3.2.2. Radial Basis Function Neural Network

Radial basis function neural network is a multilayer feed forward neural network having input layer, hidden layer and output layer. Main difference between Radial basis function neural network and back propagation neural network is that radial basis uses gaussian potential function as its activation function [31]. Functions of the form of following equations are considered as radial basis functions.

$$\delta(r) = r \tag{3.9}$$

$$\delta(r) = r^2 \tag{3.10}$$

$$\delta(r) = r^3 \tag{3.11}$$

$$\delta(r) = \exp(-r^2) \tag{3.12}$$

Input layer contains “m” number of neurons and output layer contains “n” number of neurons depending upon the features of the dataset and number of output classes respectively and hidden layer lies between the input layer and the output layer. The hypothetical connections exist between the first two layers which are input layer and the hidden layer, whereas weighted connection exists between the hidden layer and the output layer. Architecture of radial basis function neural network is shown in the figure 3.7.

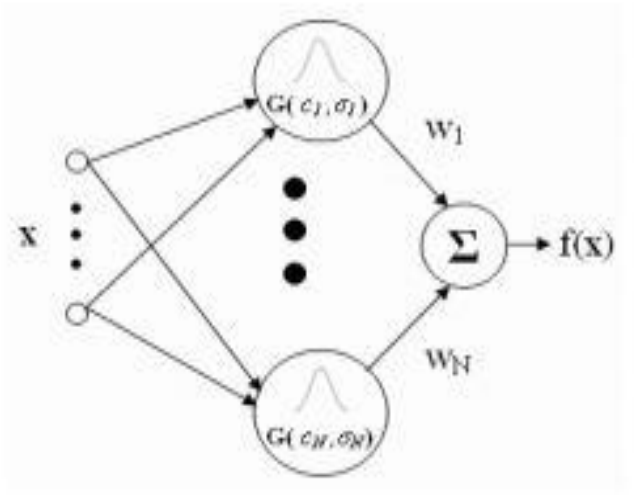

Figure 3. 7: Multilayer Feed Forward Radial Basis Function Neural Network with N hidden neurons *[32]*

Classification can be easily performed by utilizing radial basis function neural network, moreover, this network can also be utilized for approximating functions by using Gaussian potential functions [32]. Training Algorithm of radial basis function neural network [31] is given below. Gaussian activation function is used by the radial basis function [33]. Non-negative response is given by such function for all the values of r. The same function as of equation is used.

$$G(x) = \exp(-x^2) \tag{3.13}$$

Derivative of the function is calculated as

$$G'(x) = -2xexp(-x^2) \tag{3.14}$$

$$G'(x) = -2xG(x) \tag{3.15}$$

Step 1: small random values of weights are initialized.

Step 2: Perform steps 3-10 if the stopping condition is not true.

Step 3: Perform steps 4-9 for each input.

Step 4: Input signals are received by each input unit $(y_i\ , i\ =\ 1, \ldots\ldots, n)$

Step 5: Radial basis function is calculated.

Step 6: The set of input vectors are utilized for choosing the Radial basis functions centers. For guaranteed adequate sampling of the input vector space sufficient numbers of centers must be designated.

Step 7: The output of i_m unit $G_i\ (\ x_i)$ in the hidden layer

$$G_i(x_i)\ =\ exp\ (-\sum_{j=1}^{r}[x_{ji}\ -\ \hat{x_{ji}}]^2\ /\ \mu_2^1\ ) \tag{3.16}$$

Whereas $x_{ji}\ =$ Centre of the RBF unit for input variables, μ_i = Width of the i^{th} RBF unit, $x_{ji}\ =\ j_{th}$ variable of input pattern.

Step 8: Weights in the output layer are initialized by assigning small random small values.

Step 9: Neural network output is calculated

$$H_{net}\ =\ \sum_{i=1}^{N} w_{im}\ G_i\ (x_i)\ +\ Z_o \tag{3.17}$$

Whereas

N= number of hidden layer nodes, H_{net} = Output value of m_{th} node in output layer for the n_{th} incoming pattern. w_{im} = Weight between m_{th} output node and i_{th} radial basis function unit. Z_o = Biasing term at n_{th} output node.

Step 10: Error is calculated and stopping condition is tested. Changing of weights and number of iterations can be the stopping condition.

3.2.3. Naive Bayes classifier

Naive bayes classifier is the statistical classifier that uses the bayes theorem probability theory as its base. Naive bayes classifier is different from conventional classifiers because it involves calculation of posterior probability of classes hence reducing its computational complexity and does not involve any training unlike neural network-based classifiers. They can predict class membership probabilities, such as the probability that a given sample belongs to a specific class [31]. Bayes theorem of probability involves the calculation of conditional probabilities. Conditional probability is the probability of an event that have influence on another event. Bayes theorem make use prior probability that is the original probability of a hypothesis or event without any additional information. Prior probabilities are used to find posterior probabilities which are the revised probabilities of an event after getting additional information about the event [34-35].

Bayes Theorem can be explained using following equations.

$$P(X \mid Y) = \frac{\boldsymbol{P}(\boldsymbol{Y}|\boldsymbol{X})\boldsymbol{P}(\boldsymbol{X})}{\boldsymbol{P}(\boldsymbol{Y})} \tag{3.18}$$

$$P(X \mid Y) = \frac{\boldsymbol{P}(\boldsymbol{Y}|\boldsymbol{X})\boldsymbol{P}(\boldsymbol{X})}{\boldsymbol{P}(Y|X)\times\boldsymbol{P}(\boldsymbol{X})+\boldsymbol{P}(Y|-X)\times\boldsymbol{P}(-\boldsymbol{X})} \tag{3.19}$$

$P(X)$ is the probability of X, $P(Y)$ is the probability of Y without having knowledge about event X, $P(X \mid Y)$ is the posterior probability of X given Y and $P(Y \mid X)$ is the posterior probability of Y given X. $P(-X)$ is the probability of X being false and $P(Y \mid -X)$ is the probability of Y given X is false. The Naive Bayes Classifier assumes that the effect of each feature on a class is statistically independent of all other features. This assumption of statistical independence between different features of a class is called class conditional independence and is made to simplify computation. Naive Bayes classifier works best in two cases: when the features are completely independent and secondly when the features are functionally dependent. The worst performance is seen in between these two extremes. The popularity of naive bayes classifier has increased and is being adopted by many because of its simplicity, computational efficiency, and its good performances for real-world problems.

3.3. Proposed Technique

Proposed technique makes use of accelerated corrosion testing of mild steel samples to acquire acoustic emission data of corrosion process. Acquired acoustic signals are processed to extract distinct features of acoustic data. These distinct features are used by different machine learning algorithms to classify corrosion and no corrosion state and corrosion severity level classification. Figure 3.8 represents the flow chart of the proposed technique.

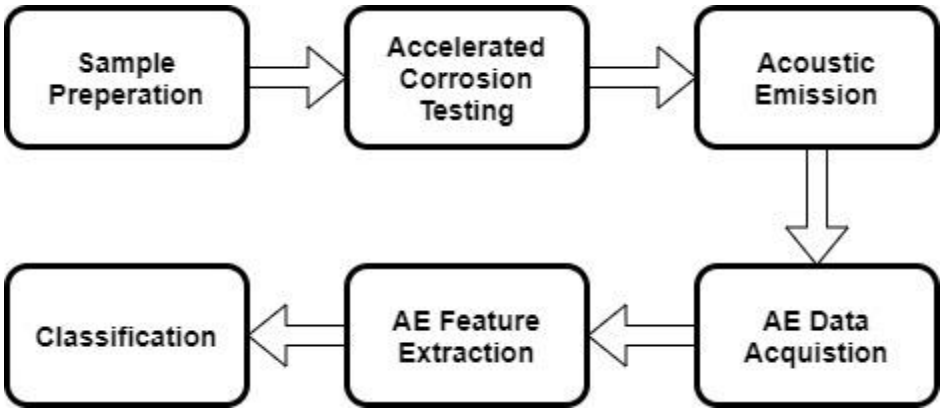

Figure 3. 8: Flow chart of proposed technique

For classification purpose, proposed technique presents a comparative study after implementation of different classifiers namely Back Propagation Neural Network (BPNN), Radial Basis Function Neural Network (RBF-NN) and Naive Bayes Classifier.

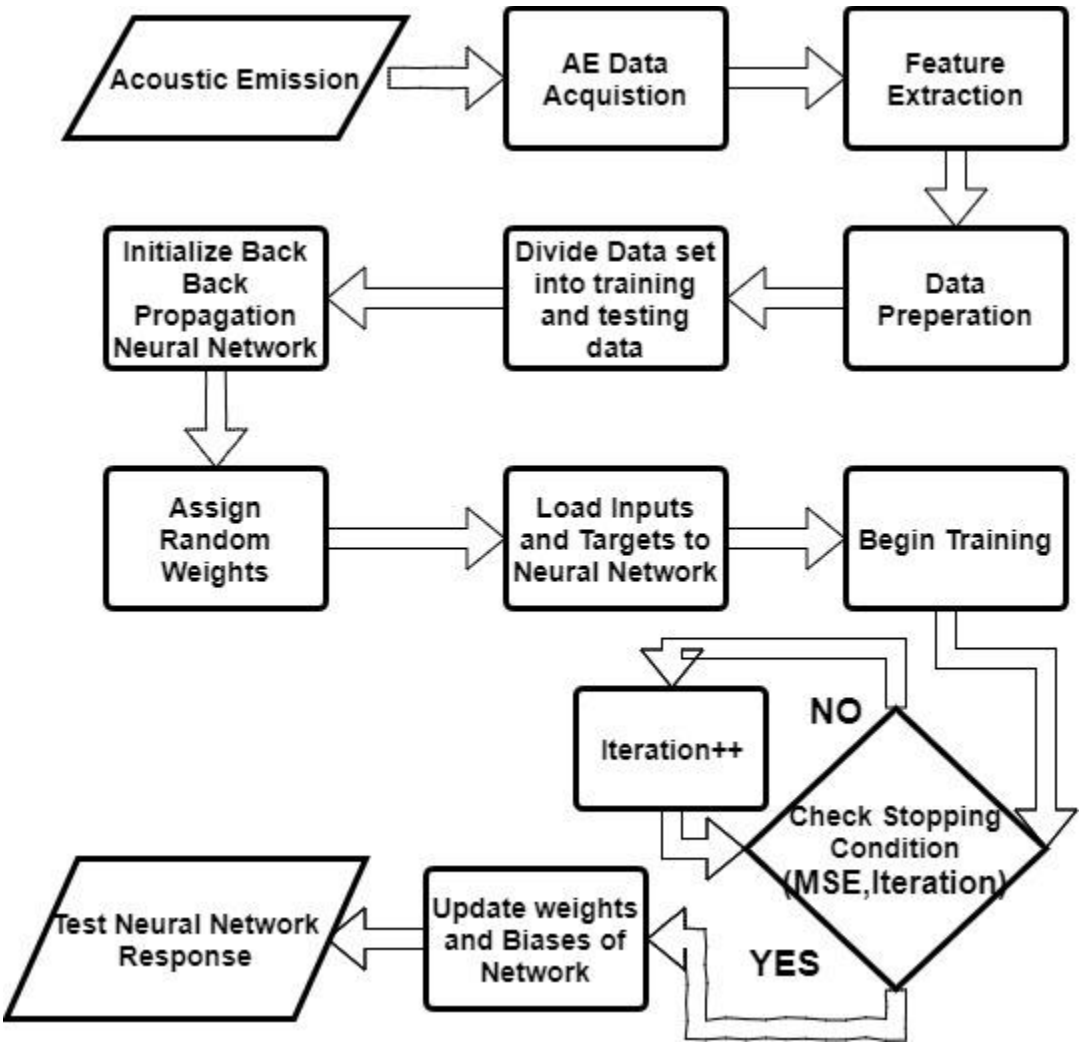

Figure 3. 9: Flow chart of proposed technique with BP-NN

Figure 3.9 represents the flow chart of the proposed technique with back propagation neural network used as a classifier here. Flow chart presents the data acquisition setup followed by feature extraction and classification with the help of back propagation neural network by elaborating all the necessary steps required to initialize, train and test the network.

Figure 3.10 represents the flow chart of the proposed technique with radial basis function neural network used as a classifier here. Flow chart presents the data acquisition setup followed by feature extraction and classification with the help of radial basis function neural network by elaborating all the necessary steps required to initialize, train and test the network.

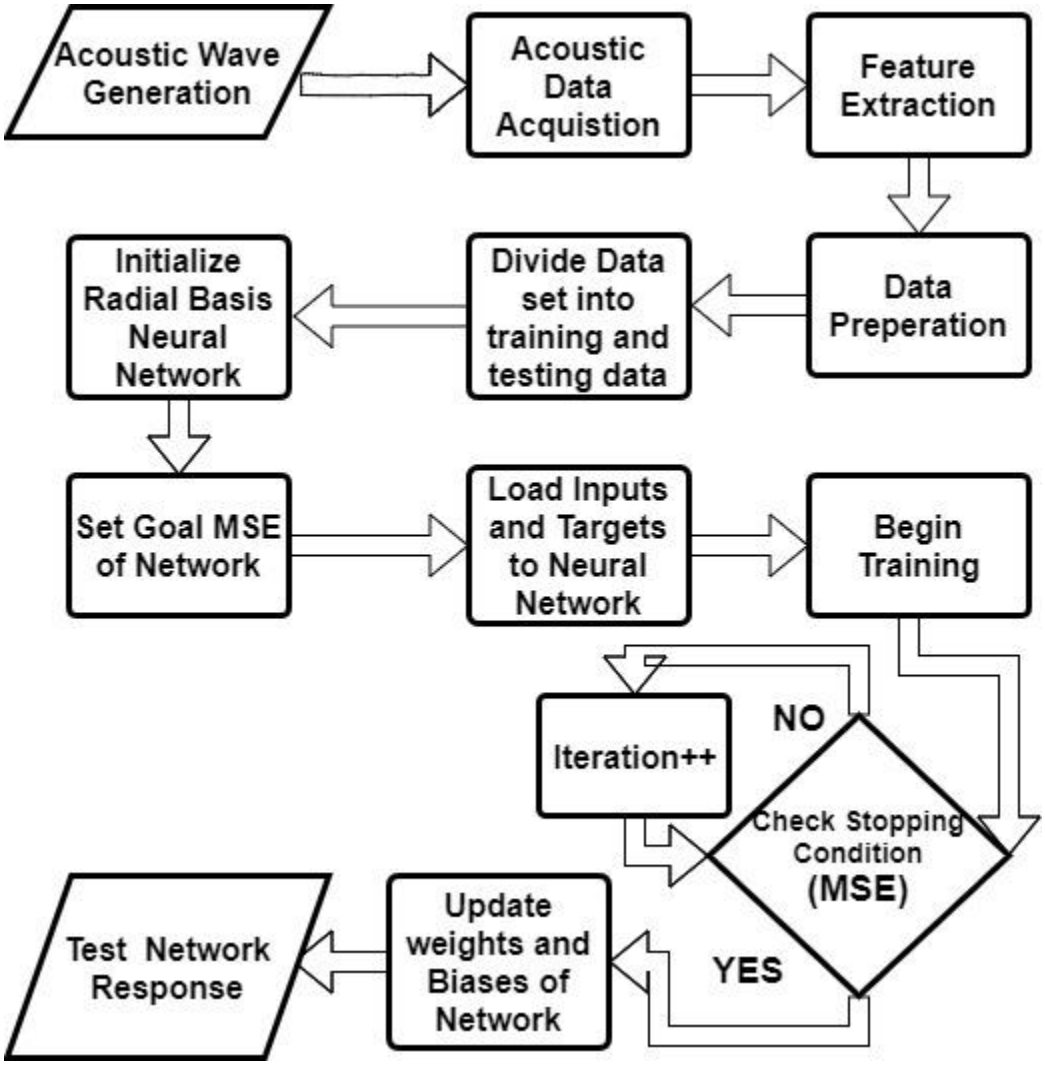

Figure 3. 10: Flow chart of proposed technique with RBF-NN

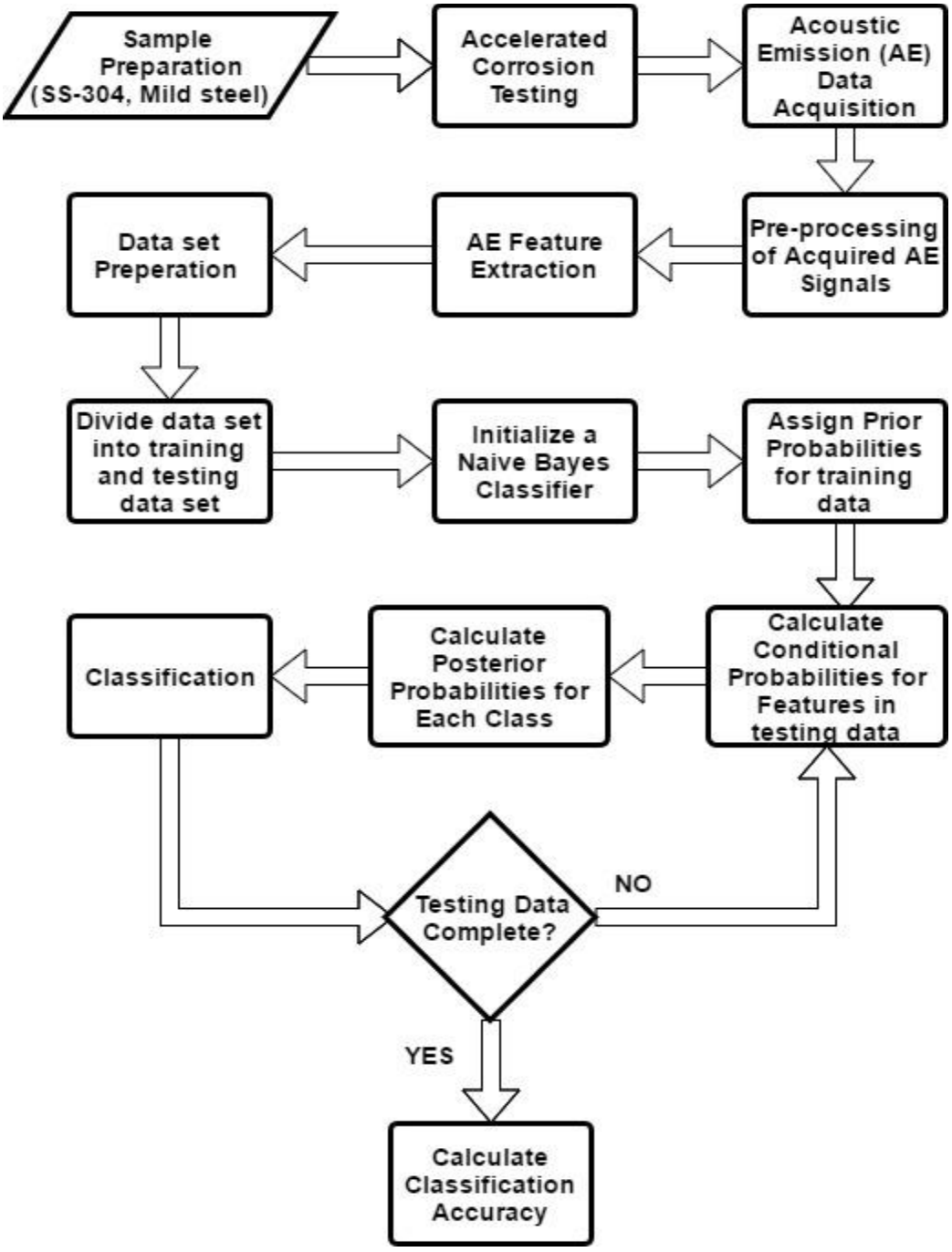

Figure 3. 11: Flow chart of proposed technique with Naive Bayes classifier

Figure 3.11 represents the flow chart of the proposed technique with Naive Bayes classifier here. Flow chart presents the data acquisition setup followed by feature extraction and classification with the help of Naive Bayes classifier by elaborating all the necessary steps required to initialize, train and test the classifier.

3.4. Summary

The chapter can be summarized as follows:

- J. Kaiser discovered Acoustic emission in 1950 and then in years coming later that AE field progressed through sensitive AE sensors, calibration methods and reliable data acquisition systems.

- Different paradigms of machine learning algorithms are selected to compare their performance. These techniques include, Backpropagation Neural Network, Naive Bayes classifier and Radial Basis Function Neural Network.

- Flow charts of proposed technique including data acquisition, feature extraction, dataset preparation, network initialization, network testing with separate classifiers are given.

4. EXPERIMENTATION

This chapter provides details about the accelerated corrosion experimental setup and acoustic emission signal acquisition. A table of various features of acquired signals is also presented.

4.1. Experimental Setup

Experiments are conducted in Embedded Systems Lab of college of EME, National University of Sciences and Technology, Islamabad, Pakistan. Accelerated corrosion testing of mild steel samples is performed in water and sodium bi-carbonate solution using high potentials. Acoustic emission signals for the process are acquired using Sound Well CG80 wideband acoustic sensor. The acoustic emission produced during corrosion process lies in high frequency ranges, so signals are acquired at higher sampling rates of 250 KHz to fulfill the Nyquist criteria. Figure 4.1 shows the flow chart of the data acquisition system.

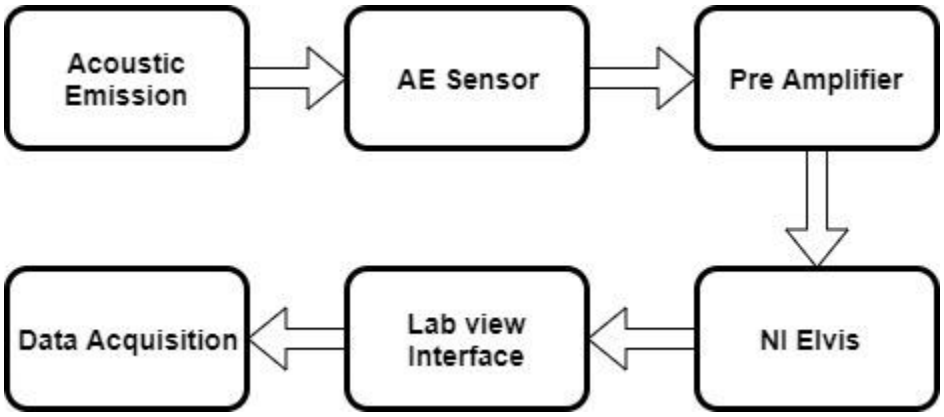

Figure 4. 1: Flow chart for the data acquisition scheme

Acoustic emission released from accelerated corrosion testing of mild steel samples is sensed by acoustic sensor. High frequency acoustic signal is initially amplified with the use of pre-Amplifiers, that amplifies the amplitude of the signal through considerable gain. NI Elvis kit is used to acquire data because it supports high frequency data acquisition and easy interface with Acquisition kit and acquisition software. Lab-view software interface is designed to acquire high frequency acoustic signals through NI Elvis kit. Figure 4.2 shows the setup of accelerated corrosion testing with data acquisition setup.

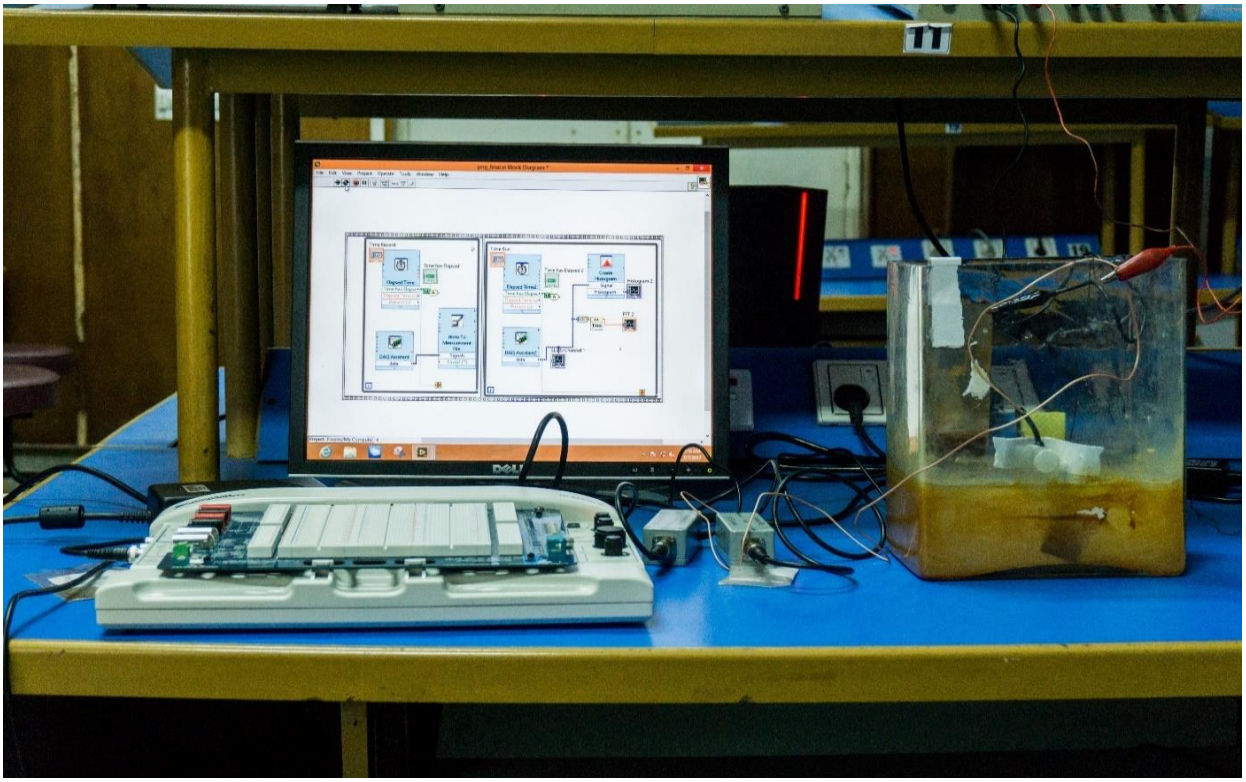

Figure 4. 2: Experimental setup for accelerated corrosion testing

More than twenty experiments were performed in which mild steel samples were used for accelerated corrosion testing for different time spans ranging from one to four hours. Mild steel samples dipped in sodium bi-carbonate and water solution, attached with a DC power supply of 24V and drawing maximum of 2 Amp current depending upon the concentration of the solution. As soon as the potential is supplied to solution and sample, solution tends to turn its color as seen in the figure above. Figure 4.3 shows the samples after accelerated corrosion test for different time spans. A clear difference in the physical appearance of sample before corrosion and after accelerated corrosion test is observed.

Figure 4. 3: Images of samples after accelerated corrosion testing

For further clarification about the corrosion, microscopic examination of samples was conducted after accelerated corrosion testing which revealed the presence of corrosion layer and disintegration of metal. Presence of corrosion layer can be observed in figure 4.4 that shows the microscopic images of a sample at different zoom levels.

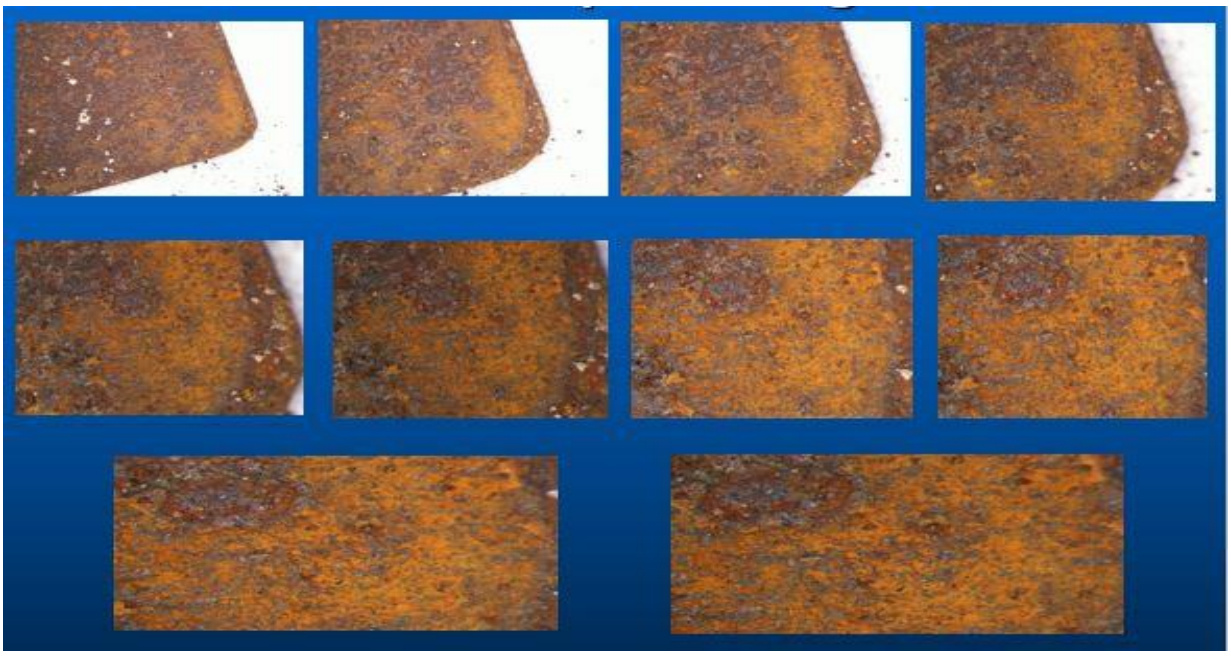

Figure 4. 4: Microscopic images of samples after accelerated corrosion testing at different zoom levels

4.1.1. Mass Loss Calculations

Besides change in physical appearance of samples and confirmation of corrosion layer after microscopic examination of samples, Mass loss calculations for each sample before and after accelerated corrosion testing was performed. Mass of each sample was recorded before and after the corrosion test. Difference in both values of mass before and after corrosion test was termed as mass loss. Table 4.1 shows the values of mass for each sample before and after the test, time for which sample was subjected to test, mass loss for each sample and percentage mass loss during each experiment. Significant percentage mass loss from samples was observed as the time goes on but the trend suggests that rate of percentage mass loss decreases goes on during accelerated corrosion test due to loss of concentration of solution during the prolonged tests.

Table 4. 1: Mass loss statistics of samples after accelerated corrosion testing

Time Exposed		1 hour		
Sample. No	**Mass Before (gram)**	**Mass After (gram)**	**Mass Loss (gram)**	**% Mass Loss**
2	9.75	9.29	0.46	4.71
3	9.82	9.1	0.72	7.33
4	10.12	9.7	0.42	4.15
10	10.2	9.8	0.4	3.92
11	9.4	9.1	0.3	3.19
15	5.85	5.3	0.55	9.4
Averaged			0.475	**5.45%**
Time Exposed		**2 hours**		
1	9.64	8.93	0.71	7.36
8	10.82	9.9	0.92	8.5
9	10.35	9.6	0.75	7.24
Averaged			0.793	**7.70%**
Time Exposed		**3 hours**		
5	11.82	10.5	1.32	11.1
7	10.55	9.47	1.08	10.2
12	10.8	9.79	1.01	9.35
Averaged			1.13	**10.21%**
Time Exposed		**4 hours**		
14	10.55	9.3	1.25	**11.84%**

Percentage mass loss occurred during accelerated corrosion testing versus the experimentation time has been plotted in Figure 4.5. Blue circles represent the percentage mass loss of mild steel samples against the time for which they have been exposed to accelerated corrosion testing. Graph shows that mass loss increases almost linearly as the experimentation time goes on. Plot suggests that the rate of mass loss for accelerated corrosion testing of mild steel samples is highest in first hour of experiment and the rate of percentage mass loss tends to decrease as the time goes on. One of the possible reason for drop in rate of percentage mass loss in prolonged tests would be the reduction in concentration of the solution.

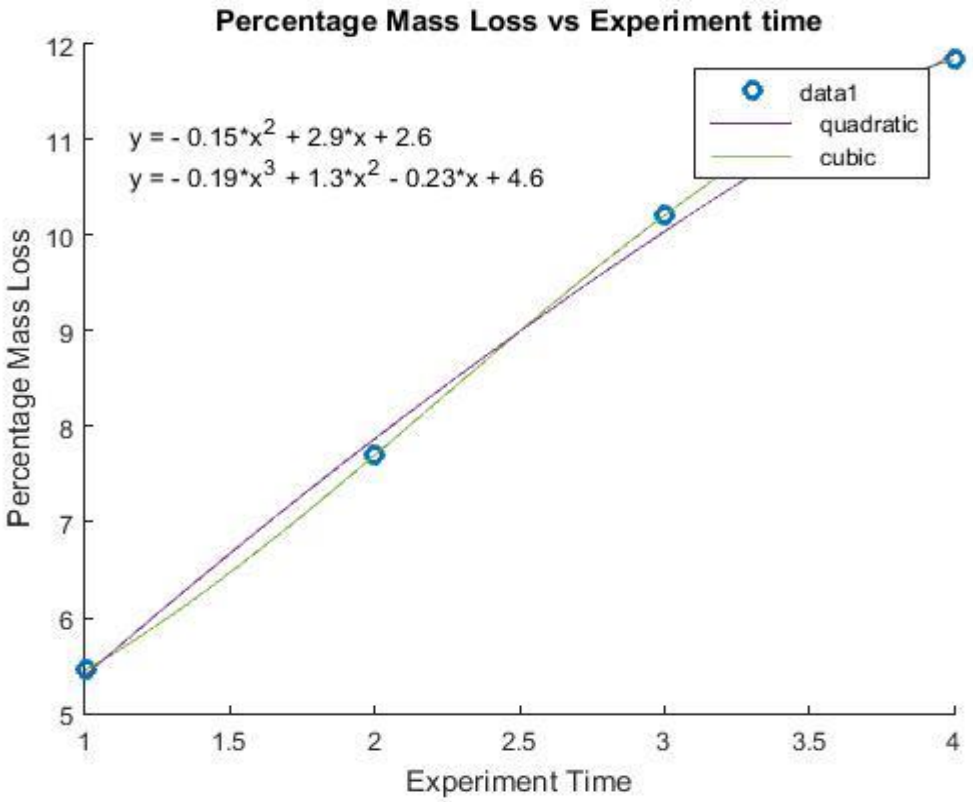

Figure 4. 5: Plot of percentage Mass Loss vs experiment time and line fitting

Figure 4.5 shows the polynomial equations after fitting quadratic and cubic lines to the plot of percentage mass loss versus experimentation time. Quadratic and cubic lines have been fitted on the plot of percentage mass loss versus experimentation time. Pink line shows the quadratic line fitting in which the original data points lie as outliers, whereas the blue line shows the cubic line fitting which passes through all data points and is more accurate fitting than quadratic fitting. With above equations, an accurate corrosion rate can be predicted in terms of percentage mass loss against the experimentation time.

4.2. Raw Acoustic Signals

Data acquisition scheme was made based on literature review. Data was acquired at start of experiment and then every fifteen minutes of the accelerated corrosion process for two seconds with sampling frequency of 250 KHz. Acoustic signal amplitude in terms of voltage is logged into Microsoft Excel sheets. Five lac values of amplitude are acquired in a single data acquisition, which is further preprocessed by windowing operation of suitable size. Data logged in these Excel files is read through Matlab. Raw acoustic signals acquired at different

time spans during accelerated corrosion testing for one hour of sample 6 are plotted against data points.

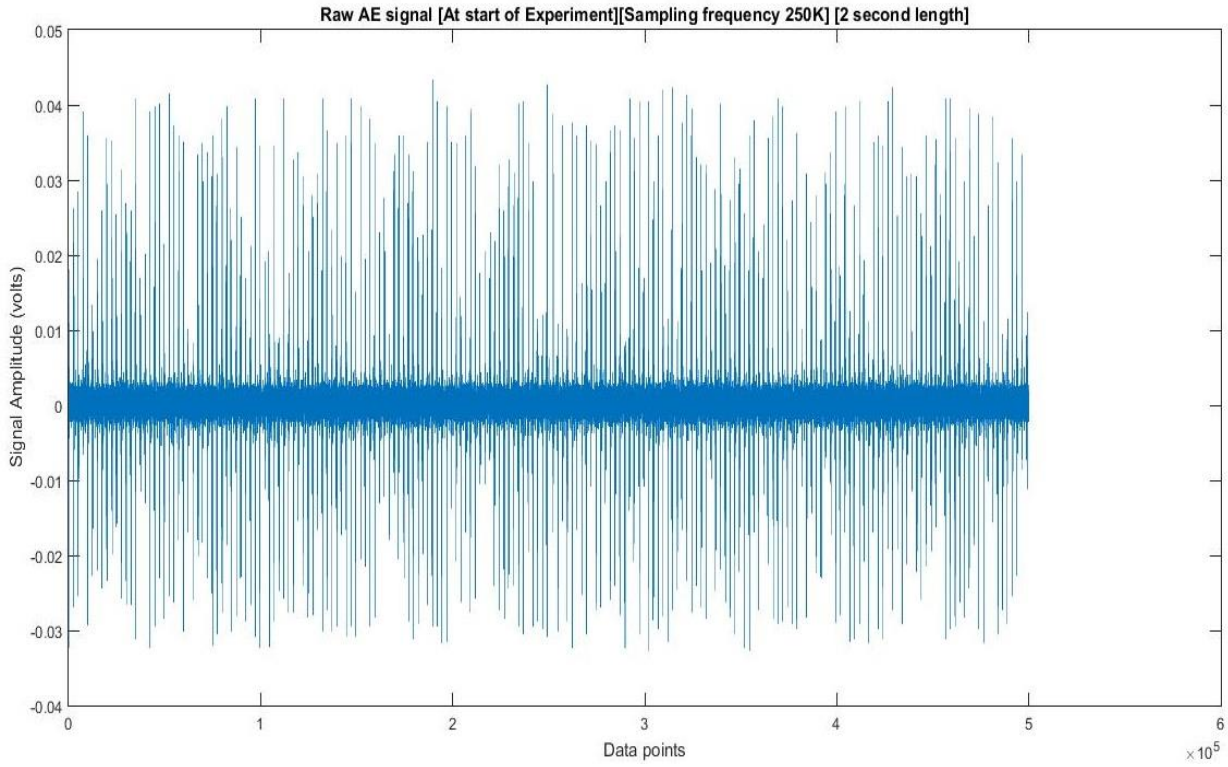

Figure 4. 6: Plot of raw acoustic signal acquired at start of experiment

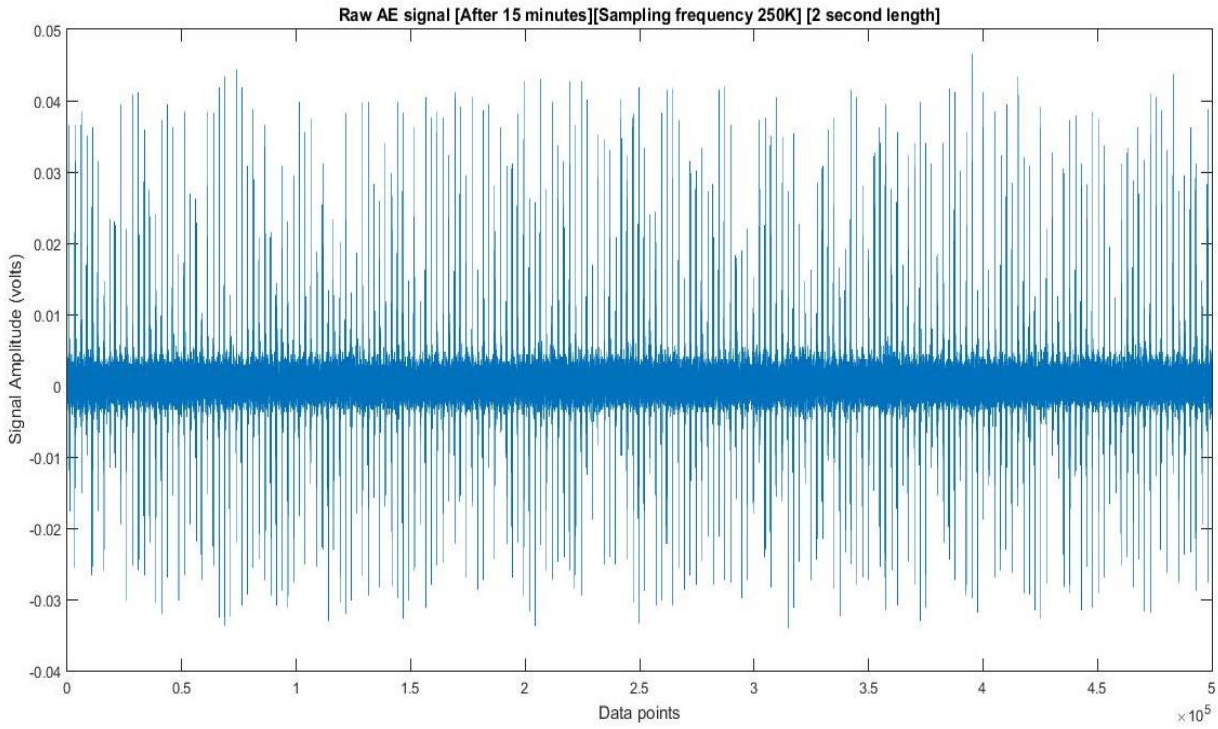

Figure 4. 7: Plot of raw acoustic signal acquired after 15 minutes

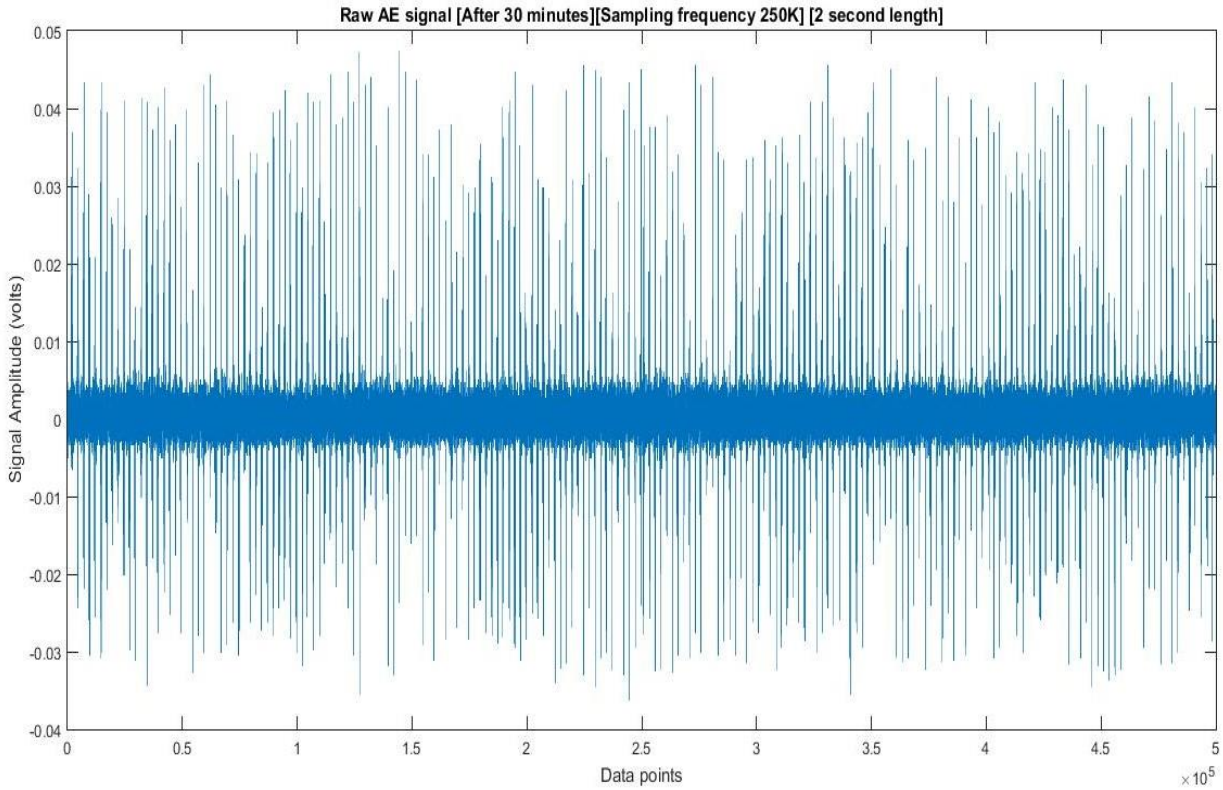

Figure 4. 8: Plot of raw acoustic signal acquired after 30 minutes

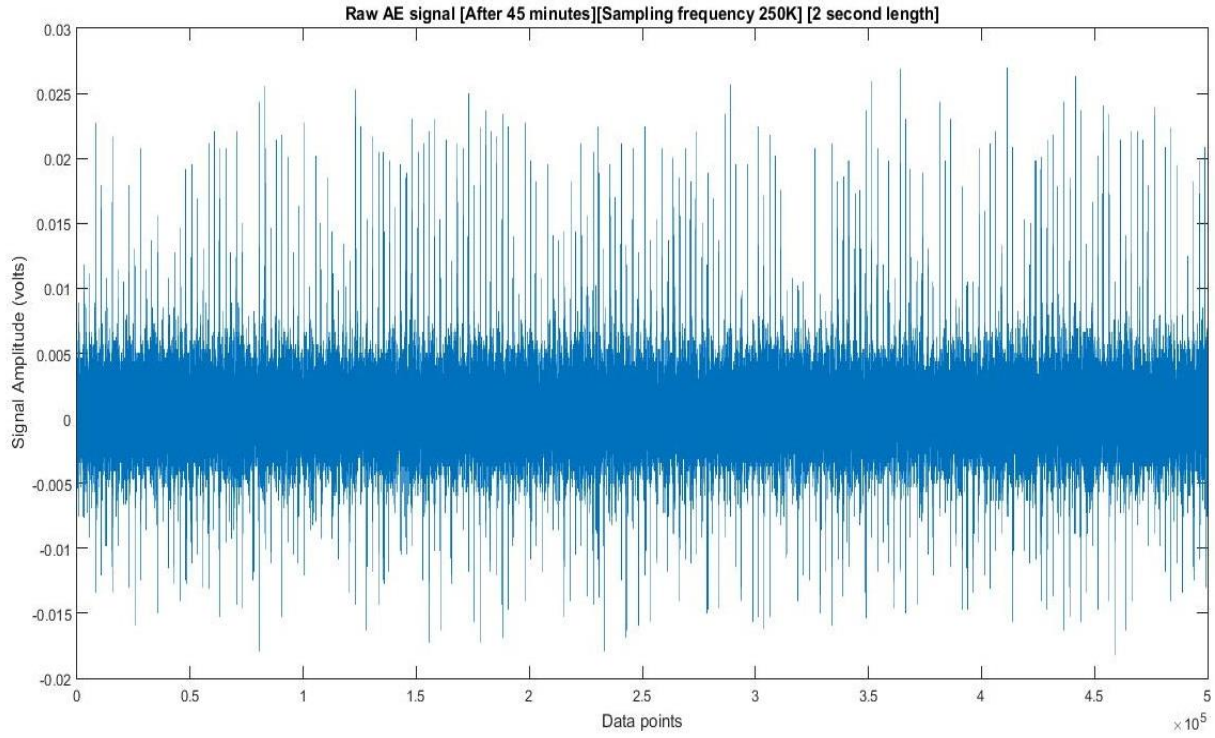

Figure 4. 9: Plot of raw acoustic signal acquired after 45 minutes

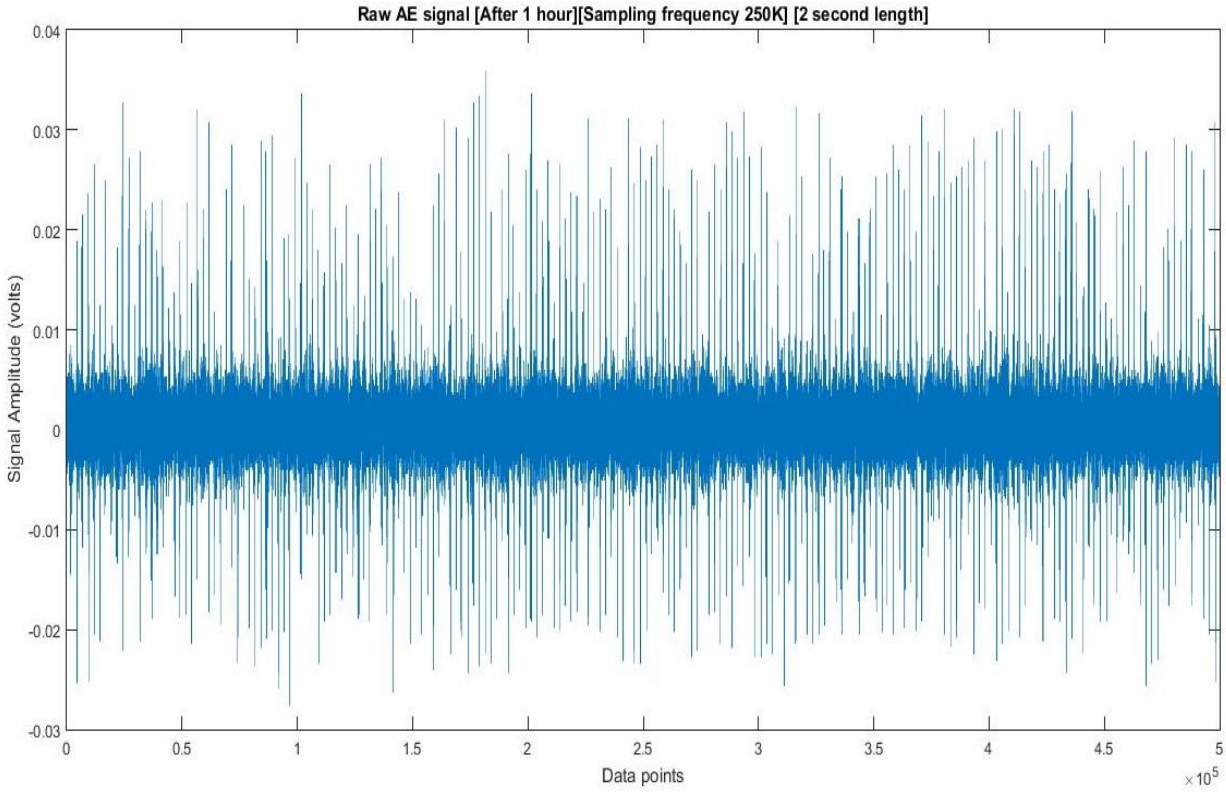

Figure 4. 10: Plot of raw acoustic signal acquired after one hour

4.3. Fast Fourier Transform (FFT) of Acoustic Signals

Frequency of acoustic emission during corrosion process is very good indicator of passive layer breakage. According to literature review frequency above 50 KHz indicates that corrosion process has been matured and material layer breaking is in progress. Data acquired during experimentation is in time domain, Fourier analysis is used here to visualize acoustic signals in frequency domain. To confirm experimentation, Fast Fourier Transform (FFT) of the acquired raw acoustic signals are calculated using Matlab script. FFT of a signal is representation of the its frequency versus amplitude at the same time. FFT of acoustic signal acquired at start of experiment is clearly distinguishable from FFTs of the acoustic signals acquired in later stages of the experiment. Higher frequency peaks are observed in FFTs of the acoustic signal confirming the on-going corrosion process. Figures below presents comparison between FFTs of a one hour accelerated corrosion test performed on sample 6.

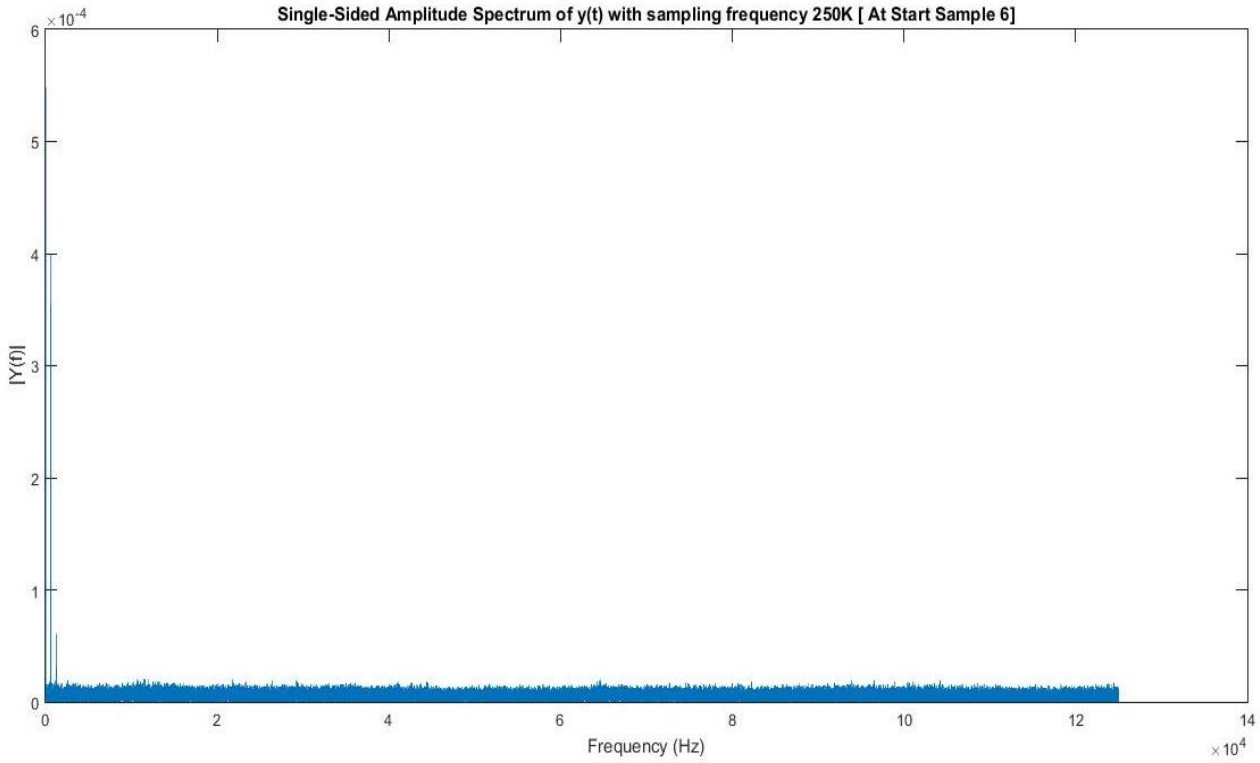

Figure 4. 11: FFT of acoustic signal acquired at start of experiment

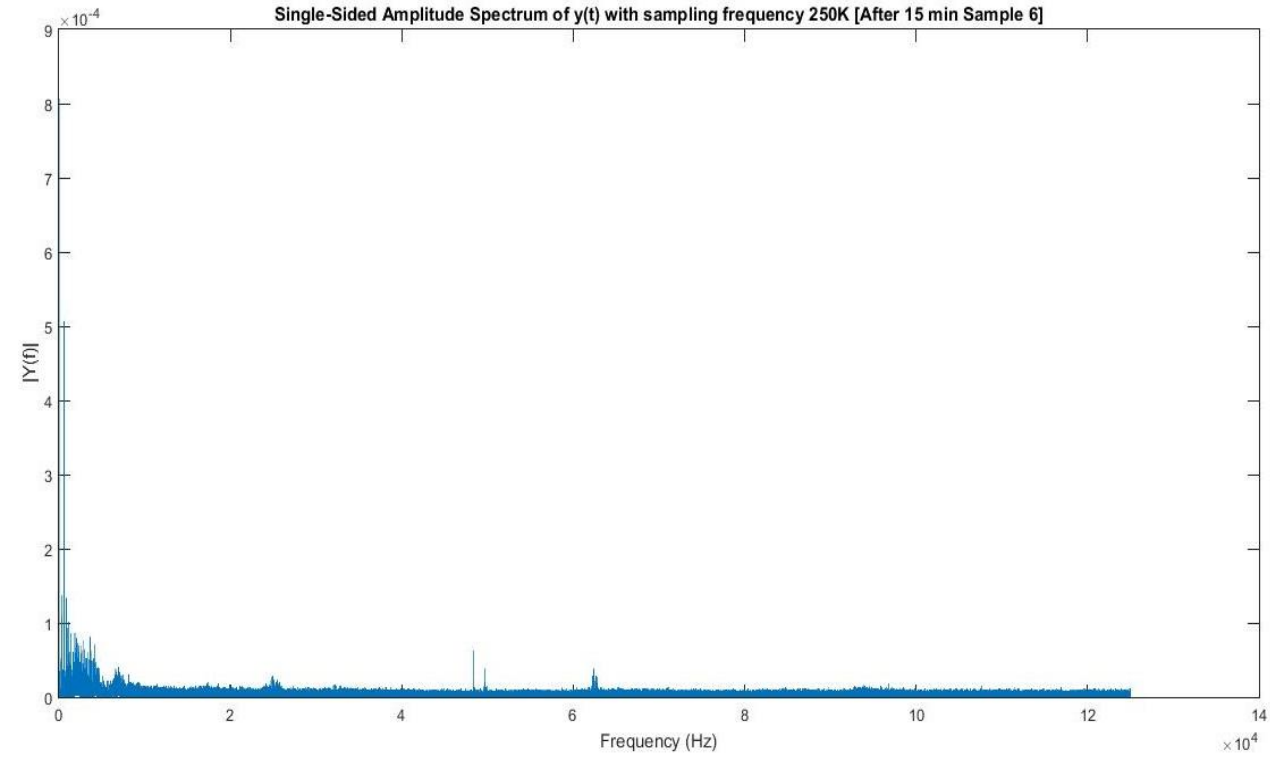

Figure 4. 12: FFT of acoustic signal acquired after 15 minutes

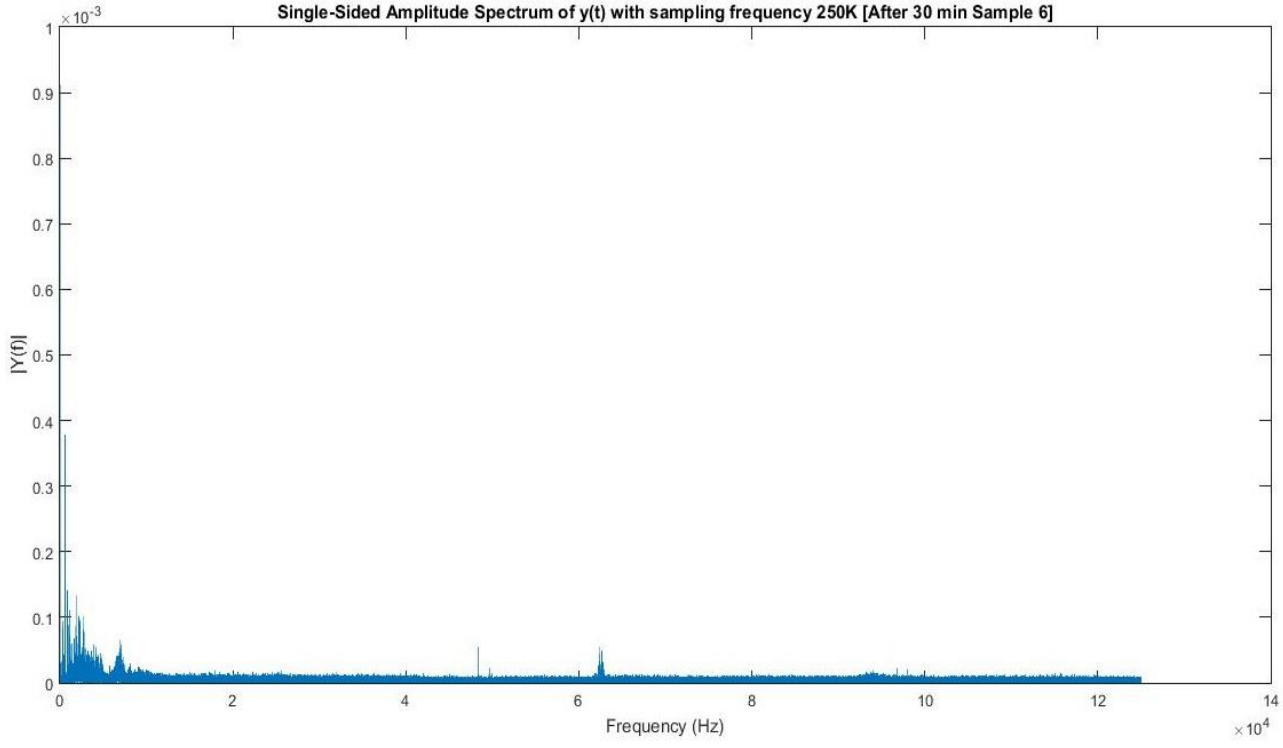

Figure 4. 13: FFT of acoustic signal acquired after 30 minutes

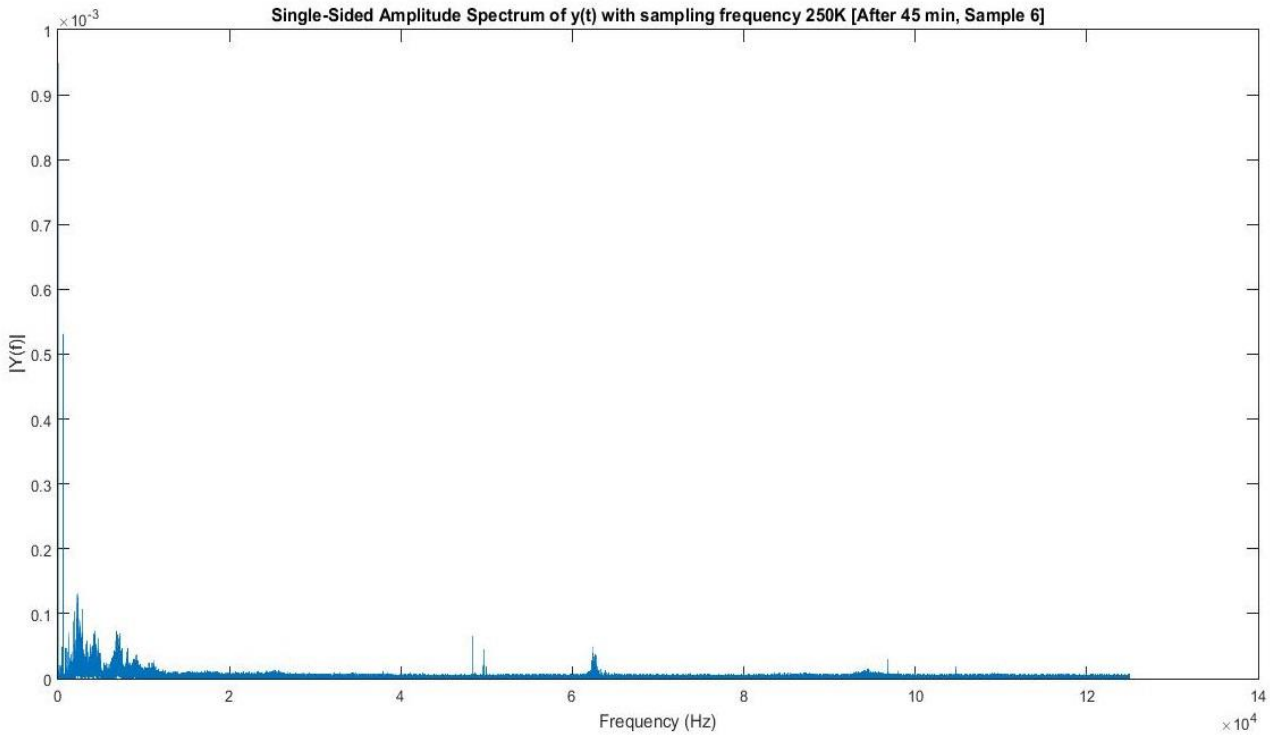

Figure 4. 14: FFT of acoustic signal acquired after 45 minutes

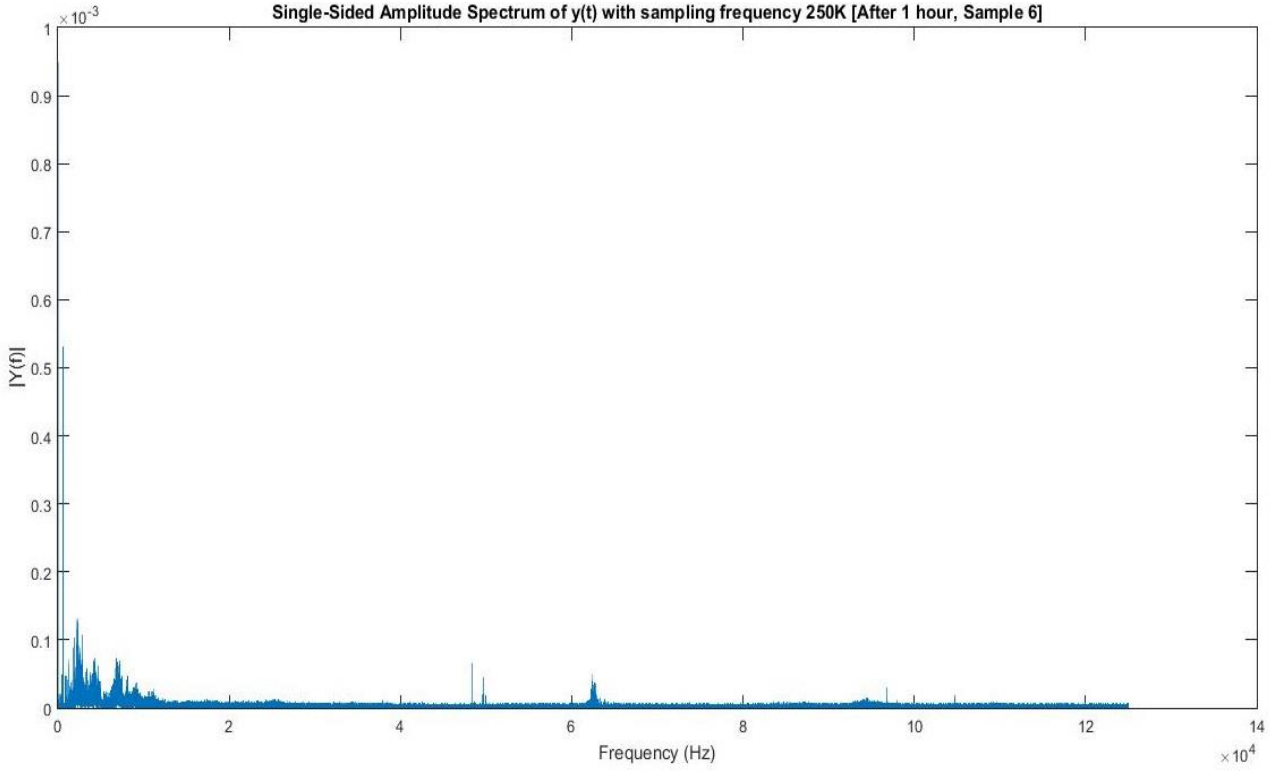

Figure 4. 15: FFT of acoustic signal acquired after 1 hour

4.4. Feature Extraction from Acoustic Signals

Raw Acoustic signals does not provide better observation about the corrosion process, so after FFT of acoustic signals, Acoustic Emission (AE) and statistical features were extracted for better understanding of the process. Common AE features such as AE Mean, AE Energy and AE RMS were computed along with several statistical features such as Skewness, Kurtosis. As the corrosion process starts and mature with time, significant change in the values of these extracted features is observed. Mass loss for each experiment was recorded and further used as an indicator of corrosion severity. Matlab script was written to automatically extract these features from logged data files. Data preprocessing step involves the application of window size of ten thousand data points after which fifty values of each feature is extracted. AE mean is the averaged value of acoustic signal obtained over a window size. AE RMS is the root mean squared values of acoustic emission signal over a specified window size. A comparison of extracted features from raw acoustic signals is presented below which shows the behavior of features as the experiment starts, mature and till the end time.

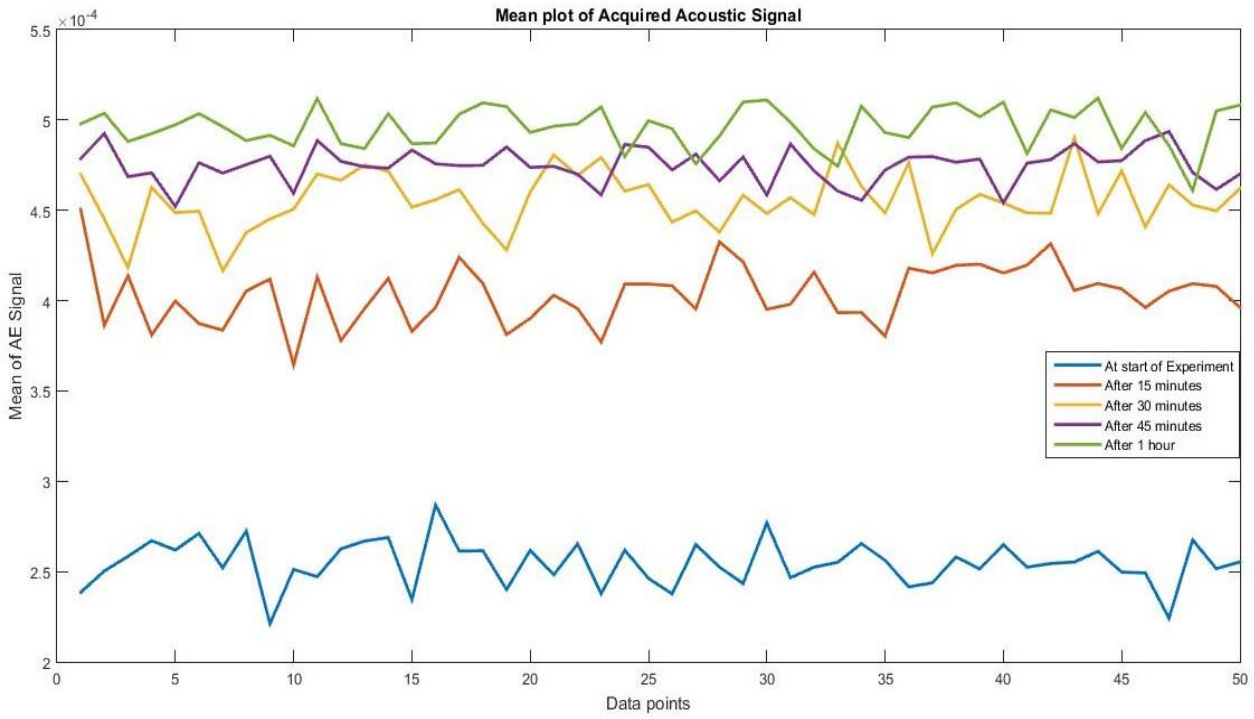

Figure 4. 16: Comparison of mean plot of acoustic signals

It can be observed from the Figure 4.16 that AE Mean at start of experiment is at its possible low and as the time of experiment goes on value of AE Mean tends to rise. Figure 4.17 shows

bar graph representation of AE Mean level increase with the increase in experiment time. As the corrosion process matures and metal loss occurs AE Mean level tends to rise.

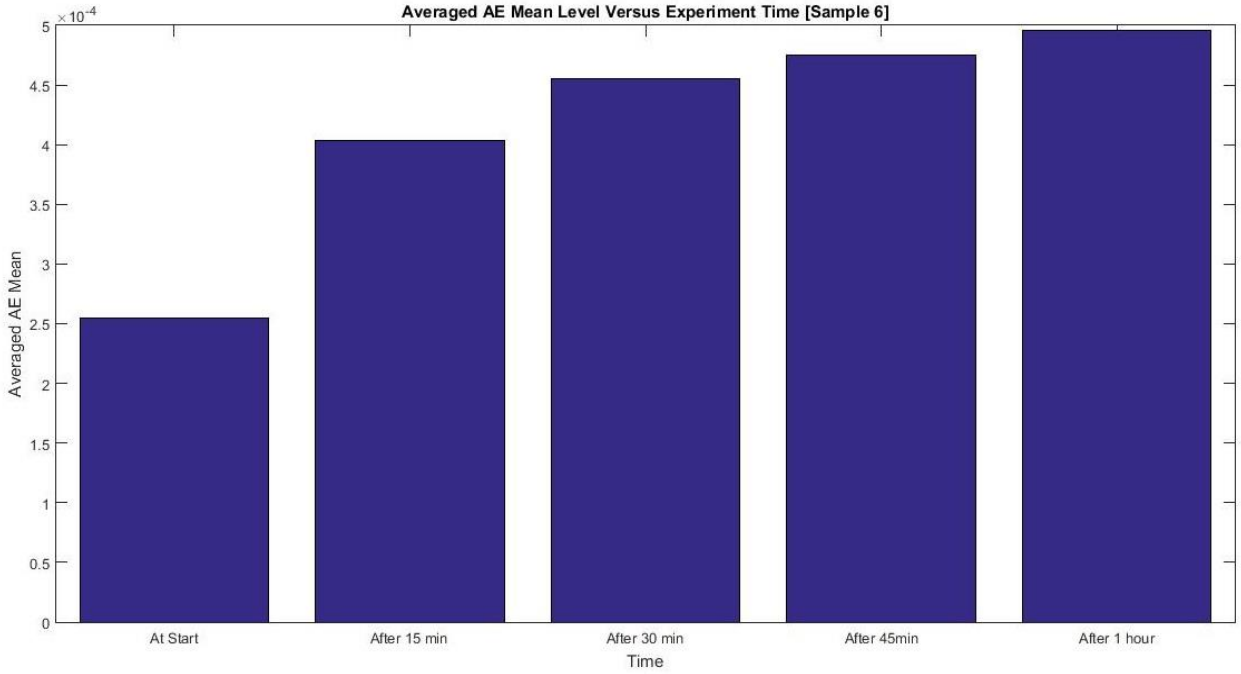

Figure 4. 17: Bar graph of averaged mean extracted from acoustic signals

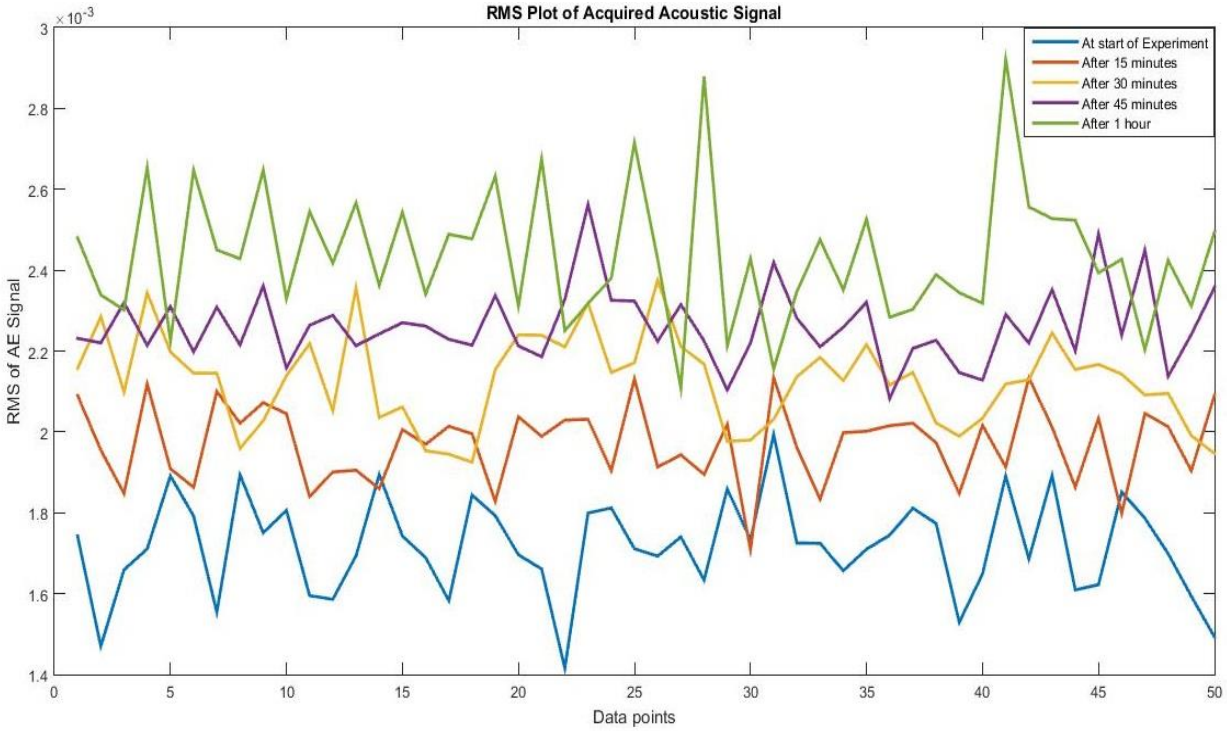

Figure 4. 18: Comparison of RMS plot of acoustic signals

It can be observed from the Figure 4.18 that AE RMS rise as the time of experiment goes on, value of AE RMS tends to rise. Figure 4.19 shows bar graph representation of averaged AE RMS level increase with the increase in experiment time. As the corrosion process matures and metal loss occurs, AE RMS level tends to rise.

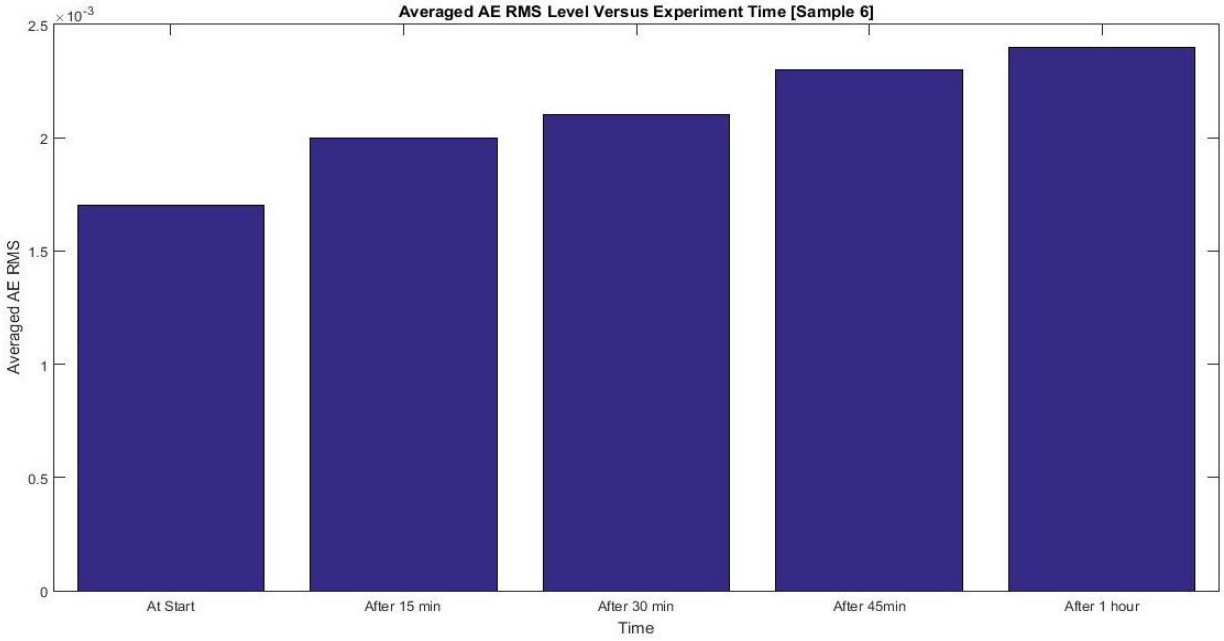

Figure 4. 19: Bar graph of averaged RMS extracted from acoustic signals

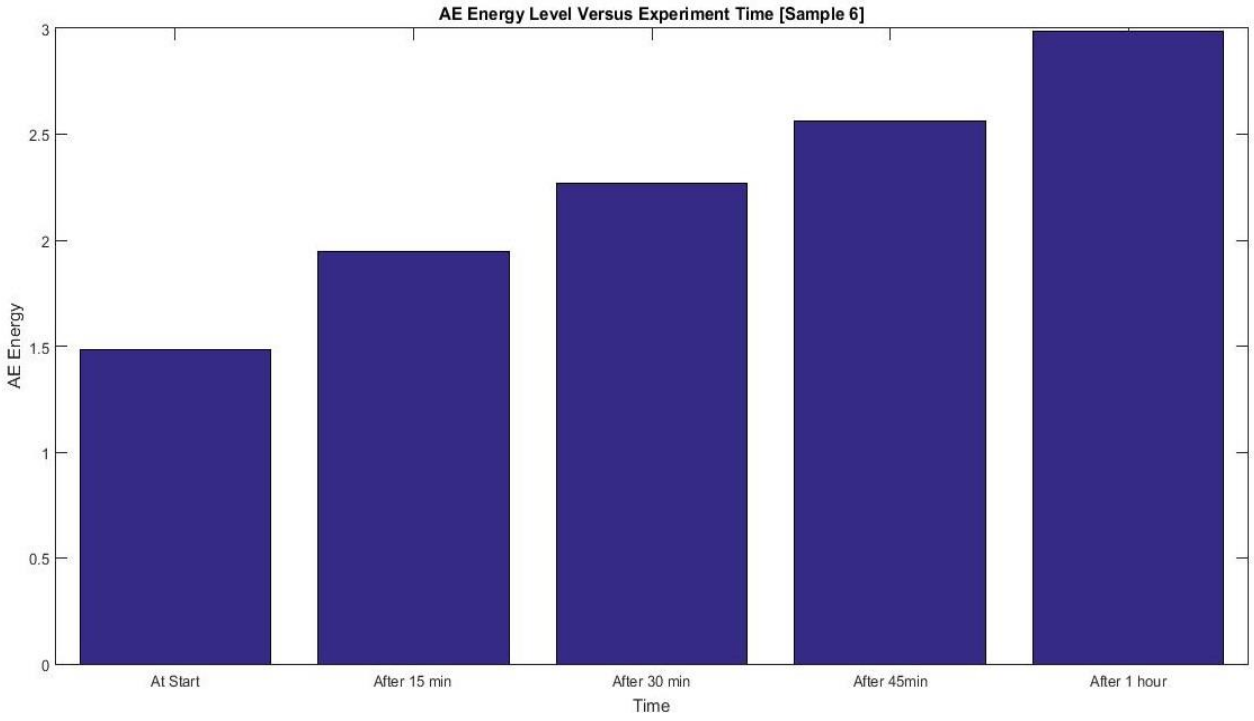

Figure 4. 20: Bar graph of averaged AE energy extracted from acoustic signals

It can be observed from Figure 4.20 that AE Energy is a distinct feature because averaged AE energy rise proportionally as corrosion process matures and metal loss occurs. Amongst statistical features kurtosis is observed as good feature. Figure 4.21 shows the averaged kurtosis level versus experiment time.

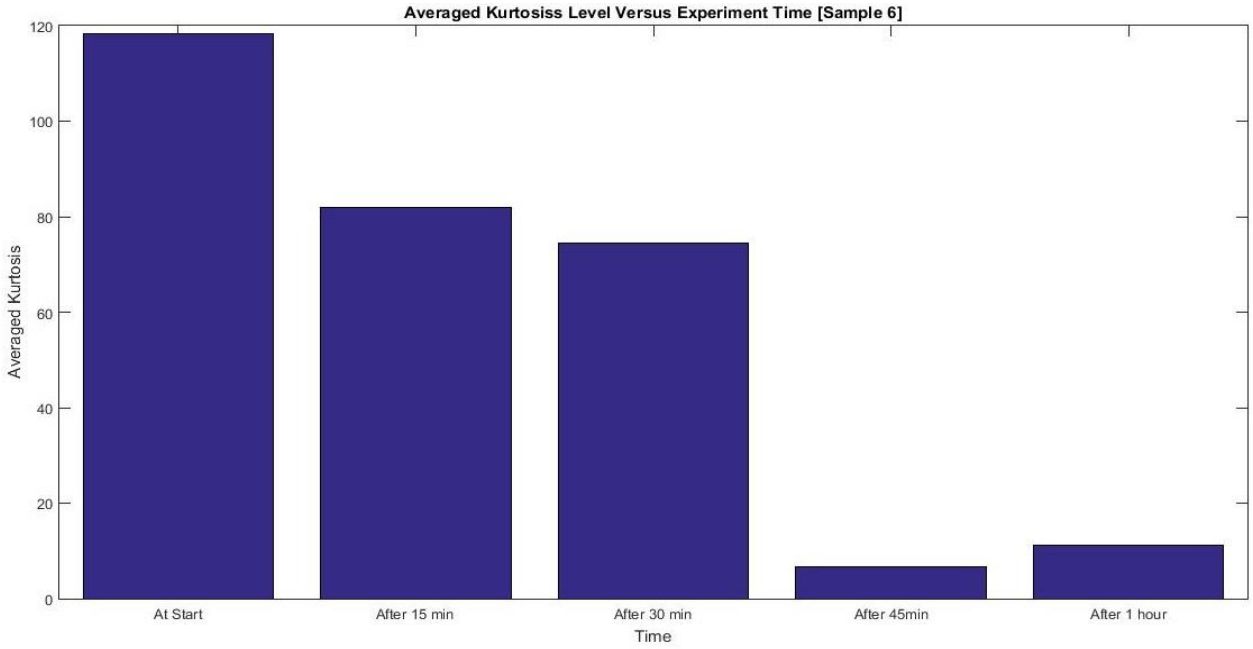

Figure 4. 21: Bar graph of averaged Kurtosis extracted from acoustic signals

Table 4.2 shows the averaged values of features extracted from the acquired raw acoustic signals. Experiments are divided into categories depending upon the time for which sample is subjected to accelerated corrosion testing. For each experiment, extracted features are tabulated according to the time span they are acquired.

Table 4. 2: Various Features of acquired Acoustic Signals

		S. No 1	**SAMPLE 2**	**Time Exposed 1 hour**	
	Averaged Mean	**Averaged RMS**	**Averaged Kurtosis**	**Averaged Skewness**	**Averaged Energy**
At start	3.36E-05	7.07E-04	5.3494	-0.0432	0.2826
After 15 min	2.13E-04	9.76E-04	5.0081	0.0791	0.4782
After 30 min	2.51E-04	0.0011	4.5212	-0.0436	0.6046
After 45 min	2.90E-04	0.0039	3.6232	-0.0312	7.4606
After 60 min	2.73E-04	0.0043	3.2152	-0.0255	9.1664
		S. No 2	**SAMPLE 3**	**Time Exposed 1 hour**	

	Averaged Mean	Averaged RMS	Averaged Kurtosis	Averaged Skewness	Averaged Energy
At start	1.82E-05	1.40E-03	80.8677	1.6301	0.9225
After 15 min	4.83E-05	0.0015	54.5341	0.962	1.0949
After 30 min	5.23E-05	0.002	49.6785	0.9041	1.9742
After 45 min	9.94E-05	0.002	67.075	1.2389	2.012
After 60 min	2.07E-04	0.0022	42.3759	0.7769	2.4745
		S. No 3	**SAMPLE 4**	**Time Exposed 1 hour**	
At start	2.74E-04	2.00E-03	16.6823	3.0839	2.1101
After 15 min	3.84E-04	0.0015	8.407	1.5981	1.1832
After 30 min	3.17E-04	0.0046	8.7271	0.1261	10.847
After 45 min	4.66E-04	0.0044	8.407	0.0861	9.6254
After 60 min	5.26E-04	0.0044	7.9702	0.4353	9.8363
		S. No 4	**SAMPLE 6**	**Time Exposed 1 hour**	
	Averaged Mean	**Averaged RMS**	**Averaged Kurtosis**	**Averaged Skewness**	**Averaged Energy**
At start	2.55E-04	1.70E-03	118.41	1.5942	1.4824
After 15 min	4.03E-04	0.002	81.954	1.5885	1.9472
After 30 min	4.55E-04	0.0021	74.492	1.5603	2.267
After 45 min	4.75E-04	0.0023	6.6386	0.191	2.5643
After 60 min	4.96E-04	0.0024	11.21	0.1937	2.9837
		S. No 5	**SAMPLE 10**	**Time Exposed 1 hour**	
	Averaged Mean	**Averaged RMS**	**Averaged Kurtosis**	**Averaged Skewness**	**Averaged Energy**
At start	2.41E-04	8.85E-04	17.958	0.0987	0.3922
After 15 min	2.63E-04	9.22E-04	19.693	0.1293	0.4255
After 30 min	2.84E-04	9.13E-04	20.0409	0.1639	0.4185
After 45 min	3.54E-04	0.001	50.6138	0.8562	0.537
After 60 min	1.71E-04	0.001	10.7298	0.0515	0.5256
		S. No 6	**SAMPLE 11**	**Time Exposed 1 hour**	
	Averaged Mean	**Averaged RMS**	**Averaged Kurtosis**	**Averaged Skewness**	**Averaged Energy**
At start	-4.12E-04	1.10E-03	89.254	0.9987	0.6469
After 15 min	9.25E-05	9.80E-04	13.2341	0.0869	0.4806
After 30 min	1.63E-04	1.10E-03	9.3506	0.093	0.5864
After 45 min	2.04E-04	0.0012	5.4642	0.0026	0.7411
After 60 min	2.37E-04	0.0012	8.0546	0.0614	0.775
		S. No 7	**SAMPLE 15**	**Time Exposed 1 hour**	

	Averaged Mean	Averaged RMS	Averaged Kurtosis	Averaged Skewness	Averaged Energy
At start	4.18E-05	9.14E-04	65.6993	0.5706	0.4192
After 15 min	1.84E-04	1.40E-03	127.6894	1.7216	1.0077
After 30 min	2.41E-04	1.60E-03	74.8692	0.7891	1.2626
After 45 min	2.59E-04	0.0018	16.6301	0.2414	1.5879
After 60 min	2.81E-04	0.0022	9.4316	0.106	2.4377

		S. No 8	SAMPLE 1	Time Exposed 2 hours	
	Averaged Mean	Averaged RMS	Averaged Kurtosis	Averaged Skewness	Averaged Energy
At start	1.82E-05	1.40E-03	80.8677	1.6301	0.9225
After 1 hr	2.07E-04	0.0022	42.3759	0.7769	2.4745
After 2 hr	2.99E-04	0.0025	63.7255	1.0109	3.2047
		S. No 9	SAMPLE 8	Time Exposed 2 hours	
	Averaged Mean	Averaged RMS	Averaged Kurtosis	Averaged Skewness	Averaged Energy
At start	3.36E-05	7.52E-04	5.3494	-0.0432	0.2826
After 1 hr	2.73E-04	0.0043	3.2152	-0.0255	9.1664
After 2 hr	3.17E-04	0.0021	5.6783	-0.0376	2.3614
		S. No 10	SAMPLE 9	Time Exposed 2 hours	
	Averaged Mean	Averaged RMS	Averaged Kurtosis	Averaged Skewness	Averaged Energy
At start	1.41E-04	9.23E-04	12.8226	0.0484	0.4299
After 1 hr	2.91E-04	0.0034	58.2011	1.1228	5.8554
After 2 hr	3.06E-04	0.0182	42.8211	3.238	4.9855

		S. No 11	SAMPLE 5	Time Exposed 3 hours	
	Averaged Mean	Averaged RMS	Averaged Kurtosis	Averaged Skewness	Averaged Energy
At start	1.39E-04	2.20E-03	23.9831	0.5377	2.4217
After 1 hr	-1.70E-04	0.0028	25.562	0.8521	4.0295
After 2 hr	1.28E-05	0.0029	19.4632	0.3456	4.2839
After 3 hr	-2.75E-05	0.0029	9.6167	0.0691	4.2967
		S. No 12	SAMPLE 7	Time Exposed 3 hours	
	Averaged Mean	Averaged RMS	Averaged Kurtosis	Averaged Skewness	Averaged Energy
At start	1.82E-05	1.40E-03	80.79	1.6301	0.9225

After 1 hr	2.07E-04	0.0022	42.3759	0.7769	2.4745
After 2 hr	2.99E-04	0.0025	63.7255	1.0109	3.2047
After 3 hr	3.22E-04	0.0024	67.035	1.1278	2.8386

	S. No 13	SAMPLE 12	Time Exposed 3 hours	
	Averaged Mean	Averaged RMS	Averaged Kurtosis	Averaged Skewness	Averaged Energy
At start	2.00E-04	1.40E-03	93.7576	0.868	0.5616
After 1 hr	3.24E-04	0.0022	257.4128	2.1414	1.2605
After 2 hr	3.43E-04	0.0025	135.7428	1.3468	1.0175
After 3 hr	3.54E-04	0.0024	143.3983	1.3268	0.6913

	S. No 14	SAMPLE 14	Time Exposed 4 hours	
	Averaged Mean	Averaged RMS	Averaged Kurtosis	Averaged Skewness	Averaged Energy
At start	4.18E-05	9.14E-04	65.6993	0.5706	0.4192
After 1 hr	2.81E-04	0.0022	9.4316	0.106	2.4377
After 2 hr	3.26E-04	0.0019	12.5481	-0.0886	1.9035
After 3 hr	3.35E-04	0.0017	5.9878	-0.0154	1.4652
After 4 hr	3.53E-04	0.0012	13.3582	0.078	0.737

4.5. Summary

The chapter can be summarized as follows

- Accelerated corrosion testing of more than twenty mild steel samples has been done using sodium bi-carbonate and water solution with 24volt DC power supply. Acoustic emission signals for accelerated corrosion process were acquired using acoustic sensor, NI Elvis kit and LabView interface.

- Data acquisition scheme have been made to acquire data based on corrosion process. Fast Fourier Transform of the acquired signals was obtained to convert the signal from time domain to frequency domain. Raw acoustic signal does not provide better information about the process, so feature extraction was done.

- AE Mean, AE RMS, AE Energy were observed as distinct features due to their linear relationship with the metal degradation during accelerated corrosion process.

5. RESULTS AND DISCUSSION

This chapter presents the results of the research. A detailed discussion on performance of different machine learning algorithms used as classifier is given in the chapter. Results of classification for corrosion detection and corrosion severity reconstruction using different classifiers are also included in the chapter.

5.1. Classification

Classification can be thought of as a pattern recognition problem. Classification is a supervised learning problem in which we assign class labels to the data in the form of teaching or target signal. Classification includes the construction of a classifier which is trained on a set of training data that already has the correct class assigned to each data point. It is then used to classify new data where the values of features are known but the class is unknown. If classification is to be done in two classes, it is called as bi-classification problem and with more than two class classification it is known as multi-class problem.

Extracted features from acquired acoustic signals are used as inputs to classifiers and arithmetic patterns are set as targets of the classifiers. Back propagation neural network and radial basis function neural network are two neural network based classifiers that are used here for classification purpose.

Naive Bayes classifier is a probability base classifier that is used here for classification. Results of classification is confusion matrix, which further reveals the performance parameters like accuracy, precision, recall, F score, sensitivity and specificity. BP-NN, RBF-NN and Naive Bayes classifiers are used, and their performance is compared by using these performance parameters given in Table 5.1.

Table 5. 1: Performance parameters of classifiers

Bi Class	Multi Class
$\textbf{Accuracy} = \frac{TP+TN}{TP+TN+FP+FN}$	$\textbf{Accuracy} = \frac{TP+TN}{TP+TN+FP+FN}$
$\textbf{Specificity} = \frac{TN}{TN+FP}$	$\textbf{Precision} = \frac{TP}{TP+FP}$
$\textbf{Sensitivity} = \frac{TP}{TP+FN}$	$\textbf{Recall} = \frac{TP}{TP+FN}$
	$\textbf{F score} = 2(\frac{Percision * Recall}{Precision+Recall})$

5.2. Bi-Classification

Problem of classification is divided into bi-class and multiclass problem. Bi-class classification problem deals with the correct classification of corrosion and no corrosion state. For one-hour experiments, acoustic data acquired at start of experiment represents 'no corrosion' state and all other acquired signals represents 'corrosion state'. For one-hour experiment, total of five acoustic signals are acquired by starting at the start of experiment, after 15 minutes, after 30 minutes, after 45 minutes and after 1 hour. Data acquisition scheme involves the acquisition of data at start of experiment than after every fifteen minutes till the end of experiment for two seconds with sampling frequency of 250 KHz. Each acquired signal has five lac voltage values logged. Features are extracted from each acquired signal using a window size of 10000. Each extracted feature has an array size of 50. AE Mean, AE RMS, skewness and kurtosis are selected as distinct features. For each one-hour experiment, input data set comprises of four features each with the feature length of 250, out of which 50 values representing the 'no corrosion' state and 200 values represents the 'corrosion' state. Targets are set according to input dataset and network is trained and tested.

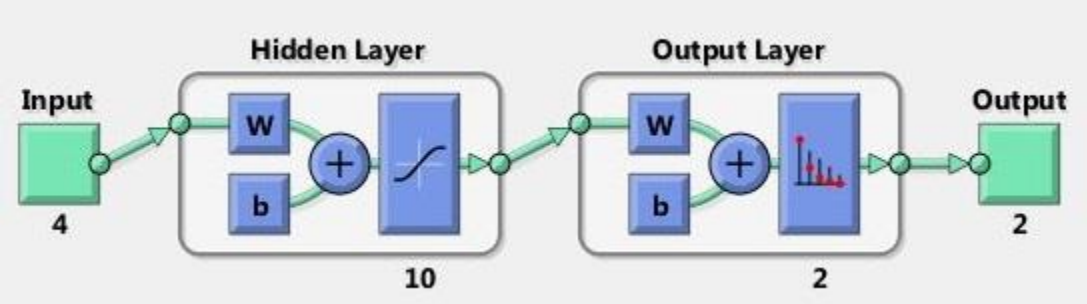

Figure 5. 1: Architecture of BP-NN used for bi-classification

Figure 5.1 shows the architecture of back propagation neural network used for classification of "corrosion" and "no corrosion" state for sample 6. Network consists of 4 input neurons, 10 hidden layer neurons and 2 output neurons. Figure 5.2 shows the neural network training, validation and testing performance with best validation performance achieved at epoch 24 with mean squared error (MSE) of 1.734×10^{-06}. Table 5.2 shows the results of back propagation neural network applied on different samples for bi-classification. Table shows the number of input neurons, hidden layer neurons, output neurons and an overall accuracy of 98.68% for BP-NN.

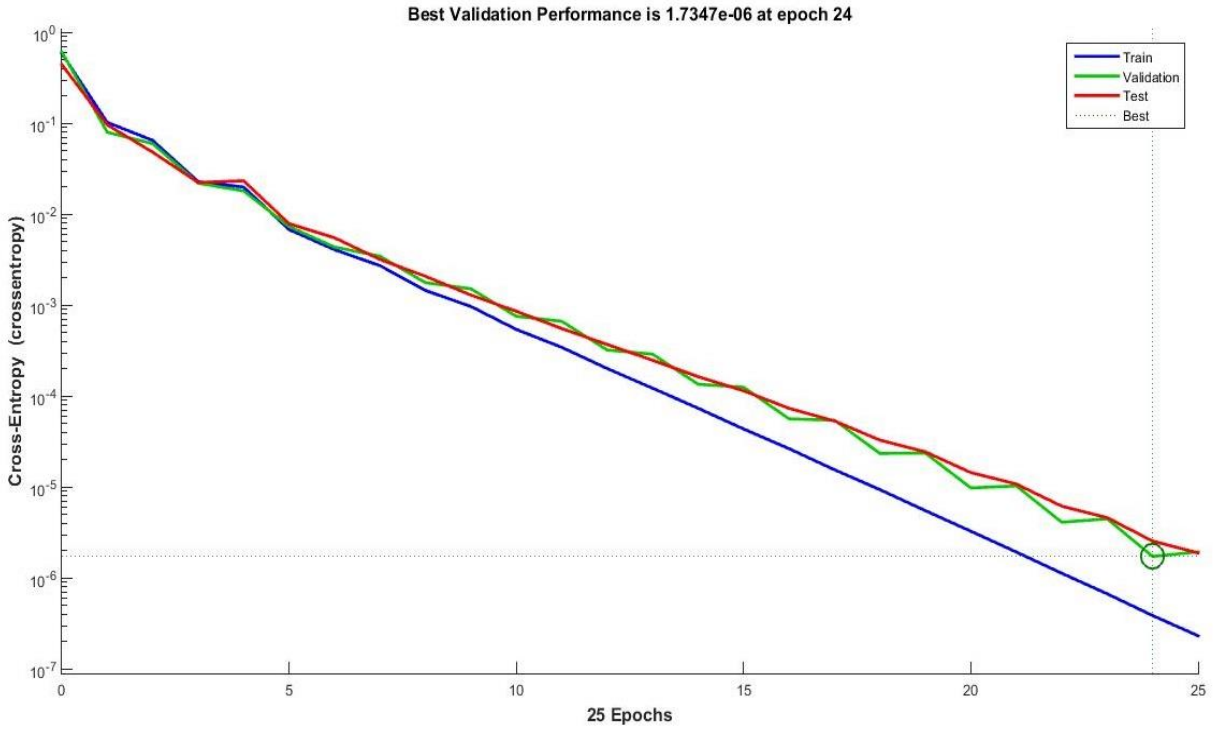

Figure 5. 2: Performance plot of BP-NN training

Table 5. 2: Results of BP-NN on bi-classification problem

S.NO	Sample	Input Neurons	Hidden Neurons	0utput neurons	Accuracy (%)	MSE	Epoch
1	**2**	4	10	2	100	3.20E-06	23
		4	20	2	100	7.67E-07	23
		4	250	2	100	2.08E-08	28
					(Averaged = 100)		
2	**3**	4	10	2	100	5.87E-06	51
		4	20	2	100	5.19E-06	43
		4	243	2	100	6.92E-06	47
					(Averaged = 100)		
3	**4**	4	10	2	100	1.44E-06	36
		4	20	2	100	9.56E-07	41
		4	212	2	99.6	1.99E-04	25
					(Averaged = 99.86)		
4	**6**	4	10	2	100	1.73E-06	25
		4	20	2	100	2.33E-07	26
		4	249	2	99.6	8.77E-02	24
					(Averaged = 99.86)		
5	**10**	4	10	2	90.4	8.05E-02	24
		4	20	2	88.8	1.12E-01	20
		4	30	2	76.4	1.66E-01	8
		4	40	2	95.3	5.26E-02	25
		4	50	2	91.6	9.04E-02	29
		4	60	2	96.8	8.38E-02	47
		4	245	2	98.4	5.04E-02	41
					(Averaged = 91.08)		
6	**11**	4	10	2	100	2.59E-07	19
		4	20	2	100	1.23E-07	16
		4	72	2	100	2.02E-07	21
					(Averaged = 100)		
7	**15**	4	10	2	100	1.83E-07	23
		4	20	2	100	1.74E-07	22
		4	167	2	100	1.03E-06	23
					(Averaged = 100)		
					(Overall Averaged Accuracy = 98.68)		

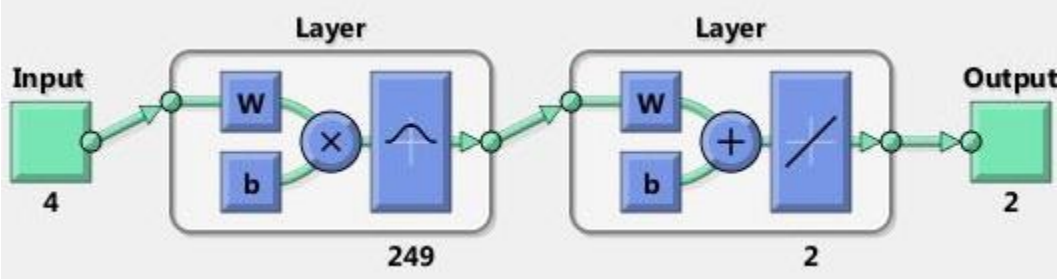

Figure 5. 3: Architecture of RBF-NN used for bi-classification

Figure 5.3 shows the architecture of radial basis function neural network used for classification of "corrosion" and "no corrosion" state for sample 6. RBF-NN has ability to select the suitable number of hidden neurons to reach to the preset goal of MSE. Here RBF-NN architecture shows 4 input neurons, 249 hidden layer neurons and 2 output neurons. Figure 5.4 shows the neural network training performance with best training performance achieved at epoch 225 with MSE of 0.000212331 while preset goal MSE of 1×10^{-05}.

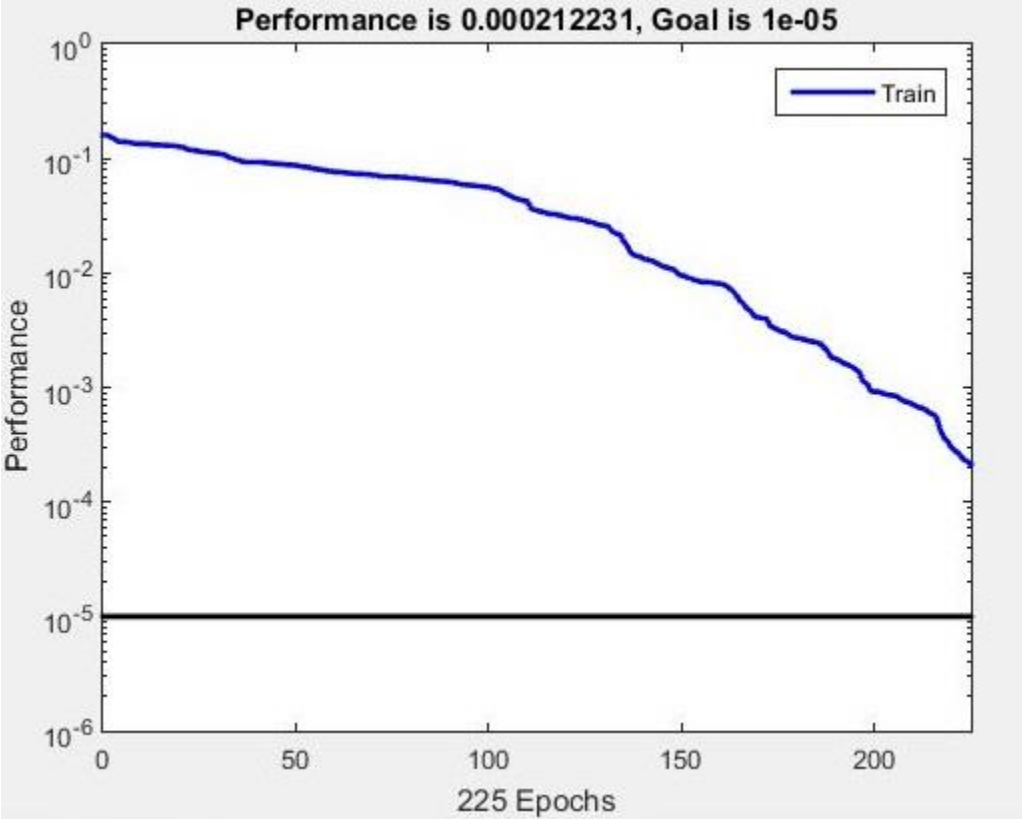

Figure 5. 4: Performance plot of RBF-NN training

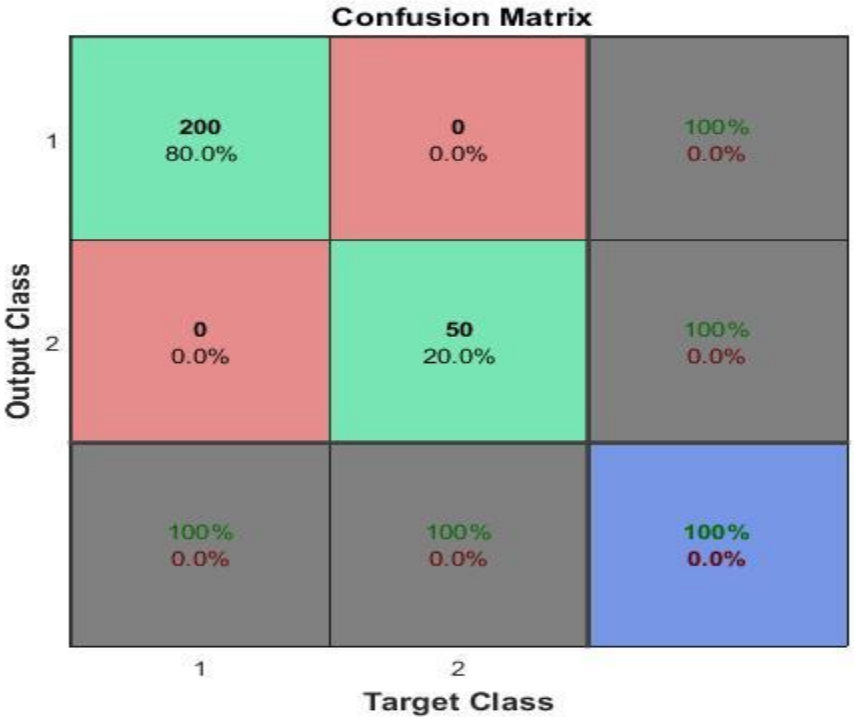

Figure 5. 5: Confusion matrix of RBF-NN used for bi-classification

Fig 5.5 shows the confusion matrix of radial basis function neural network applied on bi - classification problem of sample 6. Confusion matrix shows that RBF-NN has been able to accurately classify all samples of "corrosion" class and class "no corrosion". Table 5.3 shows the results of radial basis function neural network applied on different samples for bi-classification problem. Table shows the number of input neurons, hidden layer neurons, output neurons, MSE and an overall accuracy of 100% for RBF-NN.

Table 5. 3: Results of RBF-NN used for bi-classification

S.NO	Sample	Input Neurons	Hidden Neurons	Output neurons	Accuracy (%)	MSE	Epoch
1	**2**	4	250	2	100	2.93E-04	250
2	**3**	4	243	2	100	1.84E-04	225
3	**4**	4	212	2	100	8.12E-06	200
4	**6**	4	249	2	100	2.12E-05	225
5	**10**	4	245	2	100	1.57E-03	225
6	**11**	4	72	2	100	1.14E-03	50
7	**15**	4	167	2	100	5.05E-03	150

	Actual Class		
Predicted Class	N=250	1	2
	1	50	0
	2	0	200

Figure 5. 6: Confusion matrix for Naive Bayes Classifier used for bi-classification

Figure 5.6 shows the confusion matrix for naive bayes classifier used for bi-classification problem of sample 6. Table 5.4 represents the results of naive bayes classifier applied on different samples showing accuracy, sensitivity and specificity.

Table 5. 4: Results of Naive Bayes Classifier for bi-classification

S.NO	Sample	Accuracy (%)	Sensitivity	Specificity
1	**2**	100	1	1
2	**3**	98	1	0.975
3	**4**	100	1	1
4	**6**	100	1	1
5	**10**	92	1	0.9
6	**11**	100	1	1
7	**15**	100	1	1
		(Averaged=98.57)		

Table 5.5 shows the overall averaged accuracies of applied classifier algorithms for bi-classification problem of "corrosion" and "no-corrosion" prediction. Classifiers showed an overall healthy classification accuracy with lowest of 98.57% for Naive Bayes and highest of 100% for RBF-NN.

Table 5. 5: Accuracy comparison of RBF-NN, BP-NN and Naive Bayes for bi-classification

Classifier	Averaged Accuracy (%)
RBF-NN	100
BP-NN	98.57
Naive Bayes	98.68

5.3. Multi-class Problem (Severity Level Prediction)

Multi-class classification problem involves the classification of corrosion severity levels. Classes are assigned based on the experiment time and mass loss. Corrosion levels are decided based on mass loss calculations obtained from experimentation. Figure 5.7 represents the mass loss versus experimentation time which provides the basis of corrosion severity levels. As the experimentation goes on the mass loss occurs.

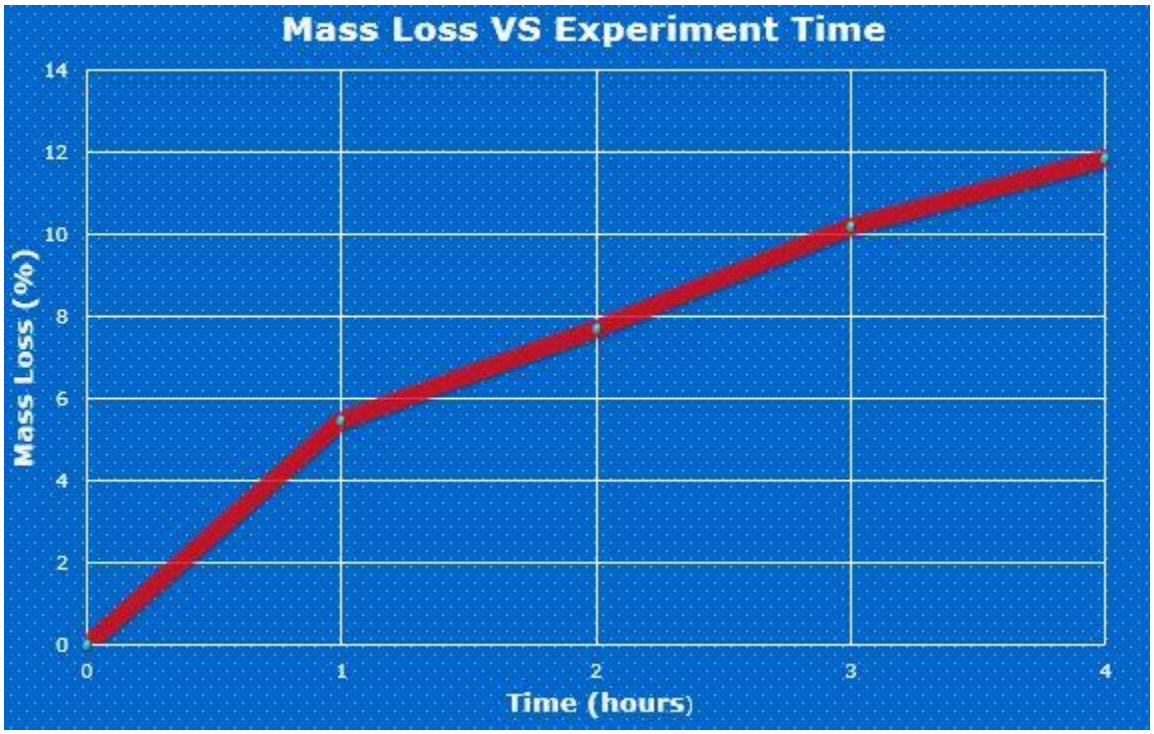

Figure 5. 7: Plot of Mass Loss versus Experimentation time

Table 5.6 shows the results of BP-NN applied on different samples of three class problem. Classes are labelled as “no corrosion”, “Grade 1” and “Grade 2” based on the mass loss. Table represents the sample number, input neurons, output neurons, accuracy, MSE and epoch with an overall accuracy of 99.92%. Output neurons for this problem are set to 3 due to three classes.

Table 5. 6: Results of BP-NN on three-class severity level problem

S.NO	Sample	Input Neurons	hidden Neurons	0utput neurons	Accuracy (%)	MSE	Epoch
1	**1**	4	10	3	100	6.23E-07	39
		4	20	3	100	2.48E-05	34
		4	146	3	99.3	1.38E-05	36
2	**8**	4	10	3	100	4.21E-05	27
		4	20	3	100	5.04E-05	33
		4	150	3	100	7.95E-08	30
3	**9**	4	10	3	100	1.95E-07	40
		4	20	3	100	5.26E-07	38
		4	121	3	100	3.60E-07	41
					Averaged= (99.92)		

Table 5.7 shows the results of radial basis function neural network applied on different samples for three class corrosion severity level problem. Table shows the number of input neurons, hidden layer neurons, output neurons, MSE and an overall accuracy of 100% for RBF-NN.

Table 5. 7: Results of RBF-NN on three-class severity level problem

S.NO	Sample No	Input Neurons	hidden Neurons	0utput neurons	Accuracy	MSE	Epoch
1	**1**	4	146	3	100	0.00179868	125
2	**8**	4	150	3	100	0.00022523	150
3	**9**	4	121	3	100	0.00054337	100

RBF-NN has ability to select the suitable number of hidden neurons to reach to the preset goal of MSE. Table 5.8 shows the performance stats for RBF-NN which showed high accuracy with precision, recall, Fscore and accuracy which chooses 146 hidden neurons to show MSE of 0.00179868.

Table 5. 8: Performance parameter of RBF-NN for high accuracy

S.NO	Sample N0	Input Neurons	hidden Neurons	0utput neurons	Accuracy	MSE	Epoch
1	**1**	4	146	3	100	0.00179868	125
	No Corrosion		**Grade 1**		**Grade 2**		
Precision	1		1		1		
Recall	1		1		1		
F score	1		1		1		
Accuracy	1		1		1		

Table 5. 9: Results of Naive Bayes on three-class severity level problem

S. No	Sample No	Accuracy (%)
1	1	99.5
2	8	100
3	9	100
		Averaged= (99.83)

Table 5.9 shows the results of naive bayes classifier applied on different samples of three-class corrosion severity level problem with an averaged accuracy of 99.83%. Table 5.10 and 5.11 shows the performance stats of naive bayes classifier precision, recall, Fscore and accuracy for low accuracy and high accuracy respectively.

Table 5. 10: Performance parameter of Naive Bayes for lowest accuracy

	No Corrosion	Grade 1	Grade 2
Precision	1	1	0.98
Recall	1	0.98	1
F score	1	0.989	0.989
Accuracy	1	0.995	0.995

Table 5. 11: Performance parameter of Naive Bayes for highest accuracy

	No Corrosion	Grade 1	Grade 2
Precision	1	1	0.98
Recall	1	1	1
F score	1	1	1
Accuracy	1	1	1

Table 5.12 shows an overall accuracy comparison of averaged accuracies of different classifiers applied on three-class corrosion severity level with lowest of 99.83% for Naive Bayes and 100% for RBF-NN.

Table 5. 12: Accuracy comparison of RBF-NN, BP-NN and Naive Bayes for three- class corrosion severity level classification

Classifier	Averaged Accuracy (%)
RBF-NN	100
BP-NN	99.92
Naive Bayes	99.83

Table 5. 13: Results of BP-NN on four-class corrosion severity level problem

S.NO	Sample	No of hidden Neurons	Accuracy (%)	MSE	Epoch
1	**7**	10	94.5	0.02674	40
		20	93.5	0.024248	22
		30	90	0.04527	21
		40	94	0.059419	38
		50	95.5	0.052291	24
		60	96	0.0099685	34
		70	94.2	0.02841	32
		198	91	0.03149	29
2	**12**	10	88	0.04006	30
		20	83	0.082404	13
		30	88.5	0.098651	21
		40	87.5	0.057164	19
		50	81.5	0.076106	17
		60	87.5	0.087661	29
		70	82.4	0.07742	27
		200	87	0.073881	26
3	**5**	10	97.5	0.0075421	35
		20	98	0.021751	35
		30	98	0.024208	23
		40	98.5	0.0061351	34
		50	98	0.022527	24
		60	98.5	0.00085106	29
		70	98.5	0.0031885	46
		189	97.2	0.00782	39
			Averaged= (92.48)		

Table 5.13 shows the results of BP-NN applied on different samples of four-class corrosion severity level classification problem. Classes are labelled as “no corrosion”, “Grade 1”, “Grade 2” and ‘’Grade 3’’based on the mass loss Table shows the accuracy and MSE at different number of hidden layer neurons and number of epochs. Table 5.14 shows the samples with highest and lowest accuracy for BP-NN on four-class corrosion severity level with hidden neurons and MSE.

Table 5. 14: Lowest and highest accuracy for BP-NN

	Sample	No of Hidden Neurons	Accuracy (%)	MSE	Epoch
Lowest Accuracy	12	50	81.5	0.076105	17
Highest Accuracy	5	60	98.5	0.00085106	29

Table 5. 15: Performance parameters of BP-NN for low accuracy (four-class problem)

	No Corrosion	Grade 1	Grade 2	Grade 3
Precision	1	0.995	0.62	0.66
Recall	1	1	0.6326	0.6346
F score	1	0.989	0.6262	0.66
Accuracy	1	0.995	0.815	0.82

Table 5.15 and 5.16 shows the performance stats of RBF-NN classifier with precision, recall, Fscore and accuracy for low accuracy and high accuracy respectively on four-class corrosion severity level classification problem.

Table 5. 16: Performance parameters of BP-NN for high accuracy (four-class problem)

	No Corrosion	Grade 1	Grade 2	Grade 3
Precision	1	0.98032	0.96	0.98
Recall	1	1	0.96	0.96
F score	1	0.989	0.96	0.965
Accuracy	1	0.995	0.98	0.985

Table 5.17 represents the results of RBF-NN applied on different samples for four-class corrosion severity level problem. Table shows the accuracy of four-class corrosion severity level with number of neurons, MSE and epoch with an averaged accuracy of 99.83%.

Table 5. 17: Results of RBF-NN on four-class corrosion severity level problem

S. No	Sample No	Accuracy (%)	No of Neurons	MSE	Epoch
1	7	100	198	0.00448	175
2	12	99.5	200	0.00125	200
3	5	100	189	0.00198	175
		Averaged = (99.83)			

Table 5. 18: Performance parameters of RBF-NN for low accuracy (four-class problem)

	No Corrosion	Grade 1	Grade 2	Grade 3
Precision	1	0.98	1	1
Recall	1	1	0.98	1
F score	1	0.989	0.989	1
Accuracy	1	0.995	0.995	1

Table 5.18 and 5.19 shows the performance stats of BP-NN classifier with precision, recall, and Fscore for low accuracy and high accuracy respectively on four-class corrosion severity level classification problem.

Table 5. 19: Performance parameters of RBF-NN for high accuracy (four-class problem)

	No Corrosion	Grade 1	Grade 2	Grade 3
Precision	1	1	1	1
Recall	1	1	1	1
F score	1	1	1	1
Accuracy	1	1	1	1

Table 5.20 represents the results of Naive Bayes classifier applied on different samples for four-class corrosion severity level problem. Table shows the accuracy of four-class corrosion severity level with an averaged accuracy of 89.1%.

Table 5. 20: Results of Naive Bayes on four-class corrosion severity level problem

S. No	Sample No	Accuracy (%)
1	7	87
2	12	81.5
3	5	99
		Averaged= (89.1)

Table 5.21 and 5.22 shows the performance stats of Naive Bayes classifier with precision, recall, and Fscore for high accuracy and low accuracy respectively on four-class corrosion severity level classification problem.

Table 5. 21: Performance parameters of Naive Bayes for high accuracy (four-class problem)

	No Corrosion	Grade 1	Grade 2	Grade 3
Precision	1	1	0.979	0.96
Recall	1	1	0.96	0.98
F score	1	1	0.968	0.969
Accuracy	1	1	0.985	0.985

Table 5. 22: Performance parameters of Naive Bayes for low accuracy (four-class problem)

	No Corrosion	Grade 1	Grade 2	Grade 3
Precision	1	1	0.625	0.644
Recall	1	0.98	0.7	0.58
F score	1	0.989	0.66	0.6102
Accuracy	1	0.995	0.89	0.82

Table 5.23 shows an overall accuracy comparison of averaged accuracies of different classifiers applied on four-class corrosion severity level problem with lowest of 89.1% for Naive Bayes and 99.83% for RBF-NN. Note able fact here is, As the severity levels grows the overall accuracy of classifier tends to drop due the inter-class mixture of acoustic data.

Table 5. 23: Accuracy comparison of RBF-NN, BP-NN and Naive Bayes for four-class corrosion severity level classification

Classifier	Averaged Accuracy (%)
RBF-NN	99.83
BP-NN	92.48
Naive Bayes	89.1

Table 5.24 shows the results of BP-NN applied on different samples of five-class corrosion severity level classification problem. Table shows the accuracy and MSE at different number of hidden layer neurons and number of epochs with averaged accuracy of 94.57% for BP-NN. Five classes that have been made, presents "no corrosion", "Grade 1", "Grade 2", "Grade 3" and "Grade 4" based on the mass loss difference for each "Grade".

Table 5. 24: Results of BP-NN on five-class corrosion severity level problem

S.NO	Sample	No of hidden Neurons	Accuracy (%)	MSE	Epoch
1	**14**	10	94.8	0.057166	54
		20	94.4	0.027748	46
		30	92	0.032199	20
		40	95.6	0.042211	46
		50	95.2	0.040906	44
		60	97.2	0.007976	70
		70	92.8	0.048229	27
		249	94.8	0.805022	33
			Averaged= (94.57)		

Table 5. 25: Performance parameters of BP-NN for low accuracy (five-class problem)

	No Corrosion	Grade 1	Grade 2	Grade 3	Grade 4
Precision	1	1	0.82	0.78	1
Recall	1	0.943	0.804	0.867	0.98
F score	1	0.9706	0.8482	0.8211	0.989
Accuracy	1	0.988	0.924	0.932	0.996

Table 5.25 and 5.26 shows the performance stats of BP-NN classifier with precision, recall, and Fscore for high accuracy of 97.2% with 70 hidden neurons and low accuracy of 92% with 20 hidden neurons respectively on five-class corrosion severity level classification problem.

Table 5. 26: Performance parameters of BP-NN for high accuracy (five-class problem)

	No Corrosion	Grade 1	Grade 2	Grade 3	Grade 4
Precision	1	1	0.94	0.92	1
Recall	1	1	0.94	0.939	0.98
F score	1	1	0.94	0.929	0.989
Accuracy	1	1	0.976	0.984	0.996

Table 5.27 shows the results of Naive Bayes classifier applied on different samples of five-class corrosion severity level classification problem with an averaged accuracy of 90.4%. Table 5.28 shows the performance parameters of Naive Bayes classifier like precision, recall, Fscore and accuracy for five-class classification problem of corrosion severity level prediction.

Table 5. 27: Results of Naive Bayes on five-class corrosion severity level problem

S. No	Sample No	Accuracy (%)
1	14	90.4

Table 5. 28: Performance parameters of Naive Bayes classifier (five-class problem)

	No Corrosion	Grade 1	Grade 2	Grade 3	Grade 4
Precision	1	0.942	0.937	0.734	0.961
Recall	1	0.981	0.64	0.94	1
F score	1	0.963	0.731	0.8251	0.98
Accuracy	1	0.984	0.912	0.92	0.992

Table 5.29 shows the results of RBF-NN applied on five-class corrosion severity level classification problem with an averaged accuracy of 100%. Table 5.30 shows the performance parameters of RBF-NN classifier like precision, recall, Fscore and accuracy for five-class classification problem of corrosion severity level prediction.

Table 5. 29: Results of RBF-NN on five-class corrosion severity level problem

	Sample	No of Hidden Neurons	Accuracy (%)	MSE	Epoch
Highest Accuracy	14	249	100	0.0005372	225

Table 5. 30: Performance parameters of RBF-NN (five-class problem)

	No Corrosion	Grade 1	Grade 2	Grade 3	Grade 4
Precision	1	1	1	1	1
Recall	1	1	1	1	1
F score	1	1	1	1	1
Accuracy	1	1	1	1	1

Table 5.31 shows an overall accuracy comparison of averaged accuracies of different classifiers applied on five-class corrosion severity level problem with lowest of 90.4% for Naive Bayes and highest of 100% for RBF-NN.

Table 5. 31: Accuracy comparison of RBF-NN, BP-NN and Naive Bayes for five-class corrosion severity level classification

Classifier	Averaged Accuracy (%)
RBF-NN	100
BP-NN	94.57
Naive Bayes	90.4

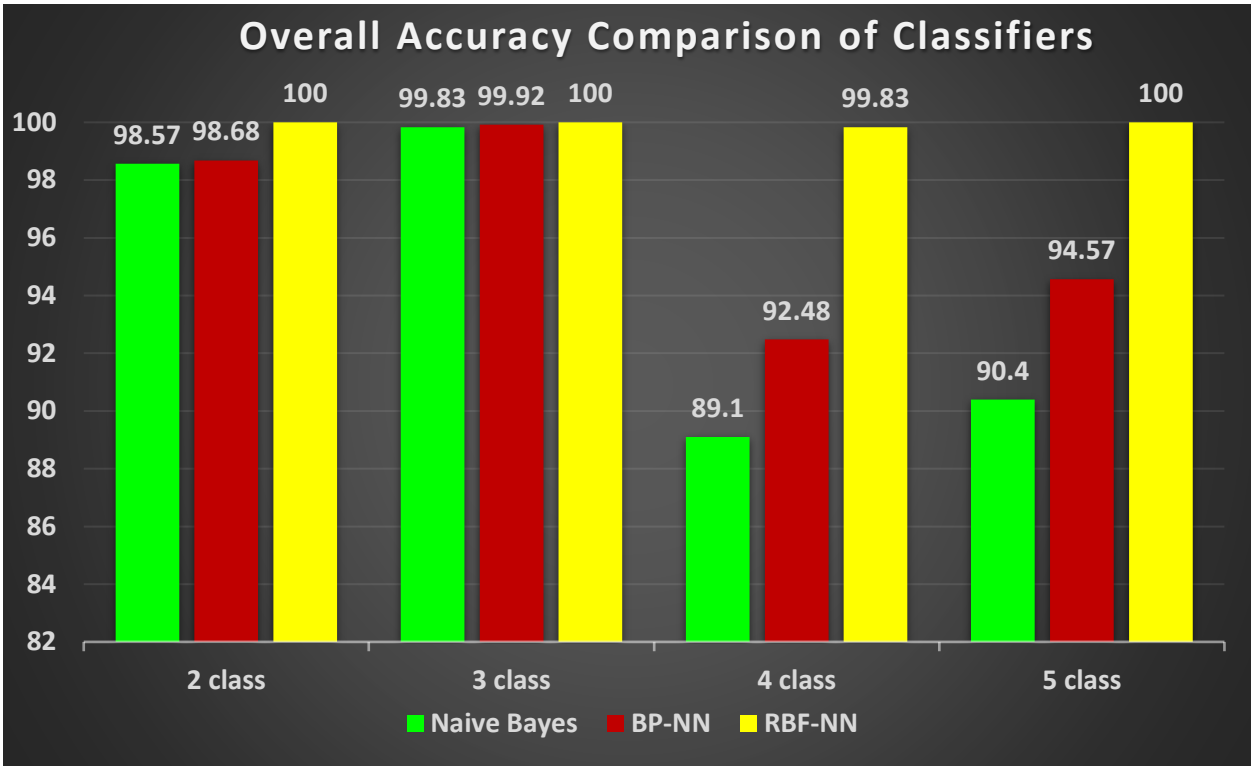

Figure 5. 8: Overall accuracy comparison of BP-NN, RBF-NN and Naive Bayes classifiers for corrosion detection and severity level prediction problem

Figure 5.8 shows an overall comparison of averaged accuracies for applied RBF-NN, BP-NN and Naïve Bayes classifiers on corrosion detection and corrosion severity level problems. Classifiers showed a higher classification rate overall, possible reasons for overall high classification rate is own acquisition scheme of acoustic emission data, distinct features of acoustic data and less variability in the data. Naive Bayes classifier due to its probabilistic nature have not been able to well handle the inter-class mixed data and showed the least accurate results. On the other hand, radial basis function neural network showed good generalization capability due to the presence of gaussian potential functions as activation functions in the hidden layer neurons and showed the highest accuracy for corrosion severity level classification problem.

5.4. Graphical User Interface (GUI) of the Proposed Technique

Graphical User Interface (GUI) is a type of user interface that is designed to interact with the software and computing algorithms through graphical icons and visual indicators. Figure 5.9 shows the GUI of the proposed corrosion monitoring technique made on Matlab. GUI can help user to easily interact with technique and initiate commands from a single window. GUI involves the loading of corrosion's acoustic data to Matlab, Raw and FFT plots of the acquired acoustic data, Feature extraction from acoustic data and finally classification of corrosion severity levels using BP-NN, RBF-NN and Naive Bayes classifiers.

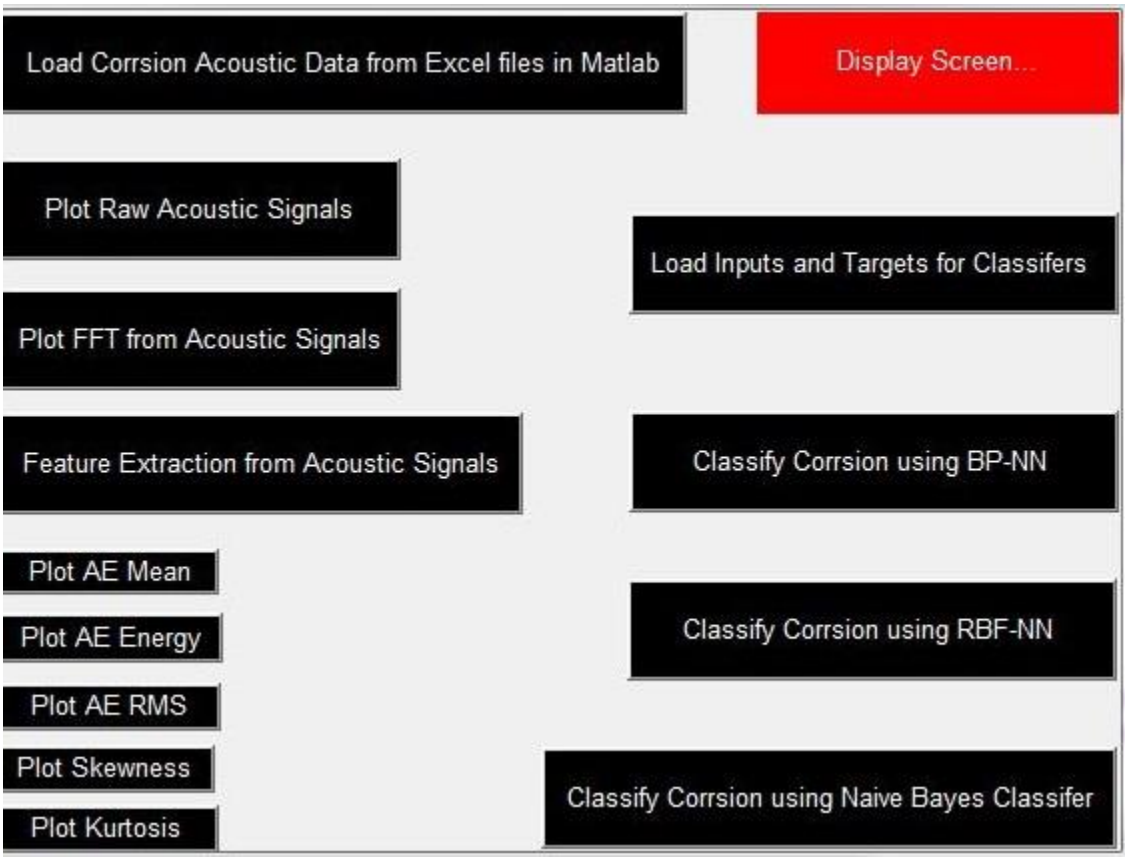

Figure 5. 9: GUI of the Proposed Technique

5.5. Summary

The chapter can be summarized as follows:

- Performance of different machine learning algorithms as classifiers has been tested under different conditions. Three different algorithms, back propagation neural network, radial basis function neural network and naive bayes classifier have been used as supervised learning algorithms for classification of ‘corrosion’ and ‘no corrosion’ state and corrosion severity level prediction.

- For classification purpose, back-propagation neural network and radial-basis function neural network have been trained using AE mean, AE RMS, skewness and kurtosis as inputs of the network and arithmetic patterns set as output classes. Networks have been trained using training dataset and tested against the testing dataset.

- For multi-class problem, five corrosion severity levels have been made based on the mass loss occurred during accelerated corrosion testing. Back-propagation neural network, radial basis function neural network and naive bayes classifier are used to accurately predict the corrosion severity levels. Radial basis function neural network outperformed the other two classifiers and showed the best classification accuracy for corrosion severity level prediction due to presence of gaussian activation function in network hidden layer neurons.

6. CHALLENGES

Corrosion detection through acoustic emission is still in its infancy. Different researchers have used different techniques for corrosion detection and monitoring, involving, visual inspection, vision based techniques, magnetic flux leakage and radiographic inspection. Literature available on corrosion detection and monitoring through acoustic emission is very limited. Researchers have used air-borne acoustic emission for corrosion detection. However, there are few challenges in implementation of the technique. Major challenge in implementation of the technique is the environmental noise such as sounds from parallel running machines, operator voice or sounds in background etc. This research tried to provide a solution to the earlier mentioned problem, by using structure-borne acoustic emission emitted during accelerated corrosion testing process. For better reliability and accuracy proposed technique uses hybrid technique that detects corrosion through acoustic emission then accurately classifies corrosion severity levels with the help of machine learning algorithms. One of the major challenges faced during implementation of the proposed technique is to identify the correct method of accelerated corrosion testing because literature found on accelerated corrosion testing was too ambiguous. Correct method of accelerated corrosion was identified by months of rigorous experimentation.

Data acquisition and data logging of high frequency acoustic emission was another big issue faced during implementation of proposed technique. NI data acquisition card was initially used to sample data at higher frequencies, but it was unable to achieve sampling rate of 250 KHz. To acquire higher frequency acoustic emission data, NI ELVIS kit with LabView interface was used. Own data acquisition scheme was made in accordance with timing of accelerated corrosion testing. For corrosion severity level prediction, prolonged accelerated corrosion tests were performed and metal loss for the samples were measured with high accuracy weighing instruments available at gold shops.

Another challenge to the proposed technique is the variability of the acoustic emission signal for prolonged accelerated corrosion tests due to decrease in the concentration of solution. To solve the above issue, features from data were extracted after preprocessing of the data. Distinct

features of acoustic emission signals showed correlation with material degradation occurred due to corrosion process.

To achieve better prediction and classification accuracy found in literature, a novel classification technique radial basis function neural network is used to classify corrosion severity levels. Classification results of radial basis function neural network were compared with back propagation neural network and naive bayes classifier.

6.1. Summary

The chapter can be summarized as follows

- There are various challenges in implementation of the proposed technique. Experimentation involved in the proposed technique demands the accelerated corrosion testing of mild steel samples, for which accurate scheme for accelerated corrosion testing could be a demanding task.

- High frequency acoustic emission data acquisition demands data acquisition scheme, usage of accurate hardware and software interface. In order to classify corrosion in different levels by machine learning algorithms, acoustic data should be preprocessed and distinct features of acoustic data to be extracted and used as inputs to classifiers.

7. CONCLUSION AND FUTURE WORK

7.1. Conclusion

Degradation caused by corrosion to complex engineering structures strongly affects the economic growth of a country. Industry demands a low cost and efficient corrosion detection method. Acoustic emission of a corrosion process can give vital information about the process. Early stage corrosion detection and monitoring can be performed through acoustic emission. Corrosion detection through non-destructive testing techniques is commonly under use, which involves techniques like radiography, vision based inspection, guided waves and magnetic flux leakage. Acoustic emission unlike other NDT techniques, is a passive NDT technique which just listens to the micro seismic activity. However, AE data needs to be interpreted to get knowledge about the system and is considered as less reliable technique due to variability. The aim of the research is to propose a hybrid technique, which detects corrosion through acoustic emission and predicts corrosion severity levels with high accuracy using machine learning algorithms.

Laboratory based experimental setup was established for accelerated corrosion testing of mild steel for different time spans and mass loss of samples were measured. Acoustic emission signals were acquired at high frequency sampling rate with Sound Well AE sensor, NI Elvis kit and NI Labview software. Acoustic emission frequency of accelerated corrosion process typically lies above 50 KHz. Data acquisition step involves the acquisition of amplitude of high frequency acoustic emission signals and logging them in Excel files. Raw Acoustic signals plot does not give clear information about the changing process. Fast Fourier Transform of acoustic signals confirms the high frequency band during corrosion process. For further interpretation of AE signals with the corrosion process, AE and statistical features of the data were extracted. AE Mean, AE RMS, AE Energy, kurtosis and skewness were selected as distinct features and represent a linear relationship with the corrosion process.

Three different algorithms, back-propagation neural network, radial basis function neural network and probability theorem based naive bayes classifier have been investigated for corrosion severity level prediction. Five Corrosion severity levels have been made based on mass loss during accelerated corrosion testing. For bi-classification problem, Naive Bayes, BP-NN and RBF-NN

showed accuracy of 98.68%, 98.57%, and 100% respectively. One of the possible reason for high accuracy is highly distinctive features representing “corrosion” and “no corrosion” state. For multi-class problem dealing with the corrosion severity level prediction, accuracies of implemented algorithms drop due to inter-class mixture of AE signals and their features. For multi-class problem RBF-NN outperformed BP-NN and Naive Bayes classifier and showed better performance. One of the possible reason for better performance of RBF-NN is the presence of non-linear gaussian activation functions in hidden layer neurons of the network. The reason for the worst performance of Naive Bayes classifier for multi-class problem lies in its probabilistic nature which calculates the posterior probability based on prior probabilities assigned to each class and does not show better efficiency when there is inter-class mixed data.

Finally, it can be concluded that the proposed technique works efficiently for lab environment, however, the proposed technique can face challenges while implementation in the industrial environment. Industrial grade acoustic sensors with manufacturer data acquisition software, prior knowledge of application industry and environment, detailed study of corrosion process and adequate machine learning skills are essentials for industrial application of proposed technique.

7.2. Future Work

Future aim of the research is to explore the suitable techniques and methods to overcome the challenges involved in industrial application of the proposed technique. Prolonged accelerated corrosion tests of samples may be performed to study the behavior of AE signals after increased timing. This may involve analysis of environmental noise in order to filter it out eventually. For practical Implementation of technique in industrial environment acoustic sensor calibration, rugged data acquisition hardware and subsequent acquisition software should be incorporated. For example, corrosion detection inside pipes during chemical flow in petrochemical industries is a challenging task, which can be addressed with the suitable sensor, acquisition software and hardware using proposed technique. Real time data acquired from industrial environment could be sent through wi-fi over a network for further analysis. Exploration of various un-supervised machine learning algorithms can be done using the real time acoustic data of corrosion process.

7.3. Summary

The chapter can be summarized as follows

- A novel hybrid technique for corrosion detection using acoustic emission and corrosion severity level prediction with radial basis function neural network has been developed. Acoustic emission signals during accelerated corrosion testing of mild steel samples were acquired using own data acquisition scheme. For classification purpose, back propagation neural network and radial basis function neural network have been trained using AE mean, AE RMS, skewness and kurtosis as inputs of the network and arithmetic patterns set as output classes. Networks have been trained using training dataset and tested against the testing dataset. Radial basis function neural network outperformed the other two classifiers and showed the best classification accuracy for corrosion severity level prediction due to presence of gaussian activation function in network hidden layer neurons.

- Future work involves the exploration of techniques and methods suitable for practical implementation in industrial application of the proposed technique. It also includes study of various other algorithms to improve the performance of proposed technique.

REFERENCES

[1] Hays, George F. "Now is the Time." *Journal of Advanced Materials Research* 95 (2010): 17-22.

[2] Agarwala, Vinod S., Perry L. Reed, and Siraj Ahmad. "Corrosion detection and monitoring-A review." *CORROSION 2000*. NACE International, 2000.

[3] Schmitt, Günter. "Global needs for knowledge dissemination, research, and development in materials deterioration and corrosion control." *World Corrosion Organization, New York* (2009).

[4] Blitz, Jack. *Electrical and magnetic methods of non-destructive testing*. Vol. 3. Springer Science & Business Media, 2012.

[5] Schweitzer, Philip A. *Corrosion Engineering Handbook, -3 Volume Set*. CRC Press, 1996.

[6] Mali, Anil R., D. I. Desai, and C. U. Nikam. "Brief Review on Corrosion & its Prevention." *Journal of Environmental Engineering and Studies* 2.1 (2017).

[7] De Force, Brian, and Howard Pickering. "A clearer view of how crevice corrosion occurs." *JOM Journal of the Minerals, Metals and Materials Society* 47.9 (1995): 22-27.

[8] Hellier, Charles. "Handbook of nondestructive evaluation." (2001).

[9] Pidaparti, R. M., Aghazadeh, B. S., Whitfield, A., Rao, A. S., & Mercier, G. P. (2010). Classification of corrosion defects in NiAl bronze through image analysis. *Corrosion Science*, *52*(11), 3661-3666.

[10] Mandal, K., and D. L. Atherton. "A study of magnetic flux-leakage signals." *Journal of Physics D: Applied Physics* 31.22 (1998): 3211.

[11] Gloria, N. B. S., Areiza, M. C. L., Miranda, I. V. J., & Rebello, J. M. A. (2009). Development of a magnetic sensor for detection and sizing of internal pipeline corrosion defects. *NDT & e International*, *42*(8), 669-677.

[12] Van der Veer, P. "Internal corrosion in small-diameter, heavy-wall pipelines: a critical phenomenon and how to measure it." *Corrosion Prevention and Control* 47.4 (2000): 103-6.

[13] Kim, D., L. Udpa, and S. Udpa. "Remote field eddy current testing for detection of stress corrosion cracks in gas transmission pipelines." *Materials Letters* 58.15 (2004): 2102-2104.

[14] Raghavan, Ajay, and Carlos ES Cesnik. "Review of guided-wave structural health monitoring." *Shock and Vibration Digest* 39.2 (2007): 91-116.

[15] Lowe, Mike JS, David N. Alleyne, and Peter Cawley. "Defect detection in pipes using guided waves." *Ultrasonics* 36.1-5 (1998): 147-154.

[16] Mokhles, M., Ch Ghavipanjeh, and A. Tamimi. "The use of ultrasonic guided waves for extended pipeline qualification prediction." *SINCE2013: Singapore International NDT Conference & Exhibition, Marina Bay Sands, Singapore*. 2013.

[17] Droubi, M. G., Faisal, N. H., Orr, F., Steel, J. A., & El-Shaib, M. (2017). Acoustic emission method for defect detection and identification in carbon steel welded joints. *Journal of Constructional Steel Research*, *134*, 28-37.

[18] Wu, Kaige, Woo-Sang Jung, and Jai-Won Byeon. "Acoustic emission of hydrogen bubbles on the counter electrode during pitting corrosion of 304 stainless steel." *Materials Transactions* 56.4 (2015): 587-592.

[19] Patil, Shilpa, Shweta Goyal, and Bilavari Karkare. "Performance evaluation of accelerated corrosion techniques using electrochemical measurements and acoustic emission parameters." *Prognostics and Health Management (ICPHM), 2016 IEEE International Conference on*. IEEE, 2016.

[20] Prateepasen, A. *Pitting Corrosion Monitoring Using Acoustic Emission*. INTECH Open Access Publisher, 2012.

[21] Mabbutt, S., Picton, P., Shaw, P., & Black, S. (2012). Review of Artificial Neural Networks (ANN) applied to corrosion monitoring. In *Journal of Physics: Conference Series* (Vol. 364, No. 1, p. 012114). IOP Publishing.

[22] Saenkhum, N., A. Prateepasen, and P. Keawtrakulpong. "Classification of Corrosion Detected by Acoustic Emission." *ASME 2003 International Mechanical Engineering Congress and Exposition*. American Society of Mechanical Engineers, 2003.

[23] Hendi, A., Behravan, A., Mostofinejad, D., Moshtaghi, S. M., & Rezayi, K. (2017). Implementing ANN to minimize sewage systems concrete corrosion with glass beads substitution. *Construction and Building Materials*, *138*, 441-454.

[24] De Masi, G., Gentile, M., Vichi, R., Bruschi, R., & Gabetta, G. (2015, May). Machine learning approach to corrosion assessment in subsea pipelines. In *OCEANS 2015-Genova* (pp. 1-6). IEEE.

[25] Liao, K., Yao, Q., Wu, X., & Jia, W. (2012). A numerical corrosion rate prediction method for direct assessment of wet gas gathering pipelines internal corrosion. *Energies*, *5*(10), 3892-3907.

[26] Jian, L., Weikang, K., Jiangbo, S., Ke, W., Weikui, W., Weipu, Z., & Zhoumo, Z. (2013). Determination of corrosion types from electrochemical noise by artificial neural networks. *Int. J. Electrochem. Sci*, *8*(2), 2365-2377.

[27]"Acoustic Emission Testing." [Online]. Available: http://mech.vub.ac.be/teaching/info/Damage_testing_prevention_and_detection_in_aeronautics/PDF/acoustic-emission.pdf. [Accessed 15 May 2016].

[28] Grosse, Christian U., and Masayasu Ohtsu, eds. *Acoustic emission testing*. Springer Science & Business Media, 2008.

[29] Murphy, Kevin P. "Naive bayes classifiers." *University of British Columbia* (2006).

[30] Basri, M., Rahman, R. N. Z. R. A., Ebrahimpour, A., Salleh, A. B., Gunawan, E. R., & Rahman, M. B. A. (2007). Comparison of estimation capabilities of response surface methodology (RSM) with artificial neural network (ANN) in lipase-catalyzed synthesis of palm-based wax ester. *BMC biotechnology*, *7*(1), 53.

[31] Sivanandam, S. N., and S. N. Deepa. *Introduction to neural networks using Matlab 6.0*. Tata McGraw-Hill Education, 2006.

[32] M. A. Selver and C. Guzelis, "Semiautomatic Transfer Function Initialization for Abdominal Visualization Using Self-Generating Hierarchical Radial Basis Function Networks," in IEEE Transactions on Visualization and Computer Graphics, vol. 15, no. 3, pp. 395-409, May-June 2009.

[33] MathWorks, "Matlab help, Design radial basis network," [Online]. Available: https://in.mathworks.com/help/nnet/ref/newrb.html [Accessed 20 May 2016].

[34] Garg, Bandana. "Design and Development of Naive Bayes Classifier." *Circulation* 701 (2013): 8888.

[35] MathWorks, "Matlab help, Train multiclass naive Bayes model," [Online]. Available: https://in.mathworks.com/help/nnet/ref/newrb.html [Accessed 26 May 2016].

Completion Certificate

It is to certify that the thesis titled "Corrosion Detection and Classification using Acoustic Emission and Machine Learning Based Approach" submitted by registration no.00000117373, NS Muhammad Fahad Sheikh of MS-86 Mechatronics Engineering is complete in all respects as per the requirements of Main Office, NUST (Exam branch).

Supervisor: _____
Dr. Khurram Kamal

Date: ____ February, 2018